

**CONSERVATION APPROACHES OF PATINA  
FORMATION ON MARBLE AND TRAVERTINE  
SURFACES IN THE ARCHAEOLOGICAL SITES**

**A Thesis Submitted to  
the Graduate School of Engineering and Sciences of  
İzmir Institute of Technology  
in Partial Fulfillment of the Requirements for the Degree of**

**DOCTOR OF PHILOSOPHY**

**in Architecture**

**by  
Fulya BADUR**

**July 2017**

We approve the thesis of **Fulya BADUR**

**Examining Committee Members:**

---

**Prof. Dr. Hasan BÖKE**

Department of Architectural Restoration, İzmir Institute of Technology

---

**Prof. Dr. Başak İPEKOĞLU**

Department of Architectural Restoration, İzmir Institute of Technology

---

**Prof. Dr. A. Bahadır YAVUZ**

Department of Geological Engineering, Dokuz Eylül University

---

**Assoc. Prof. Dr. FEHMİ DOĞAN**

Department of Architecture, İzmir Institute of Technology

---

**Assoc. Prof. Dr. Hülya YÜCEER**

Department of Architecture, Adana Science and Technology University

**31 July 2017**

---

**Prof. Dr. Hasan BÖKE**

Supervisor,  
Department of Architectural Restoration  
İzmir Institute of Technology

---

**Prof. Dr. Şerife HANIM YALÇIN**

Co-Supervisor,  
Department of Chemistry  
İzmir Institute of Technology

---

**Assoc. Prof. Dr. Şeniz ÇIKIŞ**

Head of the Department of Architecture

---

**Prof. Dr. Aysun SOFUOĞLU**

Dean of the Graduate School of  
Engineering and Sciences

## ACKNOWLEDGEMENTS

This thesis might not have existed without the support of many people.

First of all, I would like to express my special thanks to my supervisor Prof. Dr. Hasan Bke for his support and guidance throughout the study. I know that I could never complete this study without your help and patience.

I also would like to express my gratefulness to Prof. Dr. Őerife Hanım Yalçın for her scientific support during this thesis.

Thanks to Prof. Dr. BaŐak İpekođlu for her encouragement and support in several projects during my master and PhD education. Thank you for your remarkable contributions to this thesis whenever needed.

My thanks to the jury members Assoc. Prof. Dr. Fehmi Dođan, Assoc. Prof. Dr. Hlya Yceer and Prof. Dr. A. Bahadır Yavuz for their valuable suggestions to this study.

Also thanks to the research scientists of the Centre for the Materials Research of the Institute for SEM-EDS, XRD, TGA analyses and Nadir Aras for LIBS analyses.

Many thanks to my dear friends ađlayan Deniz Kaplan, Elif Uđurlu Sađın and Kerem Őerifaki who worked with, travelled, discussed, had fun together and more to write here. Thanks for your technical help and especially valuable encouragement. I tried many sentence to write here, but I think that's the best: Thanks that I met this team!

I am indebted to my mother Nilgn Murtezaođlu, my father Hızır Murtezaođlu, my brother Ufuk Murtezaođlu, and my general manager Tolga zsoy for their love, patience and support to complete this thesis.

And of course, special thanks to my husband Gkdemir Badur and my pretty son Demir Badur for their endless love and support, patiently looking at me with lovely eyes to finish this research. Good news! It's done. This thesis is dedicated to them.

## ABSTRACT

### CONSERVATION APPROACHES OF PATINA FORMATION ON MARBLE AND TRAVERTINE SURFACES IN THE ARCHAEOLOGICAL SITES

Patina, which is formed on the stone surfaces of historical buildings and monuments as a result of aging, is considered as a value of the building in the conservation of cultural heritage studies. It should be conserved on calcareous stone surfaces whether or not it represents protective characteristics, since it provides information about previous times. Within this respect, the determination of mineralogical composition, and microstructural and chemical characteristics of patina are critical for the conservation decisions. The aim of this study is to determine the characteristics of yellow patina formation on marble and yellow travertine surfaces to constitute a conservation approach in the archaeological sites.

In this study, XRD, FT-IR, SEM-EDX, LIBS and TGA were used to determine the characteristics of yellow patina formation on marble and yellow travertine surfaces in Aizanoi, Aphrodisias, Sardes and Hierapolis.

Analysis results indicated that yellow patina is mainly composed of calcium oxalate (whewellite or weddelite) minerals. CaO, MgO, Al<sub>2</sub>O<sub>3</sub>, SiO<sub>2</sub>, P<sub>2</sub>O<sub>5</sub>, K<sub>2</sub>O, SO<sub>3</sub>, FeO and Na<sub>2</sub>O were observed on the chemical analyses of the same samples. The results of LIBS and SEM-EDX showed that Ca increases, and other elements decrease from surface to the sound inner parts of the stone due to calcium oxalate and gypsum precipitation and clay deposition on the surfaces. The calcium oxalate patina forms a homogeneous film layer on calcite crystals. It is most likely formed by the reaction of calcite and oxalic acid produced by the biological formations on stone surfaces. It is colorless in original. The yellow color may be related with the FeO and clay deposition on the stone surfaces. The outcomes of the study proved the presence of a protective yellow patina formation on yellow travertine surfaces against the weathering effects of water which cannot be distinguished by naked eye. This patina presents same characteristics with the yellow patina on marble surfaces which should be conserved.

The results of this study show that the determination of yellow patina is critical to keep irreversible cleaning interventions away from surfaces especially for the monuments that yellow travertine is used as building materials.

# ÖZET

## ARKEOLOJİK ALANLARDA BULUNAN MERMER VE TRAVERTEN YÜZEYLERİNDEKİ PATİNA OLUŞUMLARININ KORUMA YAKLAŞIMLARI

Tarihi bina ve anıtların taş yüzeylerinde yaşlanma sonucu meydana gelen patina, kültürel mirasın korunması ile ilgili çalışmalarda yapının değeri olarak ele alınmaktadır. Dolayısıyla, kalkerli taş yüzeylerinde koruyucu özelliği olup olmadığına bakılmaksızın korunması gerekmektedir. Zira patina, geçmiş dönemler ile ilgili bilgiler taşımaktadır. Bu açıdan patinanın mineralojik kompozisyonu ile kimyasal ve mikro yapısal özelliklerinin belirlenmesi koruma kararlarının oluşturulmasında önemlidir. Bu çalışmanın amacı mermer ve sarı traverten yüzeylerindeki sarı patinanın özelliklerinin arkeolojik alanlarda koruma yaklaşımlarının oluşturulması için belirlenmesidir.

Bu çalışmada, Aizanoi, Aphrodisias, Sardis ve Hierapolis'te bulunan mermer ve sarı traverten yüzeylerinde oluşan sarı patina oluşumlarının özelliklerinin belirlenmesi için XRD, FT-IR, SEM-EDS, LIBS ve TGA kullanılmıştır.

Analiz sonuçları, sarı patinanın çoğunlukla kalsiyum oksalat (vedelit veya vevelit) minerallerinden oluştuğunu göstermektedir. Aynı örneklerin kimyasal analiz sonuçlarında CaO, MgO, Al<sub>2</sub>O<sub>3</sub>, SiO<sub>2</sub>, P<sub>2</sub>O<sub>5</sub>, K<sub>2</sub>O, SO<sub>3</sub>, FeO ve Na<sub>2</sub>O elementleri bulunmuştur. LIBS ve SEM-EDX sonuçlarında, yüzeyde biriken kalsiyum oksalat, alçı ve kil minerallerinden dolayı yüzeyden sağlam iç kısımlara gidildikçe Ca oranının arttığı ve diğer elementlerin azaldığı görülmüştür.

Kalsiyum oksalat kalsit kristallerinin üzerinde homojen bir film tabakası oluşturmaktadır. Bunun kalsit ve taş yüzeylerindeki biyolojik oluşumların ürettiği oksalik asitin reaksiyonu sonucu oluştuğu düşünülmektedir. Kalsiyum oksalat renksizdir. Kalsiyum oksalat patinasının sarı rengi taş yüzeylerinde biriken demir oksit ve kil minerallerinden kaynaklanabilir. Elde edilen bilgiler, traverten yüzeylerinde çıplak gözle ayırt edilemeyen suya karşı koruyucu bir sarı tabakanın varlığını ispatlamaktadır. Bu patina, mermer yüzeylerinde oluşan ve korunması gereken sarı kalsiyum oksalat tabakası ile aynı niteliktedir. Bu çalışmanın sonuçları, sarı kalsiyum oksalat patinasının tespitinin, özellikle sarı traverten kullanılan tarihi yapılarda geri dönüşü olmayan temizleme uygulamalarından kaçınılması açısından önemli olduğunu göstermektedir.

# TABLE OF CONTENTS

|  |      |
|--|------|
| LIST OF FIGURES .....  | viii |
| LIST OF TABLES.....  | xiii |
| CHAPTER 1. INTRODUCTION .....  | 1    |
| 1.1. Problem Definition .....  | 5    |
| 1.2. Aim and Scope.....  | 6    |
| 1.3. Case Study Archaeological Sites .....   | 6    |
| 1.3.1. Aizanoi.....  | 8    |
| 1.3.2. Aphrodisias .....   | 9    |
| 1.3.3. Sardes.....   | 10   |
| 1.3.4. Hierapolis.....   | 11   |
| 1.4. Characteristics of Marble and Travertine Used in<br>Case Study Areas .....  | 14   |
| 1.5. Formation of Patina Types on Stone Surfaces<br>in the Archaeological Sites .....  | 15   |
| 1.5.1. The Formation of Green Patina .....   | 20   |
| 1.5.2. The Formation of Gray/Black Patina.....   | 20   |
| 1.5.3. The Formation of Yellow/Brown Patina .....  | 23   |
| 1.6. Techniques Used in the Characterization of Patina .....   | 29   |
| 1.7. Conservation Approaches of Patina in<br>Cultural Heritage Studies.....  | 35   |
| 1.8. International Charters about Patina Formation in<br>Cultural Heritage Studies.....  | 41   |
| CHAPTER 2. METHODS .....   | 43   |
| 2.1. Site Survey and Sampling.....   | 43   |
| 2.2. Nomenclature of the Samples .....   | 48   |
| 2.3. Laboratory Studies Used in the Determination of<br>Mineralogical Composition, Microstructural and<br>Chemical Characteristics of Stones and Patina..... | 51   |

|   |     |
|---|-----|
| 2.3.1. Preparation of Samples for Laboratory Analyses .....   | 51  |
| 2.3.2. Determination of Mineralogical Composition .....   | 52  |
| 2.3.3. Determination of Micro-structural Characteristics .....  | 54  |
| 2.3.4. Determination of Chemical Composition .....  | 54  |
| <br>  |     |
| CHAPTER 3. RESULTS AND DISCUSSION.....  | 60  |
| 3.1. Mineralogical and Chemical Compositions of<br>Marble and Travertine .....  | 60  |
| 3.2. Characteristics of Patina on Marble and Travertine .....   | 65  |
| 3.2.1. Mineralogical Composition of Yellow Patina .....   | 65  |
| 3.2.2. Microstructural Characteristics of Yellow Patina.....  | 73  |
| 3.2.3. Chemical Composition of Yellow Patina .....  | 78  |
| 3.2.3.1. The Elemental Distribution of Stone Samples<br>from Surface to the Inner Cores.....                                    | 90  |
| 3.3. The Source of CaC <sub>2</sub> O <sub>4</sub> and Yellow Color of Calcium Oxalate<br>Patina on Marble and Travertine ..... | 110 |
| <br>  |     |
| CHAPTER 4. CONCLUSION .....   | 115 |
| <br>  |     |
| REFERENCES .....  | 119 |

# LIST OF FIGURES

| <b><u>Figure</u></b>   | <b><u>Page</u></b> |
|--|--------------------|
| Figure 1.1. The locations of case study archaeological sites on the historical map of Anatolia (showing the provinces of Asia Minor in 63bc)<br>(Source: <a href="http://www.thehistoryblog.com/wp-content/uploads/2012/09/Anatolia-63bc.jpg">http://www.thehistoryblog.com/wp-content/uploads/2012/09/Anatolia-63bc.jpg</a> ) ..... | 7                  |
| Figure 1.2. Zeus Temple in Aizanoi (If there is no citation, the photograph belongs to the author for the rest of the thesis) .....  | 8                  |
| Figure 1.3. Theatre and stadium complex in Aizanoi.....  | 9                  |
| Figure 1.4. Tetrapylon gate in Aphrodisias .....   | 10                 |
| Figure 1.5. The ruins of scene in theatre building in Aphrodisias.....   | 10                 |
| Figure 1.6. The temple in Sardes<br>(Source: <a href="http://www.openbible.info/geo/photos/Sardes">www.openbible.info/geo/photos/Sardes</a> ) .....  | 11                 |
| Figure 1.7. A tomb in Hierapolis necropolis .....  | 12                 |
| Figure 1.8. A tomb in Hierapolis necropolis .....  | 13                 |
| Figure 1.9. The bath building in Hierapolis.....   | 13                 |
| Figure 1.10. Patina on bronze Equestrian Sculpture of Marcus Aurelius,<br>Capitoline Museums, Rome<br>(Source: <a href="https://www.khanacademy.org/">https://www.khanacademy.org/</a> ).....  | 16                 |
| Figure 1.11. Patina formations on the stone facade of<br>Reims Cathedral, France .....   | 19                 |
| Figure 1.12. Patina formations on the facade of Academie Nationale<br>De Musique, Paris and the surfaces of marble statue<br>standing in front of it .....   | 19                 |
| Figure 1.13. Green patina formation on sculpture, Italy<br>(Source: Fitzner and Heinrichs 2002).....   | 20                 |
| Figure 1.14. Black patina formation related with air pollution on the statue<br>at Town Hall, Germany (Source: Fitzner and Heinrichs 2002).....  | 22                 |
| Figure 1.15. Black patina formation related with microorganisms<br>on the towers (a) and walls (b) of Angkor Wat, Cambodia<br>(Source: The personal archive of N. Murtezaoğlu).....  | 22                 |

|   |    |
|---|----|
| Figure 1.16. Yellow patina formation on the marble ruins as building stones (a), columns capital (b) and historical writings (c) in Ephesus, Turkey .....   | 24 |
| Figure 1.17. Brown patina formation on the stones of Cathedral, Halberstadt, Germany (Source: Fitzner and Heinrichs 2002) .....   | 28 |
| Figure 1.18. Patina on marble surface of capital before (a) and after (b) laser cleaning (Source: <a href="http://www.metmuseum.org/blogs/in-season/2014/laser-cleaning-for-stone-conservation">http://www.metmuseum.org/blogs/in-season/2014/laser-cleaning-for-stone-conservation</a> ) .....               | 29 |
| Figure 1.19. Patina formation on oil painting before (right side) and after (left side) cleaning (Source: <a href="http://www.simongillespie.com/wp-content/uploads/2013/05/Varnish-Removal-2-400x603.jpg">http://www.simongillespie.com/wp-content/uploads/2013/05/Varnish-Removal-2-400x603.jpg</a> ) ..... | 38 |
| Figure 2.1. The locations of yellow patina and marble samples taken from the wall of Zeus Temple (a) and Theatre (b) in Aizanoi.....  | 44 |
| Figure 2.2. The location of yellow patina and marble samples taken from the wall of Bouleuterion in Aphrodisias .....   | 45 |
| Figure 2.3. The representative yellow patina covered marble samples taken from the ground in the Temple of Sardes.....  | 46 |
| Figure 2.4. The location of yellow patina and yellow travertine samples taken from the Bath in Hierapolis .....   | 46 |
| Figure 2.5. The locations of yellow patina and yellow travertine samples taken from the column (a) and wall (b) of Agora in Hierapolis .....  | 47 |
| Figure 2.6. The location of yellow patina and yellow travertine samples taken from Necropolis in Hierapolis.....  | 48 |
| Figure 2.7. A representative marble sample showing its use for SEM-EDX mapping.....   | 55 |
| Figure 2.8. Graphs showing the ablation rates of elements in LIBS analyses of marble applied in different energy levels between 20 and 160 mj.....  | 57 |
| Figure 2.9. Drawings showing sample placement on the stage of LIBS device as the first method for test (a) and the second method for use during the study (b) .....   | 58 |

|   |    |
|---|----|
| Figure 3.1. XRD patterns of sound inner cores of marble samples collected from various buildings in Aizanoi, Aphrodisias and Sardes archaeological sites .....  | 61 |
| Figure 3.2. The amounts of major and minor elements in sound inner cores of marble.....   | 62 |
| Figure 3.3. XRD patterns of sound inner cores of travertine samples collected from various buildings in Hierapolis archaeological site .....  | 63 |
| Figure 3.4. The amounts of major and minor elements in sound inner cores of travertine .....  | 64 |
| Figure 3.5. Calcite crystals of sound inner cores of marble (Ai.Te.M.1) (a) and travertine (H.N.T.1) (b).....   | 64 |
| Figure 3.6. XRD patterns of patina samples formed on marble surfaces of various buildings in Aizanoi, Aphrodisias and Sardes archaeological sites .....   | 66 |
| Figure 3.7. XRD patterns of patina samples formed on travertine surfaces of various buildings in Hierapolis archaeological site.....  | 67 |
| Figure 3.8. FT-IR graphs of patina samples on marble in Aizanoi, Aphrodisias and Sardes archaeological sites .....  | 68 |
| Figure 3.9. FT-IR graphs of patina samples on travertine in Hierapolis archaeological site.....   | 69 |
| Figure 3.10. SEM images of one representative marble sample (Ai.Te.M.1) showing calcite (a) and calcium oxalate crystals formed on it (b) .....   | 73 |
| Figure 3.11. Magnified SEM images showing the outer nodular appearance of calcium oxalate layer on marble (Ai.Th.M.1 (a)) and travertine (H.N.T.1 (b)).....   | 74 |
| Figure 3.12. SEM images of yellow patina on marble (Ai.Th.M.1 (a)) and travertine surfaces (H.N.T.1 (b)), sections representing the yellow patina, inner core and intersection of both (H.Ba.T.1 (c, d))..... | 75 |
| Figure 3.13. SEM images of the intersection of marble and patina with its thickness (Ai.Th.M.1 (a), Ai.Th.M.2 (b), Ai.Te.M.1 (c), Ap.Te.M.1 (d)) .....  | 76 |
| Figure 3.14. SEM images of the intersection of travertine and patina with its thickness (H.A.T.1 (a), H.Ba.T.1 (b), H.N.T.1 (c)) .....  | 76 |

|  |    |
|--|----|
| Figure 3.15. The amounts of major and minor elements in yellow patina formation (a) and sound inner cores (b) of marble samples .....  | 79 |
| Figure 3.16. The amounts of major and minor elements in yellow patina formation (a) and sound inner cores (b) of travertine samples .....  | 80 |
| Figure 3.17. TGA graphs of patina samples taken from marble surfaces .....   | 84 |
| Figure 3.18. TGA graphs of patina samples taken from travertine surfaces .....   | 85 |
| Figure 3.19. Atomic emission lines of C, Si, Al and Fe of sound inner core (spectrum below) and yellow patina (spectrum above) by LIBS spectrum of marble (Ai.Th.M.1).....       | 86 |
| Figure 3.20. The graphs showing the ratios of C, Si, Al and Fe signals to Ca signal in the yellow patina (Ai.Th.M.1-P) and sound inner cores of marble sample (Ai.Th.M.1-I)..... | 87 |
| Figure 3.21. Atomic emission lines of C, Si, Al and Fe of sound inner core (spectrum below) and yellow patina (spectrum above) by LIBS spectrum of travertine (H.N.T.1).....     | 88 |
| Figure 3.22. Atomic emission lines of C, Ca, Mg, Si, Al and Fe of yellow patina on marble samples by LIBS spectrum.....  | 91 |
| Figure 3.23. Atomic emission lines of C, Ca, Mg, Si, Al and Fe of yellow patina on yellow travertine samples by LIBS spectrum .....  | 92 |
| Figure 3.24. Variation of C, Mg, Si, Al and Fe signal intensities normalized to Ca signal with respect to depth in LIBS (a) and SEM-EDX mapping of Ai.Th.M.2 (b).....            | 95 |
| Figure 3.25. Variation of C, Mg, Si, Al and Fe signal intensities normalized to Ca signal with respect to depth in LIBS (a) and SEM-EDX mapping of Ai.Te.M.1 (b).....            | 96 |
| Figure 3.26. Variation of C, Mg, Si, Al and Fe signal intensities normalized to Ca signal with respect to depth in LIBS (a) and SEM-EDX mapping of Ap.B.M.1 (b).....             | 97 |
| Figure 3.27. Variation of C, Mg, Si, Al and Fe signal intensities normalized to Ca signal with respect to depth in LIBS (a) and SEM-EDX mapping of Ap.Te.M.1 (b).....            | 98 |
| Figure 3.28. Variation of C, Mg, Si, Al and Fe signal intensities normalized to Ca signal with respect to depth for S.Te.M.1 in LIBS.....  | 99 |

|   |     |
|---|-----|
| Figure 3.29. Variation of C, Mg, Si, Al and Fe signal intensities normalized to Ca signal with respect to depth for H.N.T.1 in LIBS.....  | 100 |
| Figure 3.30. Variation of C, Mg, Si, Al and Fe signal intensities normalized to Ca signal with respect to depth in LIBS (a) and SEM-EDX mapping of H.A.T.1 (b).....                 | 101 |
| Figure 3.31. Variation of C, Mg, Si, Al and Fe signal intensities normalized to Ca signal with respect to depth for H.A.T.2 in LIBS.....  | 102 |
| Figure 3.32. Variation of C, Mg, Si, Al and Fe signal intensities normalized to Ca signal with respect to depth for H.F.T.1 in LIBS .....   | 103 |
| Figure 3.33. Variation of C, Mg, Si, Al and Fe signal intensities normalized to Ca signal with respect to depth in LIBS (a) and SEM-EDX mapping of H.Ba.T.1 (b).....                | 104 |
| Figure 3.34. Graph showing the average content of C, Mg, Si, Al and Fe in the superficial layer of patina (~first 5 µm depth) and inner core of marble using LIBS.....              | 108 |
| Figure 3.35. Graph showing the average content of C, Mg, Si, Al and Fe in the superficial layer of patina (~first 5 µm depth) and inner core of travertine using LIBS.....          | 109 |
| Figure 3.36. Biological formations on the marble walls of Zeus Temple in Aizanoi.....   | 111 |
| Figure 3.37. SEM images of lichen formations (H.A.T.1 (a, b), H.N.T.1 (c)) and traces of living organisms (H.N.T.1 (d)) in the yellow patina formations of travertine surfaces..... | 111 |
| Figure 3.38. Different hues of yellow patina on marble ruins of Zeus Temple in Aizanoi.....   | 113 |
| Figure 3.39. Different hues of yellow patina on travertine ruins of Necropolis in Hierapolis .....  | 114 |

## LIST OF TABLES

| <b><u>Table</u></b>   | <b><u>Page</u></b> |
|---|--------------------|
| Table 1.1. Analysis techniques used in the stone conservation studies (Source: Stuart 2007).....  | 32                 |
| Table 2.1. Marble samples collected from the site .....   | 49                 |
| Table 2.2. Travertine samples collected from the site .....   | 50                 |
| Table 2.3. Parameters used in XRD analyses .....  | 53                 |
| Table 2.4. Experimental parameters used in LIBS analyses.....   | 59                 |
| Table 3.1. The mineralogical analyses results of yellow patina formation in literature .....  | 71                 |
| Table 3.2. The table representing the determined minerals in XRD and FT-IR analyses of patina on marble and travertine samples.....   | 72                 |
| Table 3.3. The thickness of yellow patina determined in SEM-EDX analyses.....   | 77                 |
| Table 3.4. The thickness of yellow patina determined in literature survey .....   | 77                 |
| Table 3.5. Comparison of chemical composition of yellow patina in some studies in the literature .....  | 81                 |
| Table 3.6. Weight losses of the samples during TGA analyses.....  | 83                 |
| Table 3.7. C/Ca, Al/Ca, Fe/Ca and Si/Ca ratios in the patina according to the inner core of yellow patina covered marble.....   | 87                 |
| Table 3.8. The molecular weight and mass percent of each element in calcium oxalate and calcium carbonate (Source: <a href="http://www.convertunits.com/">http://www.convertunits.com/</a> )..... | 89                 |
| Table 3.9. The thickness of patina formations determined by SEM-EDX and LIBS analyses .....   | 105                |
| Table 3.10. The signal intensity ratios of elements considering the average values of ~5 µm thick area in in-depth LIBS analyses of yellow patina and sound inner core of marble.....             | 108                |
| Table 3.11. The signal intensity ratios of elements considering the average values of ~5 µm thick area in in-depth LIBS analyses of yellow patina and sound inner core of travertine.....         | 109                |

# CHAPTER 1

## INTRODUCTION

Stone monuments constitute the majority of the documents of ancient civilizations as being the most common part of built cultural heritage especially in the archaeological sites. The loss of a stone material means the loss of traces coming from the past. In this respect, weathering problems and conservation of stone monuments is still a critical issue in the conservation field. Appropriate diagnosis of stone weathering and proper conservation approaches can minimize the losses on stone in the archaeological sites.

Weathering is defined as the process that stones are broken down into smaller pieces as “a result of physical disintegration and chemical decomposition of the stone” embracing all the terms to define changes on stone material (Schaffer 1932). It is classified in three main groups as physical, chemical and biological weathering considering the driving forces of rock degradation (Kühnel 2002).

Physical weathering is the physical disintegration of stone components as a result of differential stresses without any alteration in chemical characteristics of stone (Schaffer 1932). The effects of wind and water on the stones cause physical weathering. The wind erosion, condensation, droplets and pores in the stone, capillary, absorption isotherms, rainfall and crust on the physical weathering of stone are determined as the basic factors for physical weathering (Camuffo 1995). The causes of physical weathering is also related with internal stresses and cracking in stone supporting these definition (Scherer 2006). In this respect, the freeze-thaw damage, salt crystallization and swelling of clay minerals in the pores of the stones causes changes internal stresses on the pores of the stones (Scherer 2006). These changes cause changes in pressure on the pores of stones and result with the formation of micro cracks at the inner parts and on the surface of stone (Scherer 2006). The change in thermal expansion of calcite is another factor resulting with crack formations in stone (Scherer 2006). Calcite crystals expand along two directions with the effect of increase in temperature. As a result of heating-cooling and changes in thermal expansion stresses on calcite, micro crack formations occur along grain boundaries resulting with an increase in porosity (Scherer 2006). In addition to this, anisotropic thermal expansion of calcite and dolomite crystals causes the formation of

micro cracks in various marble samples with different texture on different historical buildings (Siegesmund et al. 2000).

The mechanical forces such as natural disasters (earthquake, fire, flood etc.), war, vandalism, and previous conservation interventions are other causes of physical weathering (Press and Siever 2002).

The physical weathering of cracked particles results with the formation of soil grains in and on the surfaces of various rock types (Press and Siever 2002). These soil grains may be moved from the stone's surface by erosion which may be interpreted as material loss. These soil grains may also increase the weathering rate where they are situated (Press and Siever 2002).

Chemical weathering of stone is another critical weathering type developed on historical monuments. It is defined as the decomposition of stone components as a result of chemical processes (Schaffer 1932). The chemical weathering is determined with the chemical reactions of minerals presented in the various rock types with air and water (Press and Siever 2002). Feldspar, amphibole, mica and other silicates are the basic minerals of siliceous rocks. When they are altered in the presence of water, silica is lost and dissolved ions are released. As a result of the hydration of silicates, several clay minerals such as kaolinite, montmorillonite, quartz are left behind. It is observed as dissolution of calcite and release of calcium and bicarbonate ions which are carried away in solution in calcareous stone types (Press and Siever 2002). These processes are accelerated by the solution of natural acids presented in the air as carbonic acid ( $H_2CO_3$ ), which is the most common natural acid present in air, sulphure dioxide ( $SO_2$ ) and nitrogen dioxide ( $NO_2$ ) in water or especially in the polluted humid atmosphere (Press and Siever 2002). Considering this, acid rains are also effective in chemical weathering of stone.

Chemical weathering of stone is observed on calcareous stone materials located in the air polluted atmosphere. Carbon dioxide ( $CO_2$ ), sulphure dioxide ( $SO_2$ ) and nitrogen dioxide ( $NO_2$ ) gases are effective gasses in weathering process of calcareous stones in the polluted atmosphere that traffic or industrial dust is heavily present (Gauri and Bandyopadhyay 1999). These gases dissolve in water and react with calcite minerals by dry deposition and wet deposition on stone surfaces (Gauri and Bandyopadhyay 1999). Sulphure dioxide ( $SO_2$ ) is the main mineral present in the polluted atmosphere. It deposits on stone materials in the presence of water. As a result of a chemical reaction between the acidic material and stone substrate, gypsum is formed (Gauri and Bandyopadhyay 1999).

Chemical weathering is also observed on the stone surfaces that was subjected to conservation treatments for the long term maintenance of the historical buildings. Among them, strong acidic or basic cleaning materials as acetone and protective materials such as oil, wax, egg protein and milk are effective in the chemical weathering of stone surfaces (Siegesmund et al. 2002). The protective materials applied on limestone façades are also effective on the chemical weathering. It was proved in a case study of Palacio de Nuvo Baztan in Madrid (Buergo and Gonzalez 2003). According to the results of this study, these materials caused color changes on limestone surfaces with the chemical reaction of original material and the applied coating consisting of a mixture of lime, gypsum, milk-derived compounds as a proof of destructive effects of protective materials on limestone surfaces (Buergo and Gonzalez 2003).

The dissolution of CO<sub>2</sub> also affects iron silicates in stones chemically. As a result of their reaction in the presence of oxygen in the air, leachable iron oxides are formed and transformed in the fissures of stones (Press and Siever 2002).

Biological weathering is erosion, decay and decomposition of rock minerals by living organisms such as fungi, lichen, algae, bacteria and higher biological formations (Gadd 2007). These biological formations are investigated in two groups: macroorganisms and microorganisms (Urzi and De Leo 2001). Urzi and De Leo investigate the effects, factors, remedial techniques, color changes and weathering mechanisms of them on the historical monuments located in Italy.

Macroorganisms are birds, plant, mosses and lichens (Urzi and De Leo 2001). Birds cause deposition of guano on stone surfaces. Guano provides good medium for chemoorganotrophic bacteria growth causing corrosive effect by releasing acidic matter on stones. Plants cause mechanical force on stones and chemical reactions on stone by its growing roots. They also cause shadowing and slow down water evaporation on the stone surfaces providing good medium for physical and chemical weathering. Mosses and lichens produce acid metabolites resulting with chemical reactions with the stone material. The growths of lichen thalli cause pressure and crack formation in stone (Urzi and De Leo 2001). The lichen colonization cause physical and chemical effects on different stone types such as sandstone, basalt, granitic rock and calcareous rocks (Chen et al. 2000). The physical effects of lichens are penetration of hypae, expansion and contraction of thallus, freezing and thawing of thallus, swelling action of organic and inorganic salts formed as a result of chemical reactions formed by lichens, incorporation of mineral fragments into thallus (Chen et al. 2000). The chemical effects of lichens are

the effect of respiratory CO<sub>2</sub>, oxalic acid that lichens produce, and organic compounds abundant in lichens (Chen et al. 2000).

Microorganisms are listed as cyanobacteria, algae, diatoms, chemoorganotrophic bacteria and fungi (Urzi and De Leo 2001). They cause bio-corrosion, bio-erosion with the release of organic acids and mineral elements and microstructural destruction during their physical growing (Lian et al. 2008). The microorganisms are studied in a more comprehensive way in a research paper considering the destructive effects of each microorganism separately (Urzi and De Leo 2001). According to the results of this study, cyanobacteria are generally present together with algae and diatoms. They form biofilms and crust on stone surfaces. They cause physical and chemical weathering of stone by producing organic acids and sugar derived carbonic acids (Urzi and De Leo 2001). The colonization of cyanobacteria on a wide variety of substrata is related to physical characteristics of stone surface and nature of the substratum (Macedo et al. 2009). The aesthetic, biochemical and biophysical damage of cyanobacteria were studied on 45 case study monuments built with different stone types in Mediterranean region in a review paper (Macedo et al. 2009). In this study, the bacteria colonizing on each of the stone types were investigated and classified on marble (%30), limestone (%32) and travertine (%7) monuments. The results of this study show that the presence and destructive effects of cyanobacteria are widely observed on the stones that have more porous microstructure and surface roughness (Macedo et al. 2009). Considering all the destructive effects of them, they should be identified precisely and removed from stone surfaces for the long term stability of the monuments (Crispim and Gaylarde 2004).

Chemoorganotrophic bacteria are other type of microorganism live on stone surfaces. They cause to bound clay and crystal particles in the pores of stones, release acid metabolic products by solubilizing CaCO<sub>3</sub>, oxidize metallic compounds and cause color changes by precipitation of Fe and Mn (Urzi and De Leo 2001). Fungi are the latest microorganisms live on stone surfaces. They are determines as the most harmful agents in biological weathering of stone, especially for black fungi formations. They form crater shaped lesions, chipping and exfoliation of rock surfaces causing material losses on the stones (Urzi and De Leo 2001). At this point of view, the mechanical and chemical destructive forces they cause and bioremediation techniques on them are essential for the patina formation on different materials including building stones (Gadd 2007).

The results of all these destructive agents and physical, chemical and biological weathering mechanisms are observed on the surfaces of stone monuments. They manifest

themselves as material loss, dirty and ruined surfaces and changes in original color of stone surfaces with an unacceptable appearance (Prieto et al. 2007). This aesthetic degradation which is known as *patina* has caused to draw many of the conservation scientists' attention to weathering of stone surfaces.

*Patina* (a colored coating) is mentioned as the oldest terminology used for transformations on the stone surfaces in the research of Garcia-Valles et al. (Garcia-Valles et al. 1997). It is the formations above, at and below the rock surface by biological, physical and chemical weathering processes on the climate exposed materials (Garcia-Valles et al. 1997). The results of patina formation are mentioned as structural, textural or material change in their research about the characterization, colors and formation types of microbiological formations on limestone in a case of a cathedral building in Catalonia (Garcia-Valles et al. 1997). According to the results of this study, it was observed as color changes, crust or incrustations on exposed stone surfaces (Garcia-Valles et al. 1997).

Patina may be observed as green, gray to black, reddish/brown, orange and yellow in color. In this study, yellow patina formation, which occurs on the majority of calcareous stones in Mediterranean archaeological sites, is investigated for the purpose of conservation. The results of this study remained information about the material characteristics of yellow patina on marble and yellow travertine surfaces. It also sheds light to determine the characterization techniques and to constitute a conservation approach for yellow patina formation on stone monuments in the archaeological sites.

## **1.1. Problem Definition**

Patina is formed due to the effects of physical, chemical and biological action on stone surfaces in archaeological sites as a result of aging. Patina formations cause alteration of the aesthetic appearance of stones and monuments. However, it represents the antiquity of the monument and may have a protective function on stone surface against weathering.

Patina formation may be observed as green, gray to black or yellow to brown in color. Among them, yellow patina (which is also called *scialbatura*, *Mediterranean patina*) is easily distinguished on white colored marble and limestone surfaces. The hues of yellow patina may range from beige to brown in color. However, it may not be observed by naked eye due to the original color of yellow travertine in the archaeological

sites although it has similar mineralogical and chemical composition with marble. Hence, one of the emphasis is mostly placed on yellow patina formations on marble and limestone monuments in the previous studies, yet travertine surfaces have not been studied. From this point of view, the conservation or cleaning decision of patina becomes critical to constitute an accurate treatment technique on marble and yellow travertine surfaces for the theoreticians and practitioners studying in cultural heritage field.

This study investigates the yellow patina formation observed on the stone monuments of archaeological sites to propose a conservation approach on marble and yellow travertine surfaces.

## **1.2. Aim and Scope**

The aim of this study was to determine the mineralogical composition, microstructural and chemical characteristics of patina formation on calcareous stones focusing on the comparison of yellow travertine and white marble samples from selected case study areas in the Aegean region of Turkey for proposing a conservation approach on marble and travertine surfaces in the archaeological sites.

The results of this study reveal qualitative and semi-quantitative information and thickness of yellow patina on the surfaces of stone monuments before constituting intervention decisions in the conservation studies. The results also show the importance of the use LIBS in conservation of patina which provides a detailed information about the thickness of it. This study also sheds light to compare and evaluate the characteristics of yellow patina on white marble and yellow travertine in the archaeological sites considering the similarities and differences of their material characteristics.

For this purpose, the case study areas were selected as Aizanoi, Aphrodisias and Sardes for sampling of marble. Hierapolis was selected for sampling of yellow travertine.

## **1.3. Case Study Archaeological Sites**

The yellow patina formation on marble and limestone surfaces is observed on many of the archaeological sites at the western part of Turkey. Among them, four representative archaeological sites located in the Aegean Region of Turkey at the western

part of Anatolia were investigated for case study as Aizanoi, Aphrodisias, Sardes and Hierapolis in Turkey (Figure 1.1).

The case study archaeological sites are the important settlements of Roman period showing the common use of marble and travertine as construction materials in the whole settlements. White marble is widely used in Aizanoi, Aphrodisias and Sardes. Thus, they were selected as the case study areas for white marble samples. Travertine is a common building material in many of the archaeological sites in the same region. However, yellow travertine is remarkably used in Hierapolis due to presence of yellow travertine quarries around the site. Thus, it was selected as a case study area for yellow travertine samples. Yellow patina is widely observed on almost all of the monuments in these sites matching the aim of this research.

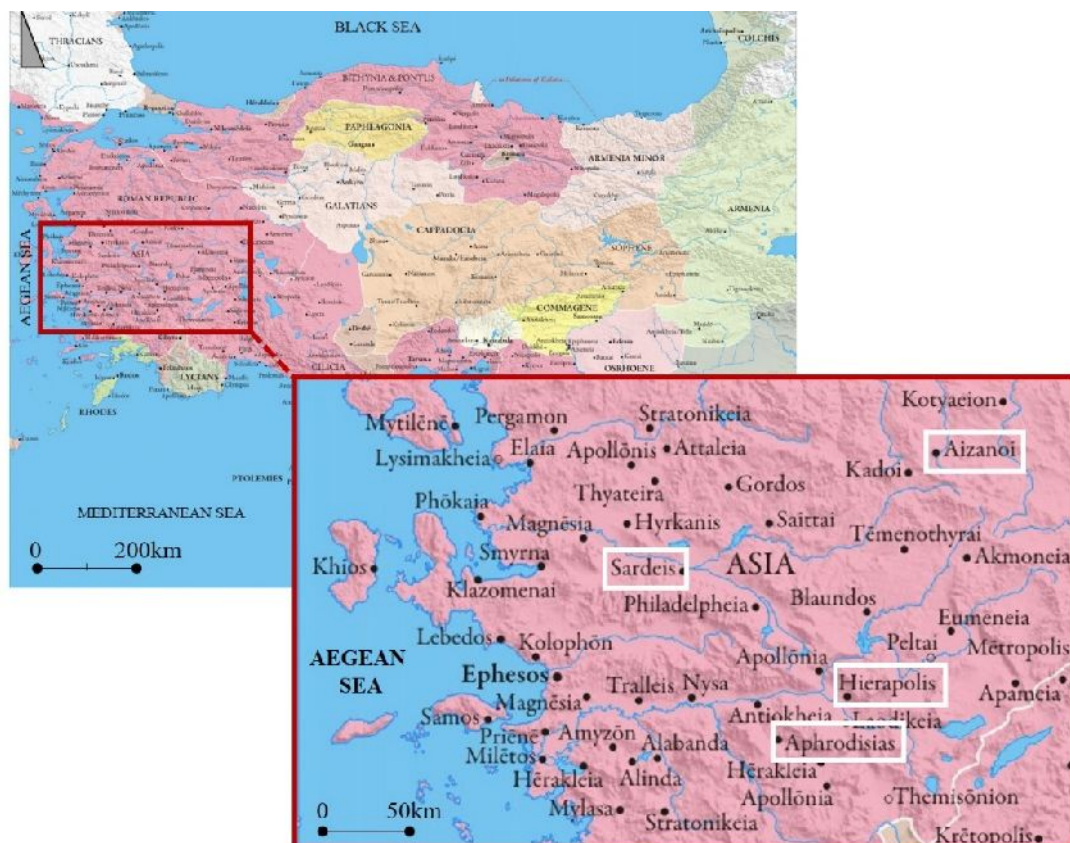


Figure 1.1. The locations of case study archaeological sites on the historical map of Anatolia (showing the provinces of Asia Minor in 63bc) (Source: <http://www.thehistoryblog.com/wp-content/uploads/2012/09/Anatolia-63bc.jpg>)

### 1.3.1. Aizanoi

Aizanoi archaeological site is located in Kütahya in Turkey. The name of the city came from the word “eksouanous” which means hent and fox. These animals were thought to be sacrificed for this city. The city was an ancient Phrygian city according to the writings of ancient historian Strabon (Çakır 2010). In Hellenistic time, the city was under the hegemony of Pergamon with 216 BC and Bithynia with 189 BC. Finally the city was ruled by Pergamon again after 188 BC (Çakır 2010). Aizanoi was under the control of Romans in 133 BC. The city was an important commercial network for Asia Minor (UNESCO 2017). In addition to this, it was used as diocese during Byzantine period.

Most of the monuments had been built in Roman period. Zeus Temple, stadium and theatre complex, macellum are important monuments that are present today. The temple is one of the best preserved Zeus Temples around the world with all its architectural characteristics, masonry walls, columns and beams (Figure 1.2). In addition to this, the city is known to be the first and only stadium and theatre complex in ancient times (Figure 1.3) (UNESCO 2017).

The city was selected as a case study for this research because marble was the main material used in the construction of these monuments in Aizanoi. The stones used in the buildings were quarried from Afyonkarahisar in Turkey (Niewöhner 2013).



Figure 1.2. Zeus Temple in Aizanoi  
(If there is no citation, the photograph belongs to the author for the rest of the thesis)



Figure 1.3. Theatre and stadium complex in Aizanoi

### 1.3.2. Aphrodisias

Dating back to 5000 BC, Aphrodisias is one of the 17 sites in UNESCO World Heritage List located in Geyre, Aydn at the southwest of Turkey (UNESCO 2017). The name of the city comes from the goddess of love and beauty, Aphrodite of Aphrodisias which was also known as Cybele of Phrygians (Zimi 2006).

The city was used as a religious center during 1<sup>st</sup> and 2<sup>nd</sup> centuries BC following the supports of Roman Empire beginning with 82 BC. It became the capital of Roman province of Caria in the 4<sup>th</sup> century AD. The settlement was under the hegemony of Seljuk during 11st-12nd centuries (Zimi 2006).

Aphrodisias was also known as the school of sculptress between the centuries 1<sup>st</sup> BC and 5<sup>th</sup> BC because of the marble rich quarries of the surrounding site (Atalay 2014). It was observed from the statues and buildings in the settlement. Marble was a vital source of local life for the settlement in the Roman period. However, it did not play an important role for the export of this abundant natural resource. The regional quarries were used for local needs and business of civic beautification of the settlement (Long 2012). This site can be evaluated as a representative area for the common use of marble in statues and in the building construction in the Mediterranean region. Temple of Aphrodite, monumental gateway Tetrastylon, theatre, Bouleuterion, stadium are some of the important monuments that represent architectural characteristics of the site (Figure 1.4, Figure 1.5).



Figure 1.4. Tetrapylon gate in Aphrodisias



Figure 1.5. The ruins of scene in theatre building in Aphrodisias

### 1.3.3. Sardes

Sardes is located in Manisa, Turkey. It was an important ancient city and the capital of Lydia around 612 BC. The city was reigned by Persians, Medes, Chaldeans and Babylons between 680 and 547 BC. After Babylons became the dominant power, Sardes was made capital where the king of Lydia lived (Hanfmann and Ramage 1978).

Sardes was under the control of Persians between 547 and 334 BC. After Alexander the Great conquered Sardes, it became a Hellenistic Greek. The Roman hegemony began after 133 BC. Tacitus mentions an earthquake during Roman period that effected the city in 13 AD. After 616 AD, the civil life in the city ended (Hanfmann and Ramage 1978). The settlement was center of trade, traffic of goods and ideas between Mesopotamia and Greek Ionian settlements. Sardes had a close relation with Ephesus in the previous times as being the center of trade, traffic of goods. It is observed from the marbles which was transported from Ephesus during the construction of Tomb of Alyattes who was the fourth king of Lydia probably by using water canals between the settlements (Tykot and Ramage 2002).

Sardes was selected as another case study area showing the common use of marble in the building construction (Figure 1.6). It was related with the marble quarries of Sardes which were located in the close-by surrounding of the settlement at three main points (Hanfmann and Ramage 1978).



Figure 1.6. The temple in Sardes  
(Source: [www.openbible.info/geo/photos/Sardes](http://www.openbible.info/geo/photos/Sardes))

#### **1.3.4. Hierapolis**

Hierapolis archaeological site is located on the travertine terraces of Pamukkale which is 18 km away from Denizli, Turkey. Hierapolis is one of 17 sites in UNESCO

World Heritage List in Turkey with its historical, architectural and environmental characteristics (UNESCO 2017).

The settlement was founded by the Pergamon king Eumenes II. He gave the name of the settlement 'Hierapolis' from the name 'Hiera' who was the wife of Telephos, the founder of Pergamon. The settlement dated back to 3000 BC. However it lost its Hellenistic characteristics after the earthquake in 60 AD. The ruins were buried in the petrified calcareous layer for centuries following with a general survey in 1887 by an excavation team (Toksöz 1996). Thus, the architectural characteristics of Roman and early Christian period are more commonly observed in the city according to the Hellenistic period.

The city was used as the capital of Phrygia. In Byzantine period, it became the center of diocese. After 4<sup>th</sup> century, it was the center of Christianity. This area was selected as a case study area because of the common use of yellow travertine in the construction of archaeological monuments related with the presence of yellow travertine quarries around the site (Figure 1.7, Figure 1.8, Figure 1.9). The Temple of Apollo, theatre, thermal baths, agora, necropolis and gymnasium are only some of the important travertine monuments that represent the architectural characteristics of Roman and early Christian period in the site (Toksöz 1996).



Figure 1.7. A tomb in Hierapolis necropolis



Figure 1.8. A tomb in Hierapolis necropolis



Figure 1.9. The bath building in Hierapolis

## 1.4. Characteristics of Marble and Travertine Used in Case Study Areas

Marble and travertine were widely used in the archaeological sites in the ancient times. They are formed by consolidation, replacement or metamorphism of carbonate sediments in the limestone (Press and Siever 2002).

Marble is a metamorphic limestone which is formed as a result of elevated pressure and temperature by deep burial conditions (Gauri and Bandyopadhyay 1999). There are two types of marble on earth: marble and dolomite. Marble is formed by the recrystallization of calcium rich limestone during metamorphism. Dolomite is formed by the recrystallization of magnesium rich limestone (dolomite). In general, marble is nearly a non-porous compact material with coarse interlocking grains of calcite or dolomite crystals (Plummer et al. 2010).

Travertine is a sedimentary limestone which is formed from eroded mineral grains, minerals precipitated from low-temperature solutions in the spring and stream waters or consolidation of the organic remains of the plants (Plummer et al. 2010). It has a crystalline texture. It is more porous compared to marble (Plummer et al. 2010).

Marble and travertine both contain more than %90 calcite minerals ( $\text{CaCO}_3$ ) (Gauri and Bandyopadhyay 1999). Calcite is the second rock material that exists on earth after silicate (Monroe and Wicander 2005). It made calcareous stones one of the most common building materials for centuries. However, it is also one of the least stable minerals against weathering in nature (Press and Siever 2002). Calcareous stones are suitable for bacterial growth with their dense calcareous matrix (Warscheid and Braams 2000). Calcareous stones are the most suitable stone types for bacterial growth according to their bioreceptibility with respect to the biogenic metabolic products and stable pH values of them with dense calcareous matrix (Warscheid and Braams 2000). Nevertheless, marble and travertine are always subject to biological attacks.

Marble and travertine are commonly observed as a building material in the archaeological sites. The mineralogical, chemical composition and microstructural characteristics are important factors to evaluate the weathering of these stones. Thus, the stones used in the archaeological sites should be investigated considering the mineralogical, chemical composition and microstructural characteristics of the studied site.

The stones used in the buildings of Aizanoi was Dokimeian marble which was quarried from the famous marble quarries in an ancient city of Phrygia in Asia Minor,

which is now known as Afyonkarahisar province of modern Turkey (Niewöhner 2013). White Dokimeian marble was a high quality stone masonry exported to the regions as central Rome and Mediterranean. This material was used in column shafts and wall revetment (Niewöhner 2013).

Aphrodisias was the center of marble quarries in the western part of Asia Minor for a long time in the past (Long 2012). The marbles used in Aphrodisias were white to tinted rose, green, purple and yellow in general (Long 2012). However, Aphrodisians preferred to use white marbles in their buildings considering the shining effect of white (Long 2012). The colored marbles were used rarely according to white marbles. The light greyish marbles were from western quarries (Conforto et al. 1975). The stones which come from the western quarries were white in color representing similar appearance with the ones studied in the scope of this study (Conforto et al. 1975).

The marble quarries of Sardes were located in the close-by surrounding of the settlement at three main points (Hanfmann and Ramage 1978). They were white with coarse-grained crystals and generally homogeneous structure (Hanfmann and Ramage 1978). However, some buildings were built using marbles which were transported from other settlements away from the local quarries (Tykot and Ramage 2002). The marbles of a tomb chamber of Alyattes was imported from Ephesus although it was 100 tons in weight (Tykot and Ramage 2002).

Travertine was commonly used in Hierapolis because it was located on the travertine terraces of Pamukkale region (Toksöz 1996).

Patina formation is observed on both marble and yellow travertine surfaces used in the archaeological sites. Thus, it should be investigated on all of the marble and travertine surfaces that were used as building materials in the archaeological sites as it was in case study areas.

## **1.5. Formation of Patina Types on Stone Surfaces in the Archaeological Sites**

Patina is a colored coating, a structural, textural and/or material change in the zone near the surface of a climate exposed rock specimen, especially on historical building materials. It has been discussed among the historians and practitioners since 1970s. The term "*patina*" was first observed in 1681 in Flippo Baldunicii's Art Dictionary via definition of "*a term used by painters, called by others a skin, a general dark tone which*

*time causes to appear on paintings”* (Weil 1977). It was latterly related with material weathering in French Encyclopedie in 1751. According to it, the origin of the “*patina*” term came from the Italian word “*patena*”, which means a shiny dark varnish applied to shoe; and latterly was used for the green formations on bronze surfaces that form by the time (Figure 1.10). Patina formation was redefined in Webster’s New World Dictionary published in 1970 under two items: a fine crust or film layer on bronze materials formed as a result of oxidation processes; and a thin coating or color change occurred as a result of aging (effect of the time passing by) (Weil 1977).



Figure 1.10. Patina on bronze Equestrian Sculpture of Marcus Aurelius, Capitoline Museums, Rome (Source: <https://www.khanacademy.org/>)

Patina formation was also defined by several researchers who specialize in the stone conservation field, too. The basic definition of it is “*the natural change of stone surfaces*” (Jokilehto 2002). This description was mentioned in a general definition of patina in stone conservation field a comprehensive book about the development of the concepts and conservation approach of cultural heritage from Antiquity and the Renaissance to the present day within the European context written by Jukka Jokilehto who has been a member of numerous advisory missions on behalf of UNESCO, ICCROM and ICOMOS (Jokilehto 2002).

Patina was defined as films, coatings, external deposits, external and internal crust formed as a result of physical, chemical and aesthetical changes of stone surfaces in a study about the characterization of colored mineral coatings on stone surfaces (Garcia-Valles et al. 1997). Supporting that, it was mentioned as the alterations that rock surfaces undergo as a result of interaction with the environment in a paper focusing on dark patinas formed on granitic outcrops and buildings (Prieto et al. 2007). In this study, Prieto et al. pointed out that patina is manifested as color changes on building exteriors supporting the previous descriptions made before.

Chemical and mineralogical composition, microstructural characteristics and surface roughness of stone, climatic condition of the site, the materials that are neighboring the stone metal oxides in mortars, metal joints etc., bio-receptivity of stone and microbiological diversity that live on it, anthropogenic factors as air pollution or man-made treatments on stone surfaces are critical factors that are affective in the formation, material characteristics and appearance of patina types observed on stone surfaces.

Patina may occur by directly transforming material itself (crust); and by depositing external material components onto the object surface (surface deposit) (Rodrigues 2006). These changes may be observed as green, gray to black, brown to yellow, orange or reddish in color. The color of patina layer may change according to the effects of global climatic shifts produced in the time period that the monument is exposed (Urzi et al. 1992). This mechanism is observed on the color change of a patina layer from orange to brown in 19<sup>th</sup> century to black or blackish in 20<sup>th</sup> century on the same monument (Urzi et al. 1992). After 1945, fungi formation causes the loss of coatings on the same areas that color changes had formed (Urzi et al. 1992).

These discolorations may also change according to the characteristics of patina. There may be changes in the hue of the patina formation on different surfaces of the same monument (Figure 1.11, Figure 1.12). The material characteristics such as crystal size,

texture, mineralogy and color of different patina layers are related with rock substrate, climate and other environmental factors (Vendrell-Saz et al. 1996). The different hues and colors of patina layers on 5 different case study buildings were compared in a research study (Vendrell-Saz et al. 1996). The results show that the darkness of the patina is mostly related to the surface condition if it is located in an open or sheltered area, the reaction of surface against UV light, the solubility of patina layer in water. Different hues of same color are mostly related to the same patina type in the same monument surface in common (Vendrell-Saz et al. 1996).

The chromatic changes from white to hues of yellow may be related with precipitation type on stones (Pinna et al. 2015). It is observed in two forms: film formation on the surfaces and precipitation in the deeper parts of stones (Pinna et al. 2015). The color gets darker when the thickness increases. So, the density of the in-depth precipitation is essential (Pinna et al. 2015). Pinna et al. state that chromatic changes do not occur in an indoor environment. Thus, the UV light should be effective on discoloration of patina layer on stone surfaces.

Besides the changes in the hue of patina layer, the color of the patina may also change according to the different causes of its formation. First of all, stone surface provides optimum conditions for the occurrence of biological growth with its porous surface morphology (Urzi and De Leo 2001). Thus, the color changes may be because of the pigmentations of the biogenic origins with various colors of biological formations and bacteria that live in the pores and on the surface of the stone considering bioreceptivity of the stone type, either (Warscheid and Braams 2000). Second, the color of the stone may also be related with weathering mechanisms that patina formation arises from (Grimmer 1988).

In this part of the study, the patina types are explained considering the color changes they cause on stone surfaces. Because of the limits of the study, yellow patina formation will be explained more comprehensively than the others.

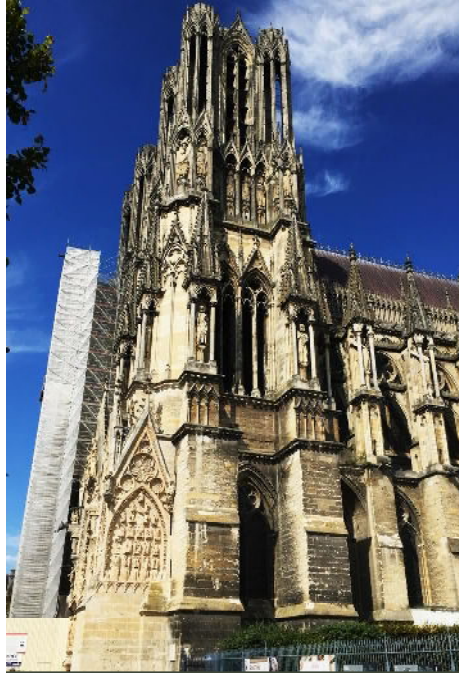


Figure 1.11. Patina formations on the stone facade of Reims Cathedral, France



Figure 1.12. Patina formations on the facade of Academie Nationale De Musique, Paris and the surfaces of marble statue standing in front of it

### **1.5.1. The Formation of Green Patina**

The green patina (film formation) on stone surfaces may be related with the presence of copper materials around the stone and biofilm formation on stone surfaces.

The copper materials neighboring the stone oxidize in the presence of water (Weil 1977). It may cause the mobilization of metal including minerals to the adjacent stones and the formation of green patina on their surfaces (Weil 1977).

The green patina is also formed as a results of green biofilm formation by settling of biological forms as lichens, mosses and algae in the pores and on the surface of the stone (Figure 1.13). Staining due to pigments present in algal cells is the most common cause of greening especially in cool and humid climates (Cutler et al. 2013). The algal biofilms have destructive effects and negative impacts on the long term stability of the stone materials which is explained in a research study by Cutler et al. discussing it on a monument surface with all its aesthetic and structural damages (Cutler et al. 2013).



Figure 1.13. Green patina formation on sculpture, Italy  
(Source: Fitzner and Heinrichs 2002)

### **1.5.2. The Formation of Gray/Black Patina**

The gray / black patina is formed by the effect of air pollution, biological attack and chemical use in the cleaning of stone surfaces.

Air pollution is related with the chemical weathering of calcareous stone materials with the effect of carbon dioxide (CO<sub>2</sub>), sulphure dioxide (SO<sub>2</sub>) and nitrogen dioxide (NO<sub>2</sub>) gases in the atmosphere (Figure 1.14) (Schaffer 1932). These are effective gases in the polluted air causing wet or dry deposition on calcareous stones (Gauri and Bandyopadhyay 1999). Dry deposition is effective on the black colored patina formation on calcareous stone surfaces. It is mostly observed grey to black or brown in color. It occurs by the accumulation of airborne pollutants such as tiny liquid droplets and solid particles suspended in the air with the winds and turbulence. As a result of the reaction between carbonate rocks and SO<sub>2</sub>, NO<sub>2</sub> and acid aerosols, gypsum (CaSO<sub>4</sub>.2H<sub>2</sub>O) is formed on the surface and in the fissures of stones. The presence of soot, dust and metallic particles assess the color of the gypsum layer although it is white in original (Gauri and Bandyopadhyay 1999).

The origin of grey to black patina may also be the pigmentation of black fungi microorganisms as fungi, cyanobacteria, green algae which contain dark pigments are also other agents of black patina (Macedo et al. 2009) (Figure 1.15). Among them, black fungi have the capacity to settle down on the stone surface and penetrate into the stone structure. They cause physical and chemical damages during their growth (Diakumaku et al. 1995). Diakumaku et al. mentioned that black fungi cause aesthetic damage when they spread over the stone surfaces including various melanin pigments that may also be observed as black in color (Diakumaku et al. 1995). The presence of black fungi formation was documented on almost all the stone monuments located in the Mediterranean Basin in a research study about the effects, isolation and identification of it on marble surfaces (Krumbein et al. 1995).

The use of lichen secondary metabolites against rock dwelling microbiological living organisms may cause black patina formations. Gazzano et al. prove this with a research article by revitalizing the effects of experimental groups of lichen secondary metabolites produced in the laboratory conditions on stone surfaces (Gazzano et al. 2013). The results of their study show that the use of biocides that lichens produce may also cause blackening on stone surfaces in the long term. The use of commercial biocides is also another method to clean these living forms such as black fungi, lichens and algae. However, black patina prevails again with different characteristic by the discoloration of these commercial pesticides left behind instead (Scheerer 2009).



Figure 1.14. Black patina formation related with air pollution on the statue at Town Hall, Germany (Source: Fitzner and Heinrichs 2002)



(a)

Figure 1.15. Black patina formation related with microorganisms on towers (a) and walls (b) of Angkor Wat, Cambodia (Source: Personal archive of N. Murtezaoglu)

**(cont. on next page)**



Figure 1.15. (cont.)

### 1.5.3. The Formation of Yellow/Brown Patina

The yellow patina formation is easily distinguished by naked eye on limestone surfaces with different hues from beige, yellow, and orange to brown in color (Figure 1.16). The yellow/brown patina is related with calcium oxalate precipitation on stone surfaces, iron containing minerals in the stone, metal compounds adjacent to stone, laser cleaning of stone surfaces or air pollution in the site. Among all, it is mostly related with calcium oxalate precipitation on calcareous stones (Adamo and Violante 2000).

The yellow patina, which is formed as a result of calcium oxalate precipitation, was observed on various building and monument types dating to different time periods beginning from 5<sup>th</sup> century BC to present in Italy, Spain, Athens, Australia, Turkey etc. according to the results of experimental studies focusing on yellow patina on marble or limestone surfaces (Watchman 1991, Fassina 1995, Garcia-Valles et al. 1997, Garcia-Valles et al. 2000, Zagari et.al. 2000, Bario et al. 2002, Buergo and Gonzalez 2003, Polikreti and Maniatis 2003, Rampazzi et al. 2004, Kalaitzaki 2005, Rodriguez et.al. 2011, Pinna et al. 2015). Their mineralogical composition represent similar characteristics including calcium oxalate in the form of whewellite or weddelite together with one or many of the minerals as quartz, brushite, kaolinite, hydroxyapatite, hematite,

potassium, feldspar, clays, dolomite, smectite, halite, fluorite etc. The thickness of this layer varies between 60 and 500  $\mu\text{m}$  which is determined by SEM - EDX or optic microscope analyses in some of these studies (Fassina 1995, Garcia - Valles et al. 1997, Garcia - Valles et al. 2000, Bario et al. 2002, Buergo Gonzales 2003, Rampazzi et al. 2004, Kalaitzaki 2005). These layers are composed of major amounts of CaO (50-60%), mostly with moderate amounts of  $\text{Al}_2\text{O}_3$  and  $\text{SiO}_2$  (2-29%) and minor amounts of MgO,  $\text{SO}_3$ , FeO (0-5%) (Lazzarini and Salvadori 1989, Fassina 1995, Garcia-Valles et al. 1997, Polikreti and Maniatis 2003, Kalaitzaki 2005). It is explained with two major causes as organic (biological) and anthropogenic (chemical) origin.

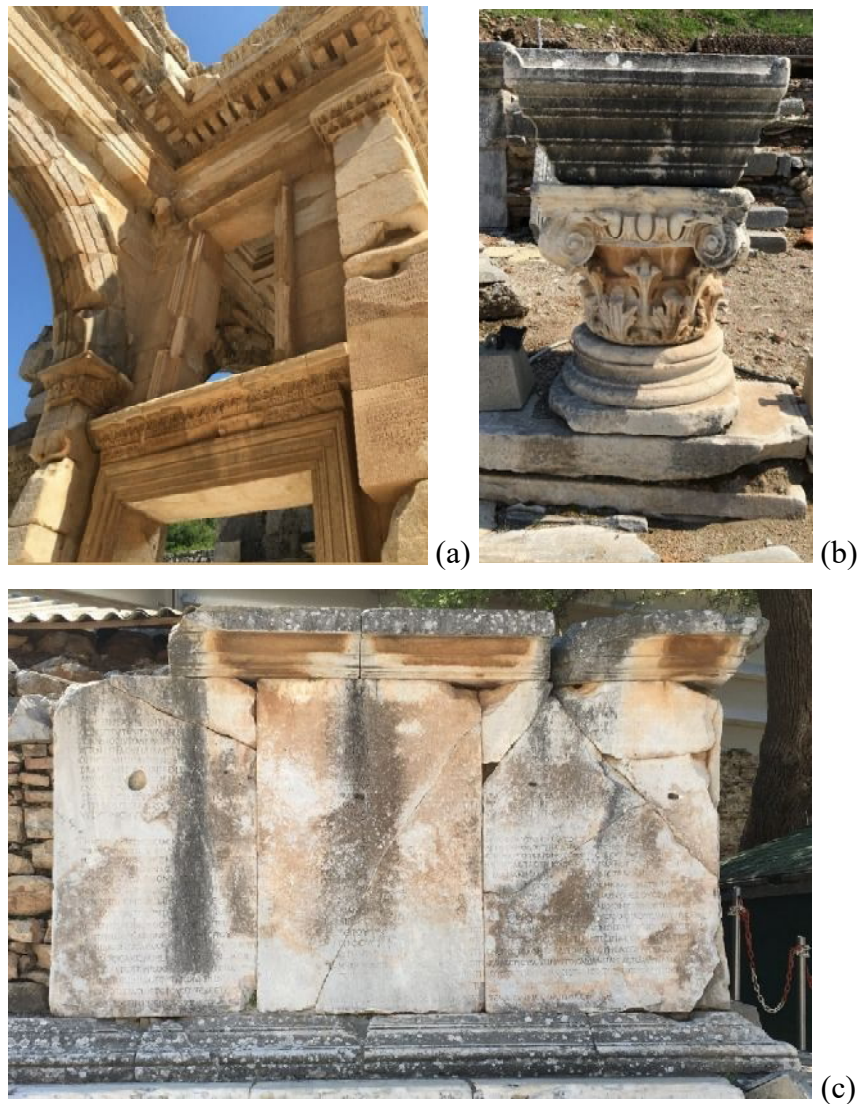
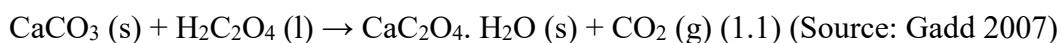


Figure 1.16. Yellow patina formation on the marble ruins as building stones (a), columns capital (b) and historical writings (c) in Ephesus, Turkey

The naturally formed calcium oxalate precipitation is related with biological formations settled on the surfaces and in the pores of limestone (Del Monte and Sabbioni 1987). This surface change is named as *Scialbatura* by Del Monte and Sabbioni who were the first focusing on the origin of yellow patina on marble surfaces of various monuments, artifacts and natural outcrops in all around Italy in 1987 (Del Monte and Sabbioni 1987). According to the results of their study, the basic reason of yellow calcium oxalate precipitation is the biological weathering formed by lichen produced oxalic acids on marble surfaces (Del Monte and Sabbioni 1987). In this process, oxalic acid reacts with calcium carbonate, which is the major mineral of limestone. As a result of this reaction, calcium oxalate occurs on stone surfaces (1.1).



Various studies agree with Del Monte and Sabbioni about the biological origin of oxalate rich yellow patina formation on limestone surfaces. Caner and Böke support this theory with an experimental study about the occurrence of calcium oxalates on the marble surfaces of Temple of Augustus in Ankara, Turkey (Caner and Böke 1989). They claim that the oxalate formation may be contributed by the presence of lichens on marble surfaces. Also, Chen et al. describes the lichen produced oxalate precipitation in their review paper about the physical and chemical effects of lichens on weathering of stones as the previous researchers did (Chen et al. 2000). In addition to this, chemoorganotrophic bacteria produce organic acids that may also cause oxalate formation on calcareous rocks (Urzi and De Leo 2001). The formation and effects of biological formations on stones are classified in six groups as photoautotrophs as cyanobacteria, lichen, algae, mosses and liverworts; chemoautotrophs as sulfur-oxidizing, nitrifying bacteria; chemoheterotrophs as heterotrophic bacteria, actinomycetes, fungi; chemoorganotrophs as sulfur-reducing bacteria; higher plants and other formations (Dakal and Cameotra 2012). Among them, some of the lichen, fungi and bacteria (cyanobacteria) formations produce oxalic acid on the stone surfaces (Dakal and Cameotra 2012). The biological origin of oxalate film formation on stone surfaces is also proved with an experimental study which was held only in laboratory conditions (Monte 2003). Differing from the previous studies, Monte achieves the production of oxalate film by fungal enzymatic reactivity on marble specimens. The results of this study show that the oxalate formations are related with fungal metabolisms whether they occur from lichenic origin or not (Monte 2003).

Oxalate formation may form on siliceous rock surfaces, also. It is proved in an experimental study which was held in Northern Territory, Australia (Watchman 1991). In this study, the formation of oxalate film was explained by the chemical reactions of biologically derived organic acids on calcium-rich dust particles, which present on weathered pre-historic paintings on siliceous rock surfaces. The study also suggests preserving oxalate layers to be latter used for carbon-14 dating to establish the time-frames of different pre-historic paintings in rock art studies (Watchman 1991).

Calcium oxalate is not formed only on the surfaces of stones. It is also observed in the fissures and pores of them. It is observed on natural outcrops and stone monuments in Touraine, France (Zagari et al. 2000). In this case, yellow patina is strongly associated with calcium oxalate formation that lichen formations cause on stone surfaces. Hence algae are effective in the production of calcium oxalate precipitation at the inner parts of the stones that are away from direct sunlight (Zagari et al. 2000). It shows that having direct sunlight is an effective factor not for algae but for lichen produced calcium oxalate precipitation on stone surfaces.

The artificially formed calcium oxalate patina is related with the previously applied treatments on stone surfaces for conservation purposes (Lazzarini and Salvadori 1989). Lazzarini and Salvadori made the first research showing the effects of previous conservation treatments on marble strongly opposing the biological origin theory that Del Monte and Sabbioni suggested in the same years (Lazzarini and Salvadori 1989). In this research, yellow patina is described as a homogeneous and well spread layer. The traces of brushstrokes are observed on stones because of previously applied man-made treatments using wax and resin (Lazzarini and Salvadori 1989). The presence of protective patina materials includes paraffin wax, lipids of animal origin and egg. The organic materials cause degradative oxidation and oxalic acid formation on calcium compounds which results with calcium oxalate precipitation on stone surfaces (Rampazzi et al. 2004).

Apart from the previously applied protective patinas, the latter formed calcium oxalate layer itself shows protective characteristics, too. Compared to carbonate, oxalate is a more resistant material against physical weathering caused by temperature changes and water (Böke and Gauri 2003). The production of oxalic acid and other organic acids, and their production by bacterial communities isolated from limestone monuments in the laboratory are experienced in a research study proving the protective effects of patina formations on stone surfaces (Di Bonaventura et al. 1999). The results of the observations

and laboratory experiments of this research prove that calcium oxalate, which is an insoluble calcium salt, represents a protective layer which is less soluble in water and more resistant to weathering formed by water or wind according to the original calcareous stone materials (Di Bonaventura et al. 1999). So, the protection of calcium oxalate layer means the protection of original stone material for the long-term stability of the historical building materials.

The calcium oxalate patina may occur in two forms in nature as whewellite (mono- hydrated calcium oxalate) and weddelite (di- hydrated calcium oxalate). They have different microstructural characteristics. Thus, their morphology may help to distinguish these two oxalate types observed on stone surfaces. Whewellite has a plate shaped morphology while weddelite exhibits a bipryramidal form in microstructure (Chen et al. 2000). Weddelite dehydrates to whewellite in nature and whewellite is more vulnerable to water. Thus, calcium oxalate is formed mostly in the form of whewellite on the surfaces of calcareous stones.

Calcium oxalate, which is observed in the form of weddelite and whewellite, is colorless to bright yellow in original (Garcia-Valles et al. 1997). However, this patina is observed yellow to brown in color on the stone surfaces in the outdoor environments. At this point of view, the yellowing of colorless calcium oxalate patina is related with precipitation of leachable iron elements and clay minerals on the stone surfaces (Press and Siever 2002, Polikreti and Maniatis 2003).

The yellow to brown color changes may be observed on the whole stone surfaces that are exposed to climatic conditions of the site they are located irrelevant from calcium oxalate formation. Hence, yellow color is observed on phosphatic layer on marble surfaces of Propylea case in Acropolis, Athens (Polikreti and Maniatis 2003). The phosphatic layer that was applied for protective purposes are also white in original. In this case, the yellow color of the patina comes from the iron products precipitated in the phosphatic layer as it is observed in calcium oxalate patinas, too. Yellow to reddish hues are related with clay minerals precipitated in the same layer carried from the environment (Polikreti and Maniatis 2003).

The yellowing of stone surfaces may also originate from the metal compounds presented in the stone composition (Oguchi 2001). The iron minerals present in the stone are dissolved and mobilized from inner parts to the surface in the presence of water. They precipitate on the surfaces of stones (Oguchi 2001). Rain and climatic conditions of the site causes the transportation of iron minerals and formation of reddish-brown stains

resulting in rust formation (Oguchi 2001, Press and Siever 2002). According to this mechanism, the water penetrates from exterior surface to the inner parts of the stone when the exterior surface of the stones gets wet. In the interior, the minerals that contain iron compounds as iron sulphides and iron carbonates are dissolved. Dissolved  $\text{CO}_2$  reacts with iron silicate which is oxidized in the presence of rain and oxygen in the air. When the exterior surface is dry, the water movement is reversed.  $\text{Fe}^{2+}$  is moved to the dry surfaces by water and oxidized to form  $\text{Fe}^{3+}$ . As a result of this process, iron containing colored minerals precipitate on the surfaces of stones as hematite ( $\text{Fe}_2\text{O}_3$ ), or limonite ( $\text{FeO}(\text{OH}) \cdot n\text{H}_2\text{O}$ ) and are observed as reddish-brown stains on stone surfaces (Oguchi 2001, Press and Siever 2002). It is clearly observed on the surfaces of marble monuments because of its desired white surface providing easy discrimination of color changes according to other stones (Spile et al. 2016).

The presence of metal compound adjacent to stone materials is another reason of yellowing of stone materials (Figure 1.17). If the stone material has metal components as bars, rods or pins, the oxidation and mobilization may occur on them. The reddish-brown patina may be formed because of the metal ions released and transferred from them (Macchia et al. 2011).



Figure 1.17. Brown patina formation on the stones of Cathedral, Halberstadt, Germany (Source: Fitzner and Heinrichs 2002)

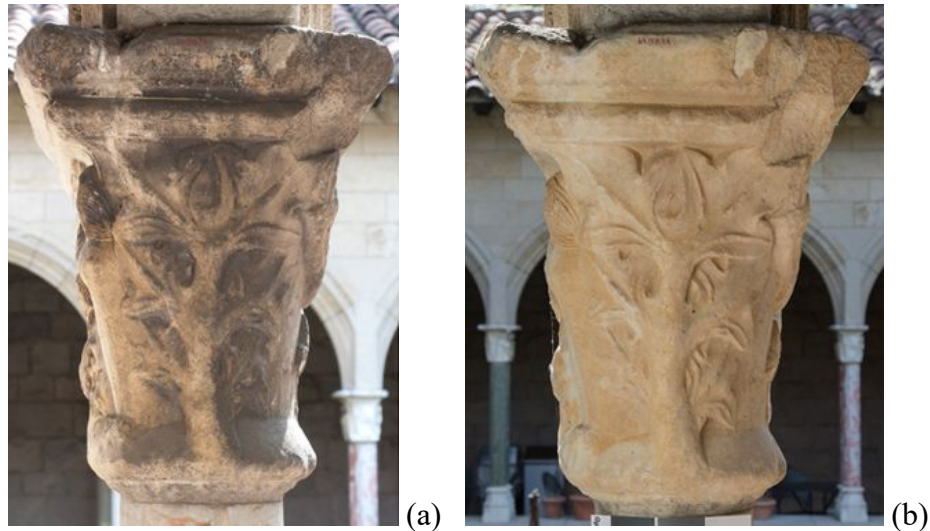


Figure 1.18. Patina on marble surface of capital before (a) and after (b) laser cleaning (Source: <http://www.metmuseum.org/blogs/in-season/2014/laser-cleaning-for-stone-conservation>)

The yellow color of stone surfaces may also be observed laser cleaning of black crust formed by air pollution on limestone surfaces (Figure 1.18). The yellow patina may be the residues of calcium oxalate precipitation that previously formed under black crust deposition. It may also be the result of laser cleaning itself. The laser pulses hits any alien soiling components that exist at the immediate vicinity of the stone surface and yellowing forms (Rodrigues 2006).

The last possible cause of yellow color is known as air pollution around the site. The residues of brown carbon are one of the basic sources of air pollution typically released through burning of biomass and garbage. In this case, SO<sub>2</sub> emissions and particulates in the air can cause the yellowing of marble or limestone surfaces (Stilgoe 2010).

## 1.6. Techniques Used in the Characterization of Patina

There are many analytical techniques used in the conservation works of stone monuments. Stuart collects these techniques under nine main titles in his book about the analytical techniques used in stone conservation studies as basic identification techniques, light examination and microscopy, molecular spectroscopy, atomic spectroscopy, x-ray

techniques, mass spectrometry, chromatography and electrophoresis, thermal and mechanical analysis and nuclear methods (Table 1.1) (Stuart 2007).

Basic identification techniques are visual examination, chemical tests, density and specific gravity, solubility and heat tests. Light examination and microscopy techniques include infrared techniques, ultraviolet techniques, x-ray radiography, refractometry, optical microscopy (polarized light microscopy), scanning electron microscopy (SEM - EDX) and scanning probe microscopy (Atomic force microscopy - AFM). Molecular spectroscopy techniques are infrared spectroscopy (Fourier Transformed Infrared Spectroscopy), raman spectroscopy, ultraviolet-visible spectroscopy, photoluminescence spectroscopy, nuclear magnetic resonance spectroscopy, electron spin resonance spectroscopy and mössbauer spectroscopy. Atomic spectroscopy techniques are atomic absorption spectroscopy, atomic emission spectroscopy and laser induced breakdown spectroscopy (LIBS). X-ray techniques are X-ray diffraction spectroscopy (XRD), x-ray fluorescence spectroscopy, electron microprobe analysis, proton induced X-ray emission (PIXE) and x-ray photoelectron spectroscopy and Auger spectroscopy. Mass Spectrometry techniques are secondary ion mass spectrometry and atomic mass spectrometry. Chromatography and electrophoresis techniques are gas chromatography and ion chromatography. Thermal and Mechanical Analysis include thermogravimetric analysis (TGA), differential scanning calorimetry/differential thermal analysis, thermal mechanical analysis. Finally nuclear methods include radio isotopic dating and neutron activation analysis (Stuart 2007).

Each of these analyses serves to determine different characteristics of stones. The conservators use proper analysis techniques considering the aim and limits of the study that they carry on. In the conservation studies of stone surfaces, determination of mineralogical compositions, micro-structural and chemical characteristics and in-depth analyses of patina are the most significant parts of the study to form a basis for the ongoing researches and treatment techniques of patina on stone surfaces.

There are several examples in the literature that various experimental methods were used for the determination of material characteristics of patina. Vazquez-Calvo et al. applied various microscopic techniques in the determination of patina formation (Vazquez-Calvo et al. 2007 (b)). XRD, XRF, TGA, FT-IR and SEM-EDX were used in the conservation studies of archaeological sites (Giakoumaki et al. 2007). Among them, XRD, XRF, TGA, FT-IR and SEM-EDX are the most widely used techniques. LIBS has become a common type of experimental method that has been used for the last two

decades (Giakoumaki et.al.2007). In this context, Lazic et al. and Kalaitzaki et al. studied on determining the qualitative and quantitative characteristics and in-depth profiling of patina on marble by using LIBS technique (Kalaitzaki et al. 2001, Lazic et al. 2004, Lazic et al. 2005).

In this context, the proper analyses techniques were selected to be used in this study in order to determine qualitative, semi-quantitative and in-depth analysis of the samples. The analyses techniques used in this study were selected as XRD, FT-IR, SEM-EDX, LIBS and TGA which are signed in bold in Table 1.1.

The use of XRD has some advantages and disadvantages in the conservation of archaeological sites. In the surface analyses, it gives detailed information about the mineralogical composition of the patina formation. However, the results may cause mistakes because of the user preparation procedure especially in porous and brittle materials which may be considered as a disadvantage of XRD analysis for patina formations.

The FT-IR analyses were also used for the determination of mineralogical composition of the materials. They are performed in the laboratory conditions because the samples and results are affected from the humidity in the atmosphere and the results may not be clear. Also, the solid samples require pellet preparation from the grounded sample powder. So, user mistakes may mislead the test results during the sample preparation. Despite this, FT-IR is still the most common infrared spectroscopy technique giving detailed information among the infrared techniques.

SEM-EDX analysis provides semi quantitative and qualitative information about the chemical composition of the materials. The micro structural characteristics of the samples are also observed in magnified images of micro scaled samples. However, this technique has some disadvantages, too. In SEM-EDX analysis, it is important to dehumidify the object in order to have fast and clear results. So, the analyses are performed in the laboratory conditions and it is not an in-situ analyses method. Hence, this technique is still one of the most common and reliable methods in the conservation studies.

Thermogravimetric analyses of the materials determine the absorbed water, organic material and CO<sub>2</sub> contents of the materials due to the weight losses in the laboratory giving information about the chemical composition of the materials as SEM-EDX. The TGA analysis is carried out on powder samples. So, user sensitivity is an important factor to have proper and accurate results.

The chemical analyses were also held by laser induced breakdown spectroscopy (LIBS) which has been widely used as an elemental analyses technique in the conservation studies (Giakoumaki et al. 2007).

The use of LIBS method has many advantages in this field. The portable LIBS can be used during in-situ analysis and does not require any sample preparation. It results with the ablation of 1 µg material on the surface and may be defined as a micro-destructive analysis technique. So, it is significant for conservation studies. Also, one who is not an expert in this area can easily learn and use this method and can analyze many materials in a very short period of time (Anglos and Miller 2009). These properties of LIBS technique draw attention of many scientists who study the conservation of cultural heritage and it has become a commonly used method by many conservators for the last two decades abroad (Giakoumaki et al. 2007, Anglos and Miller 2009). In this study, the LIBS device was not a portable one. Thus, the analyses were performed in laboratory conditions.

Table 1.1. Analysis techniques used in the stone conservation studies  
(Source: Stuart 2007)

|  | <b>Analysis Technique</b>    | <b>Aim / to determine</b>                          | <b>In situ/<br/>In lab.</b> | <b>Destr./<br/>Non-<br/>destr.</b> | <b>Used /<br/>Not<br/>Used</b> |
|--|------------------------------|--|-----------------------------|------------------------------------|--------------------------------|
| <b>Basic Identification Techniques</b> | <b>Visual examination</b>    | Useful info before embarking on more detailed exp. | In situ /<br>In lab.        | Non-<br>dest.                      | <b>Used</b>                    |
|  | Chemical tests               | Chemical characteristics of materials              | In lab.                     | Dest.                              | Not used                       |
|  | Density and specific gravity | Volume of the void in the objects                  | In lab.                     | Dest.                              | Not used                       |
|  | Solubility                   | Differentiating materials                          | In lab.                     | Dest.                              | Not used                       |
|  | Heat tests                   | The presence of certain elements                   | In lab.                     | Dest.                              | Not used                       |

(cont. on next page)

**Table 1.1. (cont.)**

|   |  |  |                      |                     |  |
|---|--|--|----------------------|---------------------|--|
| <b>Light examination and Microscopy</b> | Infrared techniques  | Type of pigments (and alterations mostly on wall paintings)      | In situ/<br>In lab.  | Non-dest.           | Not used (mostly for wall paintings)                                     |
|   | Ultraviolet techniques   | Surface details of objects                                       | In situ /<br>In lab. | Non-dest.           | Not used (for paintings/<br>paper)                                       |
|   | X-Ray Radiography  | The evidence of determination, examination of artifacts          | In lab.              | Non-dest.           | Not used (mostly for paintings/<br>papers/<br>examination of sculptures) |
|   | Refractometry  | RI (Index of refraction) of the material                         | In lab.              | Dest.               | Not used (not proper for limestone)                                      |
|   | Optical microscopy (Polarized light micr.)                               | The structural characteristics of samples                        | In lab.              | Non-dest.           | Not used   |
|   | <b>Scanning electron microscopy (SEM - EDX)</b>                          | Chemical compositions, micro structural charac.                  | In lab.              | Dest./<br>Non-dest. | <b>Used</b>  |
|   | Scanning probe microscopy (Atomic force microscopy - AFM)                | The nature of the topography at the interfaces of mortar & stone | In lab.              | Non-dest.           | Not used   |
| <b>Molecular Spectroscopy</b>           | <b>Infrared spectroscopy (Fourier Transformed Infrared Spectroscopy)</b> | Mineralogical characteristics of the samples                     | In lab.              | Dest.               | <b>Used (Effective for patina formation)</b>                             |
|   | Raman spectroscopy   | Pigment analysis, surface degradation, gemstone characterization | In lab.              | Dest.               | Not used (for gemstone mostly)   |
|   | Ultraviolet-visible spectroscopy   | Gemstone characterization (considering their colors)             | In lab.              | Non-dest.           | Not used (for gemstone)  |
|   | Photoluminescence spectroscopy   | To differentiate the natural and synthetic gemstones             | In lab.              | Non-dest.           | Not used (for gemstones mostly)  |

(cont. on next page)

**Table 1.1. (cont.)**

|                            |   |   |                   |           |  |
|----------------------------|---|---|-------------------|-----------|--|
|                            | Nuclear magnetic resonance spectroscopy                 | Molecular structure both in solution and in solid state                                   | In lab.           | Dest.     | Not used   |
|                            | Electron spin resonance spectroscopy                    | Characterize the stones   | In lab.           | Dest.     | Not used   |
|                            | Mössbauer spectroscopy                                  | The analyses of ceramics and clay content of heritage stones                              | In lab.           | Non-dest. | Not used   |
| <b>Atomic Spectroscopy</b> | Atomic absorption spectroscopy                          | The concentration of an element in solution   | In lab.           | Dest.     | Not used   |
|                            | Atomic emission spectroscopy                            | The concentration of an element in solution   | In lab.           | Dest.     | Not used   |
|                            | <b>Laser induced breakdown spectroscopy (LIBS)</b>      | The elemental composition of the materials (qualitative and semi-quantitative (in-depth)) | In situ / In lab. | Non-dest. | <b>Used (Effective for patina formation)</b>                         |
| <b>X-ray Techniques</b>    | <b>X-ray diffraction spectroscopy (XRD)</b>             | Mineralogical composition of the materials  | In lab.           | Non-dest. | <b>Used</b>  |
|                            | X-ray fluorescence spectroscopy                         | Measurements of elemental composition of the materials                                    | In situ/ In lab.  | Non-dest. | Not used   |
|                            | Electron microprobe analysis                            | Measurements of elemental composition of the materials                                    | In lab.           | Non-dest. | Not used   |
|                            | Proton induced X-ray emission (PIXE)                    | Concentration of elements in a material   | In lab.           | Non-dest. | Not used (paintings, glass, precious stones etc.)                    |
|                            | X-ray photoelectron spectroscopy and Auger spectroscopy | Effects of pollutants on the surfaces of stones   | In lab.           | Non-dest. | Not used (not practical and less commonly used on hydrated elements) |
|                            |   |   |                   |           |  |
| <b>Mass Spectrometry</b>   | Secondary ion mass spectrometry                         | The molecular weight of a molecule (and often other structural information)               | In situ/ In lab.  | Non-dest. | Not used   |
|                            | Atomic mass spectrometry                                | Characterization of stone   | In situ           | Non-dest. | Not used   |

(cont. on next page)

**Table 1.1. (cont.)**

|   |   |  |                     |           |  |
|---|---|--|---------------------|-----------|--|
| <b>Chromatography and Electrophoresis</b> | Gas chromatography  | Characterize the crust formation on stone  | In situ/<br>In lab. | Non-dest. | Not used<br>(Effective for black crust and gypsum formation)                                       |
|   | Ion chromatography  | Measure the concentrations of ions on stone surfaces (sulfates, chlorides, nitrates) | In situ/<br>In lab. | Dest.     | Not used   |
| <b>Thermal and Mechanical Analysis</b>    | <b>Thermogravimetric analysis (TGA)</b>                         | The absorbed water, organic material and CO <sub>2</sub> contents                    | In lab.             | Dest.     | <b>Used</b>  |
|   | Differential scanning calorimetry/differential thermal analysis | Degradation reactions of inorganic materials, quantifying salt efflorescence etc.    | In lab.             | Dest.     | Not used<br>(used for polymers commonly)   |
|   | Thermal mechanical analysis                                     | Deformation of a sample under a static load as function of time or temperature       | In lab.             | Dest.     | Not used   |
| <b>Nuclear Methods</b>                    | Radioisotopic dating  | The age of an object ( <sup>14</sup> C method)                                       | In lab.             | Dest.     | Not used<br>(strontium isotope analyses may help to determine the provenance of material (marble)) |
|   | Neutron activation analysis                                     | The characteristic decay patterns to identify the elements present                   | In lab.             | Dest.     | Not used   |

## 1.7. Conservation Approaches of Patina in Cultural Heritage Studies

Patina occurrence causes some changes on appearance and color of the original building materials or objects that have cultural significance. These changes have been perceived in different ways by the conservators with respect to the positive and negative impacts of it on the materials.

Patina is perceived as a weathering phenomenon on the surfaces of limestone monuments. This thought derives from the negative visual effects of it on the observer. According to this approach, patina is perceived as a dirty surface on monument surfaces. It obviously causes various changes to the original characteristics, color and appearance of historical materials. These changes may cause the loss of traces coming from the ancient cultures, too. Dirt, color changes, structural and material failures which are the possible results of patina formation have negative effects on the observer. This leads this group consider patina as an aesthetical problem that should be obliterated from the material surfaces. Thus, removing patina becomes often the first step in the conservation studies of stone monuments after documentation phase. However, preventive conservation should be regarded as the first treatment method instead of cleaning considering international charters and today's conservation approaches.

According to this approach, the conservation strategies and cleaning decision of patina layer should be away from subjective interpretations and being one's sensory reaction for dirty surfaces. The conservators follow the recent conservation principles requiring a multidisciplinary way of work to decide the protection or cleaning of patina formations in the conservation studies of stone monuments. It should be decided according to the international principles. At this point of view, patina should be considered as a part of the historical building material or object that should be protected. The material characteristics and effects of patina on stone should be well determined to decide if it is protective, harmful or inefficient on stone surfaces. The irreversible treatments as cleaning and removal of patina should be avoided. Cleaning should be applied if only harmful agents are present on the stone surface.

In this sense, the international charters are guiding principles. The conservator should have a full knowledge of charters about conservation. In addition to this, material characteristics, causes and effects, aesthetical, functional characteristics and formation of patina to constitute an accurate diagnosis and to determine the proper treatment techniques in the conservation studies of stone monuments. Within this context, the basic principles of international charters, the results of previous laboratory studies and the theoretical discussions among theoreticians and practitioners since 19<sup>th</sup> century have prepared a basis for the recent conservation approach in theory and in practice for the conservation of patina formation on monument surfaces.

Considering all theoretical and practical improvements about the cleaning and conservation of patina, the present conservation approach was constituted. At this point

of view, the conservator should follow some basic principles in the conservation studies of patina formation. First of all, he/she should regard patina formation as a value and a component of the monument giving information about the past, providing a connection between today and past and creating a historical sense of the age and unique appearance of the building. It is exemplified in an extensive research about the controversies in conservation of patina on monument surfaces between theoreticians and practitioners including the patina types, their possible causes and discussions on cleaning strategies of them (Rodrigues 2006). In this paper, Rodrigues contributes in redefining the material significance of patina in conservation field. The results of this research show that patina formation may include much information carried from the past. Cleaning of patina results with the loss of information carried from the previous cultures to the future generations. Thus, cleaning should be decided if only it is indispensable for the long term stability of the stone monument itself. He suggests being sensitive not to lose the original characteristic of the stone surfaces in cleaning interventions (Rodrigues 2006).

The discussions on cleaning of patina began among restorers in the 1840s beginning with John Ruskin's extended essay on *Seven Lamps of Architecture* (Ruskin 1849). In this essay, the glorious effect of time on the building surfaces is mentioned as the representation of the age the building. The protection of the actual beauty of the stone formed by years with all its traces such as fissures, color and dirt, representing the active life binding old and new together is suggested (Ruskin 1849). In the same time period, Manifesto of the Society for the Protection of Ancient Buildings was declared by William Morris (SPAB 1877). In this Manifesto, the restoration applications are rigidly criticized. Morris states that the restoration treatments of the last 50 years damaged the ancient buildings instead of protection. It caused the loss of living spirit of the monuments. He suggests minimum intervention to the stone monuments corresponding Ruskin's ideas (SPAB 1877).

These arguments are followed by *patina dilemma* with the published articles on cleaning controversy between 1949 and 1962 (Weil 1977). Among them, patina cleaning is recommended to be studied with respect to the aesthetic and historic criteria, and stylistic and technical data in an interdisciplinary way of work according to the suggestions of a Belgian conservation scientist Paul Coreman (Weil 1977).

The cleaning of patina was a contentious subject for oil paintings and bronze artifacts in the same time period (Figure 1.19). The patina formation on oil paintings is considered as a special addition to the materials according to Brandi, an art historian

(Brandi 1949). According to him, the pictures may have been painted with an expectation of patina formation by painter or designer. Thus, the cleaning interventions may mislead the future generations about the original state of the cleaned material (Brandi 1949). The ideas of Brandi are supported by the definition of patina made by Philippot. It is defined as a mark of time that cannot be erased on paintings (Philippot 1966). According to him, the cleaning of patina may lead to the misunderstanding that the restorer can cause. Because the degree of cleaning is based on an idea of finding the original state of the material according to the evaluation of the conservator himself (Philippot 1966). It is impossible to know when to stop cleaning because the original state of the surface could never be totally known. The cleaning interventions end when the clean surface is reached which will be the result of a personal inception which must be avoided in the conservation works.



Figure 1.19. Patina formation on oil painting before (right) and after (left) cleaning  
(Source: <http://www.simongillespie.com/wp-content/uploads/2013/05/Varnish-Removal-2-400x603.jpg>)

The physical and chemical weathering that has formed by time cause a change on material surfaces which is impossible to bring back the original state of them. Hence, patina formation is evaluated as an irreversible formation on material surfaces. It is illustrated with the dust formation on bronze materials (Weil 1977). Dust is formed as a result of chemical and physical transformation of bronze material itself. A ruined bronze object is impossible to be restored to the original appearance because it is resulted with a chemical change on bronze surfaces (Weil 1977). Weil determines this change as a trace of the past giving information about the previous environmental conditions of the objects. It can give us an idea if it was located in an urban area, under the soil, or in a humid temperature etc.

This perception, which is constituted for the cleaning of patina formed on oil paintings and small objects, is also conceived for the patina formation observed on stone surfaces of historical buildings and monuments, also.

Patina layer may help to get information about the previous restoration and building applications carried out in history. The use of wax, resin, egg protein or animal glue on building surfaces for the protection of stone surfaces, the preparation of the surface for the application of polychromy, artificial aging of later added architectural elements and maintenance for the purpose of renewal of stone surfaces are the gathered information taken from the case study buildings in literature reviews that studied on man-made treatments (Rampazzi et al. 2004). So, it is clearly observed that the protection of these layers is also essential to have information about the details of historical applications on stone surfaces instead of cleaning.

The theoretical discussions about cleaning of patina were reinforced with laboratory analyses with the progresses in material science by determining the material characteristics of patina layers as protective, harmful or ineffective formations on material surfaces (Scheerer 2009). Considering the material characteristics of patina formed on stone materials, patina should be protected if it is an artificially applied protective material, calcium oxalate layer or the living organism that have protective function on the original stone substrata for the long term stability of the original material. The artificially applied protective patinas may give information about the historical techniques of intervention techniques in the past (Vazquez-Calvo et al. 2007 (a)). Thus, these artificial patinas should be protected on stone surfaces if they do not damage the underlying layer regardless of their protective function (Vazquez-Calvo et al. 2007 (a)).

The protection of yellow calcium oxalate patina, which was formed by the effects of microbiological organisms, is critical in the conservation studies. Because it is more durable against the destructive effect of wind and water according to calcite which is the major mineral of calcareous stone materials (Barri et al. 2002). In addition to this, the living organism itself may also be protective apart from the calcium oxalate precipitation it causes. For instance, the lichen growth on the tuff buildings of Cappadocian monuments are protective on stone surfaces (Garcia-Valles et al. 2003). The lichen formation living on Cappadocian tuffs act as a protective coating, reducing the weathering velocity by limiting the penetration of water (Garcia-Valles et al. 2003). Thus, protecting lichen coating for the conservation of the whole area and the monuments is critical to reduce the erosion on stone surfaces (Garcia-Valles et al. 2003). Supporting this, the formation of green algal biofilms on four sandstone building surfaces in Belfast are presented as bio protective biofilms against moisture although they cause aesthetic damage on the sandstone surfaces (Cutler et al. 2013).

The cleaning of patina layer may be necessary and indispensable in some cases. The growth of microorganisms effect the stone chemically and physically in some cases (Urzi and De Leo 2001). They may cause the formation of a destructive coating instead of a protective one as mentioned above. For instance, the biological weathering results with bio pitting and evaluated as destructive agents on marble surfaces of Ephesus, Turkey (Garcia-Valles et al. 2000). The black fungi formation cause mechanical destructive forces in marble statues located in Florence, Italy considering the results of laboratory analysis (Marvasi et al. 2012). The harmless patina layer and original stone surface should be protected as a part of the historical monument. However, the biological formations, chemical agents or harmful materials should be cleaned from the monument surfaces instead of cleaning the whole surface to slow down the weathering process. In such a case, constituting proper diagnosis and the use of appropriate cleaning methodology is essential to minimize the damages of cleaning on stone surfaces (Grimmer 1988). The selection of an inaccurate technique or insufficient use may accelerate the weathering of building stones. The use of water causes water and moisture penetration to the stone. It causes the occurrence of correlating physical and chemical weathering mechanisms in the stone structure. The use of chemicals in the cleaning interventions causes efflorescence and subflorescence, physical abrasion and material loss (Grimmer 1988, Doehne and Price 2010). In addition to this, cleaning interventions make stone vulnerable to pollutants and biological growth for further damage (Doehne

and Price 2010). Thus, the use of the appropriate cleaning technique is also another critical issue in the conservation intervention of a patina layer formed on the surfaces of historical building materials.

The theoretical discussions on cleaning of patina, the results of previous studies and the declarations of international charters show that there are several factors affecting to constitute the conservation approaches for a patina formation on historical or archaeological stone monument. The conservator should follow the rules of international charters. He/she should regard patina formation as a value and a component of the monument giving information about the past, providing a connection between today and past and creating a historical sense of the age and unique appearance of the building. The cleaning intervention should be decided if only the patina layer is harmful to the original building material.

### **1.8. International Charters about Patina Formation in Cultural Heritage Studies**

Patina formation is a value for the historical buildings and monuments representing the authenticity and age of them. It is a part of the building that formed by the years which give information about past times. These values of patina formation had been disregarded in the international charters until the last century. In 2010, the patina of age was mentioned in Article 18 of in ICOMOS New Zealand Charter for the Conservation of Places of Cultural Heritage Value reminding the importance of preservation of a place with little intervention (ICOMOS 2010). The term patina was used in the definition of “fabric” including physical materials of a place including patina of age (ICOMOS 2010). It emphasizes the preservation of patina of age as an essential value of the monument where it contributes to the authenticity and integrity of the place, or the structural stability of the materials. According to its articles, stabilization of decay, long term planned maintenance and repair is essential. It requires respect for the existing fabric. It also puts emphasis on the reversible intervention, no adverse effects and compatibility for the restoration works on original fabric. The cleaning interventions should be taken into account if only it causes advanced decay on original materials. However, the word “patina” was not precisely used as the term including the definition handled as in the scope of this study.

There are some charters which shed light on the intervention decisions related to the original building materials of historical and archaeological monuments without mentioning patina evidently. Among them, Venice Charter (1964) forms a basis for the recent approaches about the protection and conservation of historical and archaeological building materials (ICOMOS 1964). It declares keeping historical buildings and monuments away from irreversible interventions. With respect to this concern, cleaning of patina is an irreversible treatment technique for stone surfaces that should be avoided for the long-term stability of the monument.

The Nara Document on Authenticity (1994) supports the suggestions of Venice Charter focusing on the values of the historical monuments with all their authentic characteristics including all kinds of sources coming from any components of cultural heritage as traditions and techniques, location and setting, and spirit and feeling, form and design, use and function, materials and substance, and other internal and external factors (ICOMOS 1994). This definition should be evaluated considering authentic value of patina formation as an original characteristic of the historical building material with respect to the recent conservation approaches.

Following Nara Document, ICOMOS Charter, Principles for the Analysis, Conservation and Structural Restoration of Architectural Heritage in Zimbabwe (2003) describes the basic principles of methods to be used in conservation studies for the whole historic building materials (ICOMOS 2003). The evaluations of treatment techniques are clearly declared in this charter referring to the all components of historic building materials. According to this charter, the interventions on historical building materials should be reversible supporting the Venice Charter. Removal of any historic material is unadvisable. Thus, this charter points out the best therapy as preventive maintenance for conservation treatments of cultural heritage components (ICOMOS 2003). This prescription may be correlated with conservation interventions and treatment techniques of patina formation on the surfaces of stone monuments in cultural heritage studies.

Considering all the international charters about the conservation of original building materials, patina formation should be evaluated as value and a part of the historical buildings and monuments representing the authenticity and age of them which should be conserved according to the recent conservation approaches.

## CHAPTER 2

### METHODS

In this study, laboratory studies aimed to determine the chemical and mineralogical composition and micro structural properties of yellow patina formed on marble and yellow travertine surfaces in the archaeological sites to form a basis for the intervention decisions of patina formations for the purpose of conservation.

In this part, site survey and sampling phases and the experimental processes are presented in detail. The visual determinations of yellow patina formations were carried out and the samples were collected with the site survey held in 2010. The experimental data was collected from several experiments as X-ray Diffraction (XRD), Fourier Transformed Infrared Spectroscopy (FT-IR), Scanning Electron Microscope (SEM) equipped with X-Ray Energy Dispersive System (EDS), thermo-gravimetric analysis (TGA) and Laser Induced Breakdown Spectroscopy (LIBS).

The analyses were applied on sound inner cores and yellow patina formed surfaces of marble and travertine samples. The results were compared in order to determine and compare the material characteristics of yellow patina formation on both of the stone types.

#### 2.1. Site Survey and Sampling

The first step of the study was the determination of yellow patina formed surfaces on marble and yellow travertine monuments in the archaeological sites by naked eye. The photographs of the yellow colored surfaces of the monuments in Aizanoi, Hierapolis, Aphrodisias and Sardes were taken within this respect. Following this step, patina samples were scraped from the surfaces of yellow colored limestone. The stone samples were collected corresponding to the underlying stone and the patina coating the surface of large and small scaled marble and yellow travertine monuments and blocks of the walls without detriment to original building materials.

Six marble samples were collected from temple (117 AD) and theatre (160 AD) in Aizanoi (Kütahya); bouleuterion (200 AD) and temple (30 BC) in Aphrodisias (Aydın) and temple (300 BC) in Sardes (Manisa) (Figure 2.1, Figure 2.2, Figure 2.3). The samples

were taken from the areas where yellow patina was observed on marble surfaces. Six yellow travertine samples were collected from necropolis (300 BC), agora (60 AD), bath (300 AD) and fountain (300 AD) in Hierapolis (Denizli) (Figure 2.4, Figure 2.5, Figure 2.6). However, the yellow patina formation on yellow travertine surfaces was not as appreciable as on marble surfaces. The locations where the samples were collected were documented with photographs. The collected samples were put in pockets separately and named considering an order in nomenclature (Table 2.1, Table 2.2).



Figure 2.1. The locations of yellow patina and marble samples taken from the wall of Zeus Temple (a) and Theatre (b) in Aizanoi

(cont. on next page)



(b)

Figure 2.1. (cont.)



Figure 2.2. The location of yellow patina and marble samples taken from the wall of Bouleuterion in Aphrodisias



Figure 2.3. The representative yellow patina covered marble samples taken from the ground in the Temple of Sardes



Figure 2.4. The location of yellow patina and yellow travertine samples taken from the Bath in Hierapolis



(a)



(b)

Figure 2.5. The locations of yellow patina and yellow travertine samples taken from the column (a) and wall (b) of Agora in Hierapolis



Figure 2.6. The location of yellow patina and yellow travertine samples taken from Necropolis in Hierapolis

## 2.2. Nomenclature of the Samples

The nomenclatures of the samples were prepared considering an order (Table 2.1, Table 2.2). According to this order, the first letter represents the settlement where the sample was taken from (Ai: Aizanoi, H: Hierapolis, Ap: Aphrodisias, S: Sardes); the second represents the monument type where the sample was taken from (Th: theatre, Te: temple, N: necropolis, B: bouleuterion, A: agora, F: fountain); the third represents the stone type if it is marble or travertine (M: marble with yellow patina formation on its surface, T: travertine with yellow patina formation on its surface); and the last represents the sample number (as 1, 2, 3).

In addition to this, the analyses were performed on the previously prepared inner cores and patina formations of the samples. In this case, the fifth letter which was placed at the end of each sample after a dash was observed as P: Patina scraped from the surface of the sample; I: Sample prepared from the sound inner core of the stone.

Table 2.1. Marble samples collected from the site

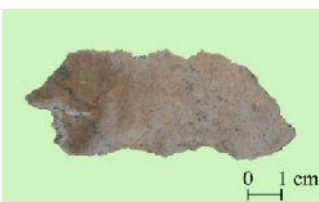
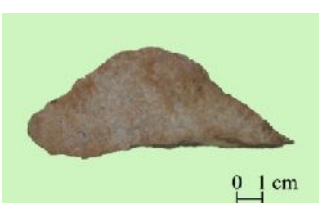
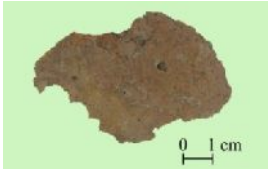
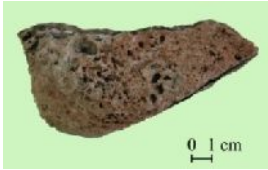
| STONE TYPE  | SAMPLE  | SAMPLE PHOTOGRAPH   | SAMPLE DEFINITION  |
|---|---|---|--|
| MARBLE  | <b><u>Ai.Th.M.1</u></b><br>Ai.Th.M.1-P<br>Ai.Th.M.1-I |    | Marble taken from the surface of stone wall of theatre in Aizanoi                              |
|   | <b><u>Ai.Th.M.2</u></b><br>Ai.Th.M.2-P<br>Ai.Th.M.2-I |    | Marble taken from the surface of stone wall of entrance building to the theatre in Aizanoi     |
|   | <b><u>Ai.Te.M.1</u></b><br>Ai.Te.M.1-P<br>Ai.Te.M.1-I |   | Marble taken from the surface of the stone wall of Zeus Temple in Aizanoi                      |
|   | <b><u>Ap.B.M.1</u></b><br>Ap.B.M.1-P<br>Ap.B.M.1-I    |  | Marble taken from the surface of the stone wall in the entrance of Bouleuterion in Aphrodisias |
|   | <b><u>Ap.Te.M.1</u></b><br>Ap.Te.M.1-P<br>Ap.Te.M.1-I |  | Marble taken from the surface of the column in Temple in Aphrodisias                           |
|   | <b><u>S.Te.M.1</u></b><br>S.Te.M.1-P<br>S.Te.M.1-I    |  | Marble taken from the in Temple in Sardes  |
| <p><b>Codes:</b><br/>           Ai: Aizanoi; Ap: Aphrodisias, S: Sardes<br/>           B: Bouleuterion; Te: Temple; Th: Theatre<br/>           M: Marble with yellow patina formation on its surface<br/>           P: Patina scraped from the surface of the sample; I: Sample prepared from the sound inner core of the stone</p> |   |   |  |

Table 2.2. Travertine samples collected from the site

| STONE TYPE   | SAMPLE   | SAMPLE PHOTOGRAPH   | SAMPLE DEFINITION   |
|--|--|---|---|
| TRAVERTINE   | <b><u>H.A.T.1</u></b><br>H.A.T.1-P<br>H.A.T.1-I    |    | Travertine taken from the surface of column of Agora in Hierapolis          |
|  | <b><u>H.A.T.2</u></b><br>H.A.T.2-P<br>H.A.T.2-I    |    | Travertine taken from the surface of stone wall of Agora in Hierapolis      |
|  | <b><u>H.Ba.T.1</u></b><br>H.Ba.T.1-P<br>H.Ba.T.1-I |   | Travertine taken from the surface of stone wall of Bath in Hierapolis       |
|  | <b><u>H.F.T.1</u></b><br>H.F.T.1-P<br>H.F.T.1-I    |  | Travertine taken from the surface of stone wall of Fountain in Hierapolis   |
|  | <b><u>H.N.T.1</u></b><br>H.N.T.1-P<br>H.N.T.1-I    |  | Travertine taken from the surface of stone wall of Necropolis in Hierapolis |
|  | <b><u>H.N.T.2</u></b><br>H.N.T.2-P<br>H.N.T.2-I    |  | Travertine taken from the surface of stone wall of Necropolis in Hierapolis |
| <p><b>Codes:</b><br/> H: Hierapolis<br/> A: Agora; Ba: Bath; F: Fountain; N: Necropolis<br/> T: Travertine with yellow patina formation on its surface<br/> P: Patina scraped from the surface of the sample; I: Sample prepared from the unweathered parts of the stone</p> |  |   |   |

## **2.3. Laboratory Studies Used in the Determination of Mineralogical Composition, Microstructural and Chemical Characteristics of Stones and Patina**

In this study, the mineralogical composition, microstructural and chemical characteristics of marble and travertine were determined by laser induced breakdown spectroscopy (LIBS), scanning electron microscopy equipped with energy dispersive spectrometry (SEM-EDX) and x-ray diffraction (XRD) analyses. The characteristics of yellow patina formation on marble and travertine surfaces were determined by Laser induced breakdown spectroscopy (LIBS), scanning electron microscopy equipped with energy dispersive spectrometry (SEM-EDX), x-ray diffraction (XRD), Fourier transform infrared spectrometry (FT-IR) and thermogravimetric analysis (TGA).

### **2.3.1. Preparation of Samples for Laboratory Analyses**

The marble and travertine samples and yellow patina samples were prepared from the collected samples separately for laboratory analyses.

During the whole phase of laboratory studies, the preparation of marble was relatively easier according to travertine. It was related with the coarse grained well interlocking crystals of marble and porous and brittle microstructure of travertine. It caused travertine to break into smaller pieces during preparation. The yellow patina samples were mostly fragmented and the patina was lost at every step of sample preparation for travertine analyses. The analyses were held on the most durable patina samples for travertine. Thus, some of the tests could not be relatively completed for some travertine samples necessitating sample preparation.

The sound marble and travertine samples and patina formation formed on their surfaces were prepared for XRD and SEM-EDX analyses. The patina samples were also analyzed by FT-IR and TGA, either. XRD and TGA analyses necessitated powder preparation. In addition to this, FT-IR and TGA necessitated pellet preparation to apply the tests.

In the preparation of the powder specimens of marble and travertine, sound parts of stones were taken out from the inner cores of previously cut cubes of the collected samples. Differing from sound inner cores, yellow patina samples on white marble

surfaces were scraped from sample surfaces by naked eye easily. However, the powder preparation of yellow patina involved some problems for the same colored yellow travertine samples. It was almost impossible to distinguish them from each other by naked eye. Thus, the patina samples were scraped under stereo microscope (Olympus SZ40). The scraped patina samples and sound inner cores of marble and travertine surfaces were ground to particles less than 53 $\mu$ m as powder specimens. Then, the pellets of sound inner cores and patina samples were also prepared from the obtained powder specimens and heated to remove absorbed water before SEM-EDX and FT-IR analyses.

The powder specimens of sound parts were used for XRD analyses. The pellets of sound inner cores were used for SEM-EDX analyses.

The powder specimens of patina samples were used for XRD and TGA analyses. The pellets of patina samples were used for FT-IR analyses.

SEM-EDX analyses were performed on the surfaces of yellow patina formed marble and travertine prisms with the dimensions of 0.5x0.5x1.0cm. The samples were heated to remove absorbed water to have better results in SEM-EDX analyses. SEM-EDX mapping was also performed on sections of the same samples from surface to the inner cores. The thin section device could not be used in the preparation of sample sections for LIBS or SEM because it caused the patina layer to break into pieces and the yellow patina was lost in most of the samples. Thus, the tests were applied on the collected samples without any sample preparation. The samples were selected from the broken parts showing the patina formation on the stone surface as a section for SEM-EDX mapping analyses. SEM images were also taken from the same specimens used for mapping analyses.

LIBS were performed for in-depth analyses from surface to the sound inner cores of the same marble and travertine specimens used in SEM-EDX mapping analysis.

### **2.3.2. Determination of Mineralogical Composition**

The determination of mineralogical composition of sound inner cores of marble and travertine and yellow patina was an important part of the study for its characterization on both of the stone types. For this purpose, X-ray diffraction (XRD) was performed on the prepared powder samples of sound inner cores and yellow patina on them. Fourier

transform infrared spectrometry (FT-IR) analyses were also applied on the prepared powder specimens of yellow patina on marble and travertine in the laboratory.

X-ray Diffraction (XRD) analyses were applied on the prepared powder samples less than 53 $\mu$ m using a Philips X-Pert Pro X-ray Diffractometer in order to define mineralogical compositions of the materials. The experimental XRD parameters were applied as follows (Table 2.3).

Table 2.3. Parameters used in XRD analyses

|                                |                         |
|--------------------------------|-------------------------|
| <b>Anode material</b>          | Cu                      |
| <b>K-Alpha1 wavelength</b>     | 1.5405600               |
| <b>K-Alpha2 wavelength</b>     | 1.5443900               |
| <b>Ratio K-Alpha2/K-Alpha1</b> | 0.500                   |
| <b>Divergence slit</b>         | Fixed,0.76mm            |
| <b>Generator voltage</b>       | 45                      |
| <b>Time per step</b>           | 10                      |
| <b>Scan range</b>              | 2 $\Theta$ -60 $\Theta$ |
| <b>Scan step size</b>          | 0.0334225               |
| <b>No. of points</b>           | 1735                    |
| <b>Scan type</b>               | Continuous              |

Fourier transform infrared spectrometry was another method that was used to determine the mineralogical compositions of the materials. The ground yellow patina powders (less than 53 $\mu$ m) were mixed with 100 unit of KBr to 1 unit of sample. The prepared mixtures were pressed into pellets. KBr and sample pellets were heated to 100°C to remove the absorbed water to avoid mistakes in FT-IR analyses. Samples were analyzed using Perkin Elmer FT-IR System Spectrum BX by scanning each of the samples four times in order to evaluate their mineralogical properties in the laboratory.

### **2.3.3. Determination of Micro-structural Characteristics**

The microstructural characteristics of patina layer were investigated on different scaled magnified SEM images of surfaces and cross-sections.

The morphology and crystal structure of yellow patina layer was evaluated on the different scaled SE and BSE images with different scales varying from 250 to 5000 magnification showing the intersection zone of yellow patina and sound inner cores of marble and travertine samples. The sections from patina surface to the inner parts were prepared and analyzed in order to observe the intersection area of yellow patina on limestone samples by mapping using 250x and 500x magnified images.

The thickness of patina layer was also investigated on the magnified SEM images of prepared cross sections of marble and travertine samples that patina layer was observable.

### **2.3.4. Determination of Chemical Composition**

The chemical composition of sound inner cores of marble and travertine and yellow patina formed on them were determined by using scanning electron microscopy equipped with energy dispersive spectrometry, laser induced breakdown spectroscopy and thermogravimetric analyses. The results were controlled to have a better knowledge on the chemical composition of yellow patina covered marble and travertine samples.

The SEM-EDX was performed using FEI Quanta 250 FEG Scanning Electron Microscope (SEM) equipped with X-Ray Energy Dispersive System (EDX). The samples were prepared and heated to remove absorbed water in the materials for SEM-EDX analyses. The powder pellets were used to analyze the sound inner cores of marble and travertine. The small pieces of yellow patina covered sample surfaces were used to analyze the yellow patina formation on the sound inner cores. The EDX analyses were held to determine the concentrations of major and minor elements in yellow patina formations of the surfaces of each of the marble and travertine samples. The concentrations of major and minor elements were determined on three different areas of each sample. The results were evaluated considering the averages and standard deviations of these three areas on the samples.

SEM-EDX analyses were also performed on the prepared cross-sections of stones showing the presence of patina layer and intersection of yellow patina and limestone surfaces by using 250x and 500x magnified images. Mapping was also held on the same cross sections to observe the elemental distribution from surface to the inner core of the stones (Figure 2.7).

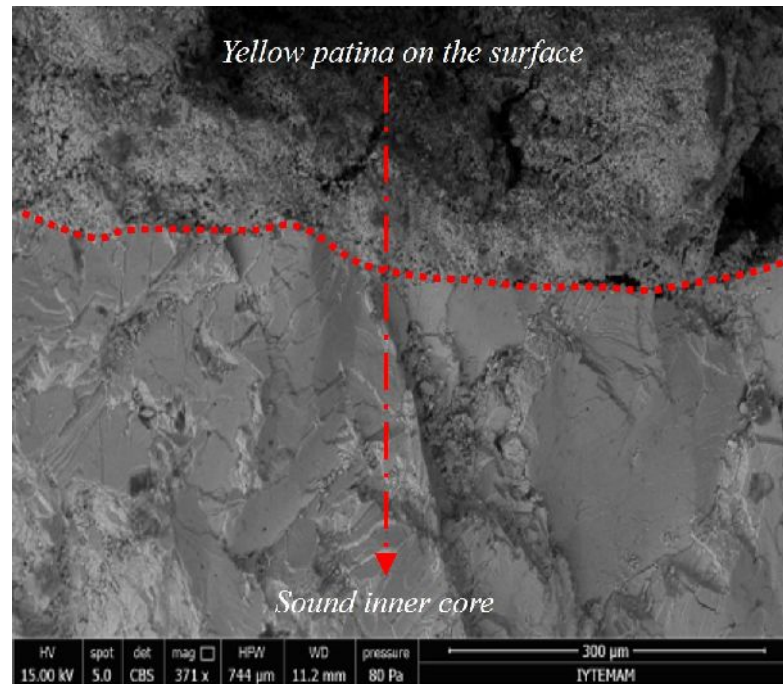


Figure 2.7. A representative marble sample showing its use for SEM-EDX mapping

This study differs from the other studies by using in-depth profiling Laser Induced Breakdown Spectroscopy (LIBS) in the determination of yellow patina on marble and travertine surfaces. The results of LIBS analyses give information about the elemental variation from surface to the sound inner core of calcareous stones considering the thickness of patina on their surfaces. LIBS results were compared with SEM-EDX mapping analyses and the compositional change from the surface to the sound inner cores are clearly observed in the laboratory analyses.

In this study, the plasma was produced by a Q-switched Nd: YAG laser and analyses were performed by measuring the spectral line intensities of the neutral calcium, silicon, carbon, iron, magnesium and aluminum for the chemical analyses of stones. In

LIBS, the material was lost after each laser shot. Thus, it was critical to use the minimum energy level during analyses to minimize material losses in micro scale to have better results in LIBS analyses. Considering this, one marble sample was tested using 20, 40, 60, 80, 100, 120, 140 and 160mj energy levels as the first step of LIBS analysis (Figure 2.8). The marble sample was first analyzed with 50 shots at one point in-depth. The results showed that the signals were very weak or lost at very low and high energies such as 20mj and 160 mj energy levels especially for Al and Si elements. The ablation and Ca rates of all elements were satisfactory for all elements around 40 mj and 60 mj energy levels. Among them, 40 mj was selected as proper level for marble and travertine to apply repetitive shots in order to keep the patina or deposition on the stone surface longer to have better information about the patina with respect to 60mj.

In the evaluation of LIBS analyses, the ablation rates of C, Mg, Si, Al and Fe signals normalized to Ca signal were determined in the spectrums. S, which is a commonly observed element on patina, could not be investigated in LIBS because its signal intensity was very weak and could not be determined in LIBS spectrum with the accompanying minerals on patina samples.

The in-depth profiling was performed on a specific point for each sample to determine the elemental variation from yellow patina to the inner cores of all the marble and travertine samples (Figure 2.9). It was tested by applying the LIBS placing the samples on the stage of the device in two different ways in order to decide the proper experimental method for LIBS accurately. In the first method the LIBS analyses were held on three specimens as yellow patina formed surface, sound inner parts and a section. The chemical compositions of surface and inner parts were calculated for marble and travertine separately. In-depth LIBS analyses were made on the section of one marble sample. Each sample were cut approximately 0.5x0.5x1.0cm cubes and used in the analyses. The results were evaluated from the sections of the surfaces laterally and the results were compared (Figure 2.9(a)). The samples were exposed to 100 laser shots on the cross sections laterally and analyzed by measuring the spectral line intensities of the calcium, silicon, carbon, iron, magnesium and aluminum on marble and travertine samples. The patina layer was tent to broken easily during sample preparation and the patina surface was lost on the samples.

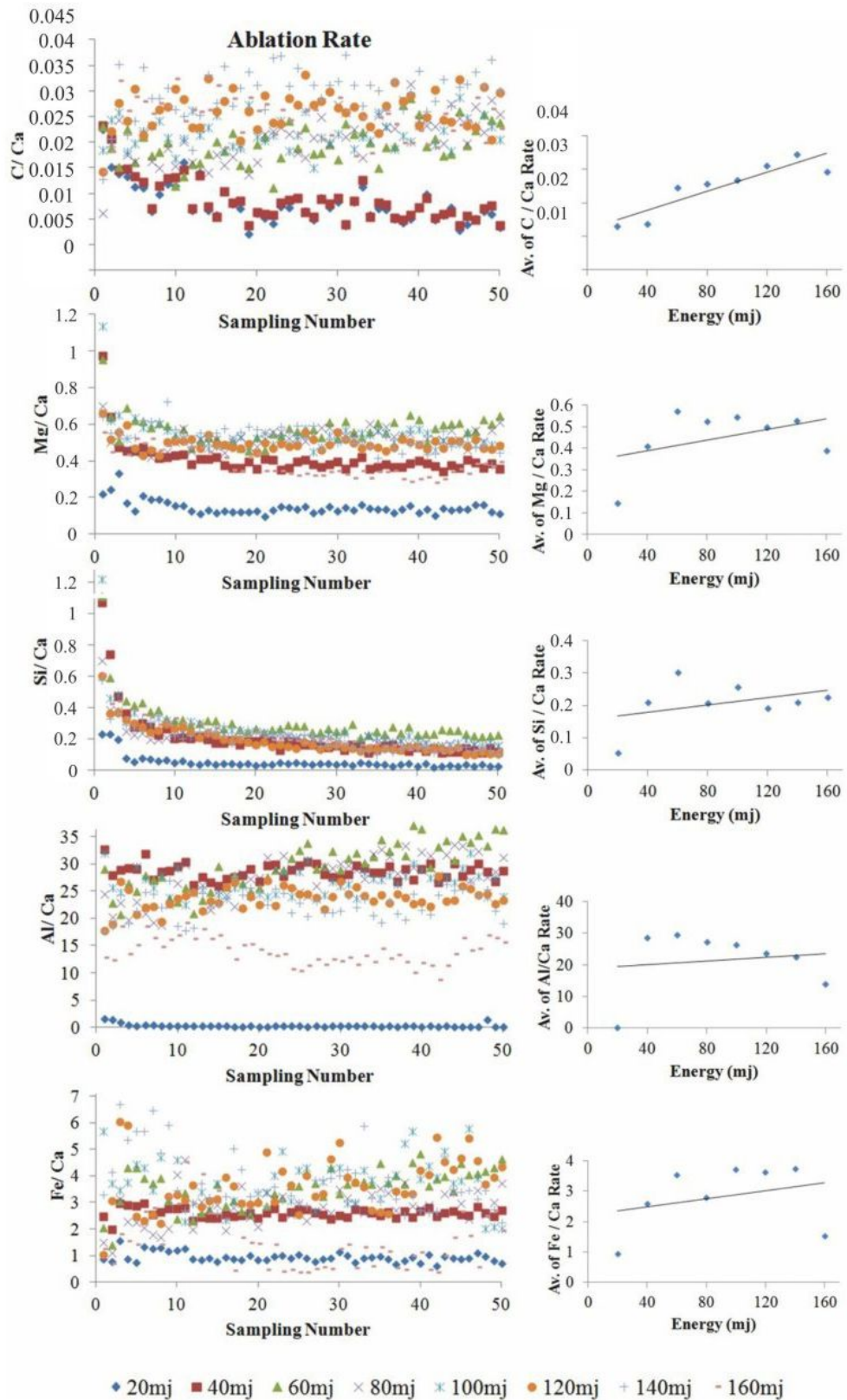


Figure 2.8. Graphs showing the ablation rates of elements in LIBS analyses of marble applied in different energy levels between 20 and 160 mj

In the second method, which is traditionally applied, a sample from weathered exterior surface to the sound inner part was cut for the analysis (Figure 2.9(b)). Analysis was applied in order to determine the change of chemical compositions of stone from the surface (patina) to inner parts of it. The samples were exposed to 100 in-depth laser shots on one point. However, the shots were evaluated considering the first 50 shots for each sample because of the dispersal of signal intensities in the deeper parts of marble and travertine. The spectrums were analyzed by measuring the spectral line intensities of calcium, silicon, carbon, iron, magnesium and aluminum on marble and travertine.

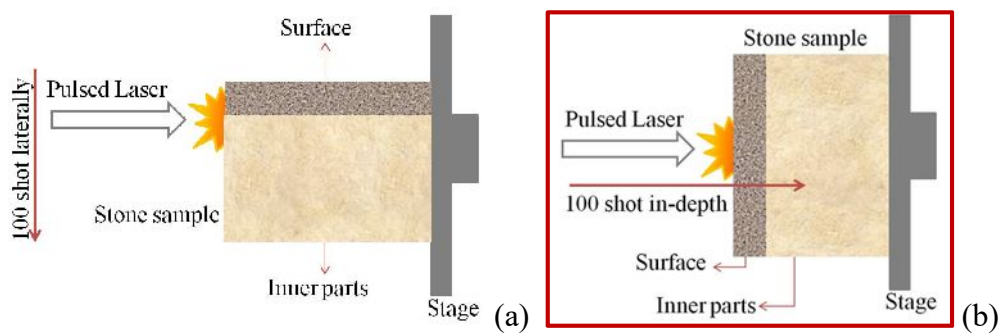


Figure 2.9. Drawings showing sample placement on the stage of LIBS device as the first method for test (a) and the second method for use during the study (b)

The changes in the trend lines of Ca, C, Si, Al, Fe and Mg distribution according to depth referred to the layer transitions from surface to the sound inner cores of the stones in LIBS graphs. It revealed semi-quantitative information about patina layer on the specimens to estimate its thickness. The same elements were determined by SEM-EDX mapping on the cross sections of the samples separately on the studied marble and travertine samples.

The results of the preliminary tests showed that in-depth analyzing (Figure 2.9(b)) was a suitable technique to have proper results using 40 mj for LIBS analyses with the experimental parameters in Table 2.4. With the given parameters, each laser shot with 40mj caused the formation of a 1 $\mu$ m depth crater on the surface of the calcareous stone samples which would be later used for the evaluation of thickness of patina during in-depth analyses.

Table 2.4. Experimental parameters used in LIBS analyses

|                       |             |
|-----------------------|-------------|
| <b>Laser energy</b>   | 40mj        |
| <b>Single Shot hd</b> | 1000ns      |
| <b>tg</b>             | 200 $\mu$ s |
| <b>gain</b>           | 100         |

The absorbed water, organic material and CO<sub>2</sub> contents of the materials were determined by thermogravimetric analysis (TGA) due to the weight loss of the materials. These results helped to evaluate the chemical composition of the materials which were also determined by SEM-EDX and LIBS analyses.

For TGA analysis, the prepared powder samples, less than 53 $\mu$ m, were analyzed using Perkin Elmer Diomand TG/DTA in static nitrogen atmosphere at a temperature range of 25-1000 °C with a heating rate of 10°C/min.

## CHAPTER 3

### RESULTS AND DISCUSSION

In this chapter, mineralogical composition, micro structural and chemical characteristics of marble, travertine and yellow patina that formed on their surfaces are expressed and discussed for the purpose of their conservation.

#### **3.1. Mineralogical and Chemical Compositions of Marble and Travertine**

Mineralogical and chemical composition of marble and travertine stones were determined by XRD and SEM-EDX analyses.

XRD analyses indicated that marble is composed of primarily calcite minerals (Figure 3.1). Also, quartz was determined according to the results of XRD analyses of marble specimens (Figure 3.1). Marble is mainly composed of CaO with the ratio of 94% and over (Figure 3.2). The minor elements are determined as MgO, Al<sub>2</sub>O<sub>3</sub>, SiO<sub>2</sub>, SO<sub>3</sub>, K<sub>2</sub>O, FeO and P<sub>2</sub>O<sub>5</sub> within the range of 0.2 and 3 in sound marble samples (Figure 3.2).

Similarly with marble, travertine is mainly composed of calcite minerals as a calcareous stone. In addition to this, quartz is also present in the XRD spectrums of travertine samples (Figure 3.3). CaO is the major element with 89% approximately. MgO, Al<sub>2</sub>O<sub>3</sub>, SiO<sub>2</sub>, K<sub>2</sub>O, SO<sub>3</sub>, FeO and P<sub>2</sub>O<sub>5</sub> are the minor elements determined in the SEM-EDX analyses of sound travertine samples with the varying percentages between 0.05 and 4.5 (Figure 3.4).

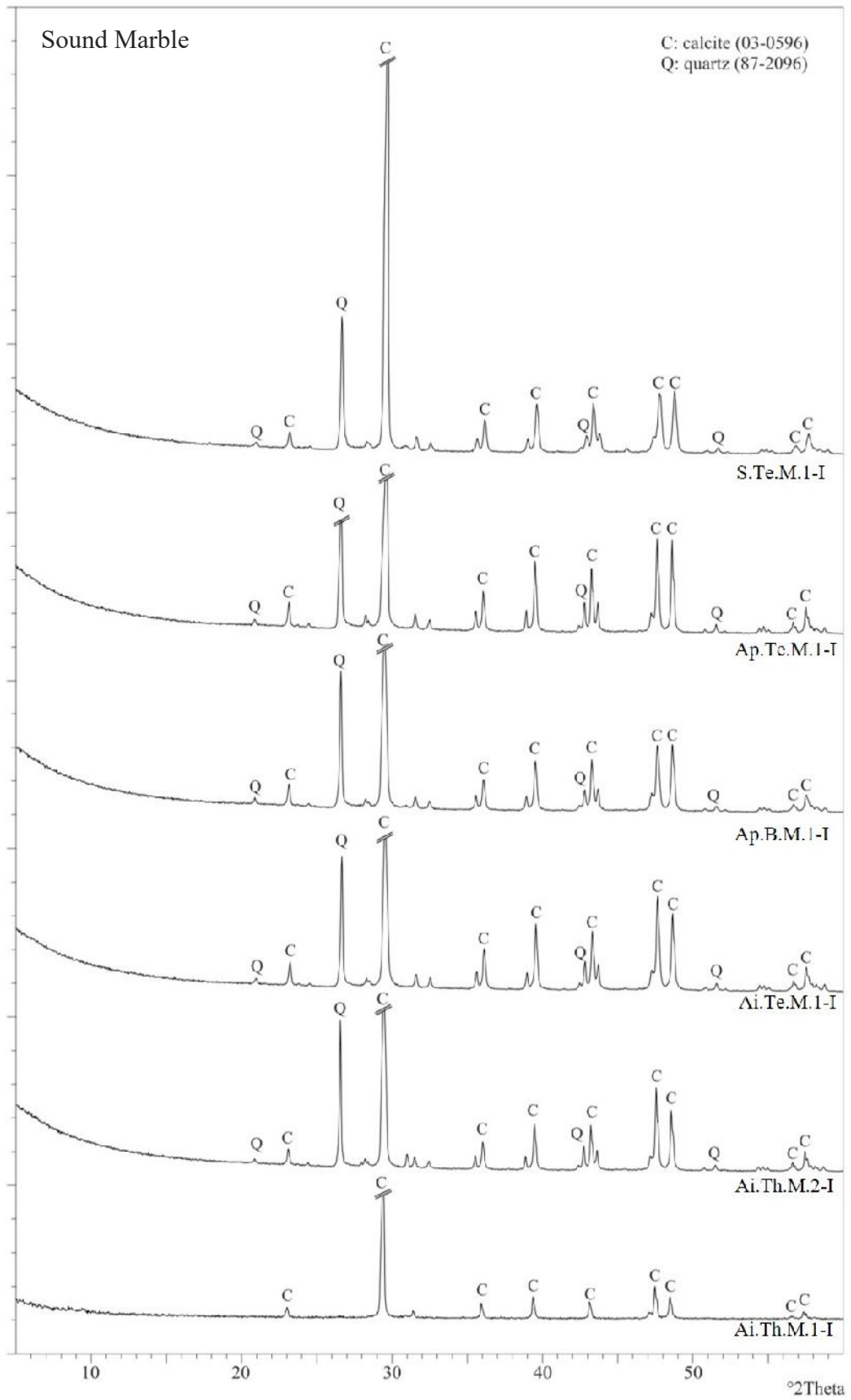


Figure 3.1. XRD patterns of sound inner cores of marble samples collected from various buildings in Aizanoi, Aphrodisias and Sardes archaeological sites

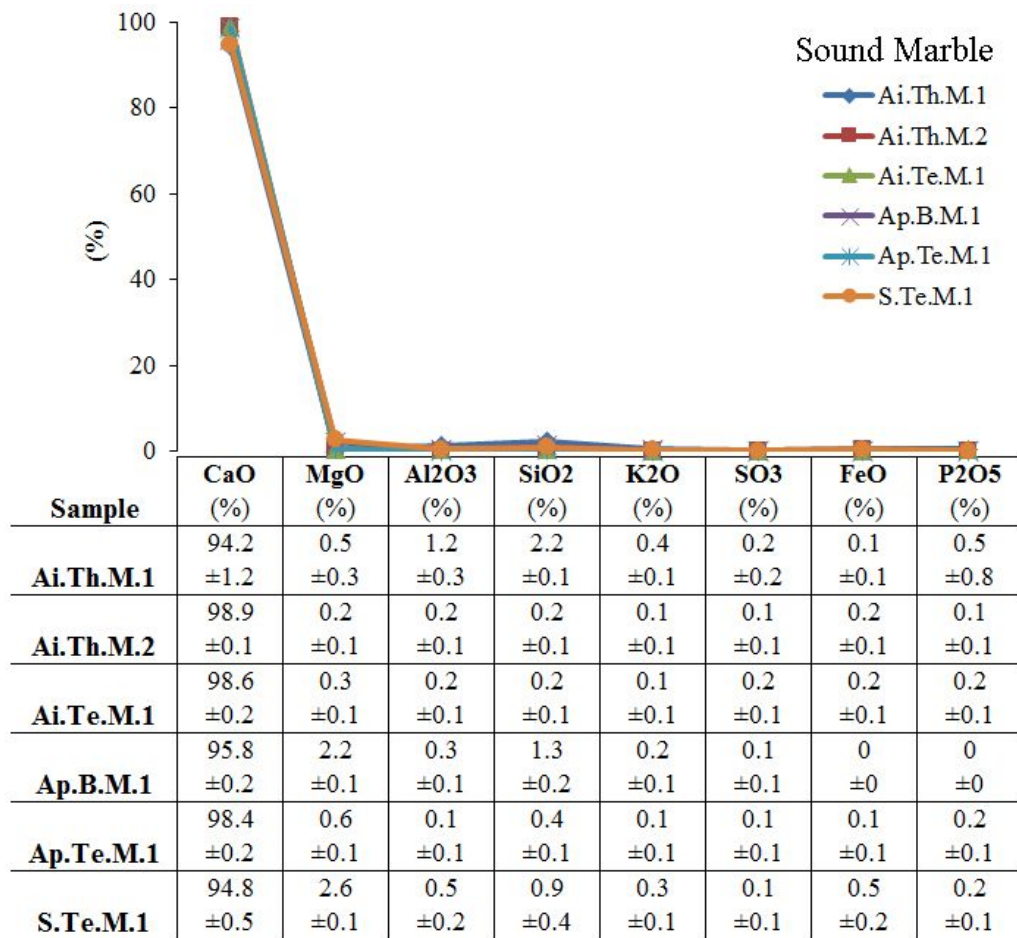


Figure 3.2. The amounts of major and minor elements in sound inner cores of marble

Marble and travertine are mentioned as carbonate stones in the literature (Press and Siever 2002). Thus, the presences of calcite minerals are related with the material characteristics of these two types of calcite rich carbonate stones.

The chemical composition of marble and travertine samples are in accordance with the mineralogical compositions representing calcite minerals as the main material of studied calcareous stones. When the mineralogical composition of marble and yellow travertine are considered, calcite crystals compose more than 90% of calcareous stone materials which is the main source of CaO (Press and Siever 2002). As a proof of this, the coarse grained calcite crystals were clearly observed in the magnified SEM images of sound inner cores of studied marble and travertine samples. The calcite crystals are well interlocked with each other in marble samples (Figure 3.5(a)). However, travertine is more porous than marble as observed from the bounding and microstructure of calcite crystals of both stone types (Figure 3.5).

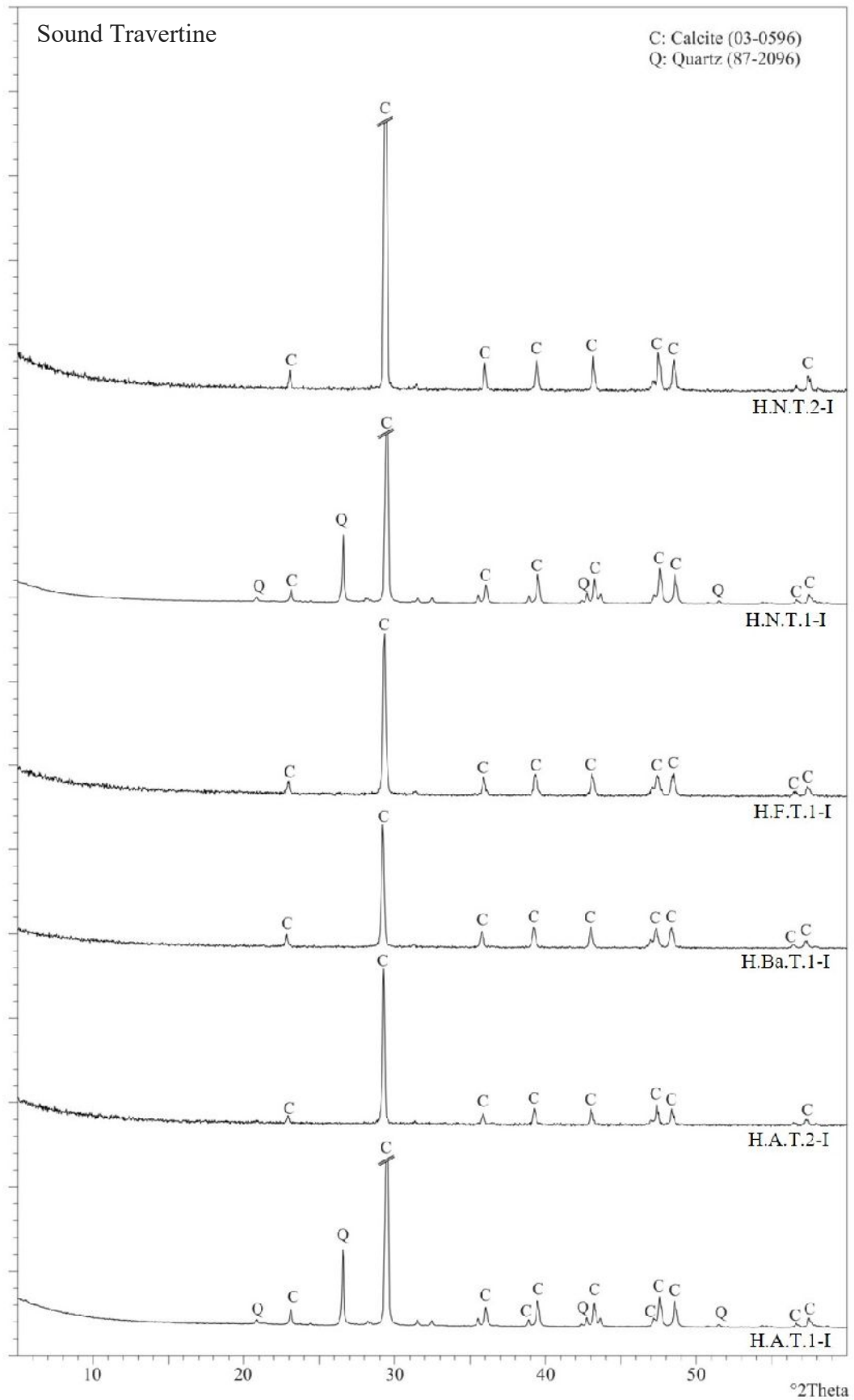


Figure 3.3. XRD patterns of sound inner cores of travertine samples collected from various buildings in Hierapolis archaeological site

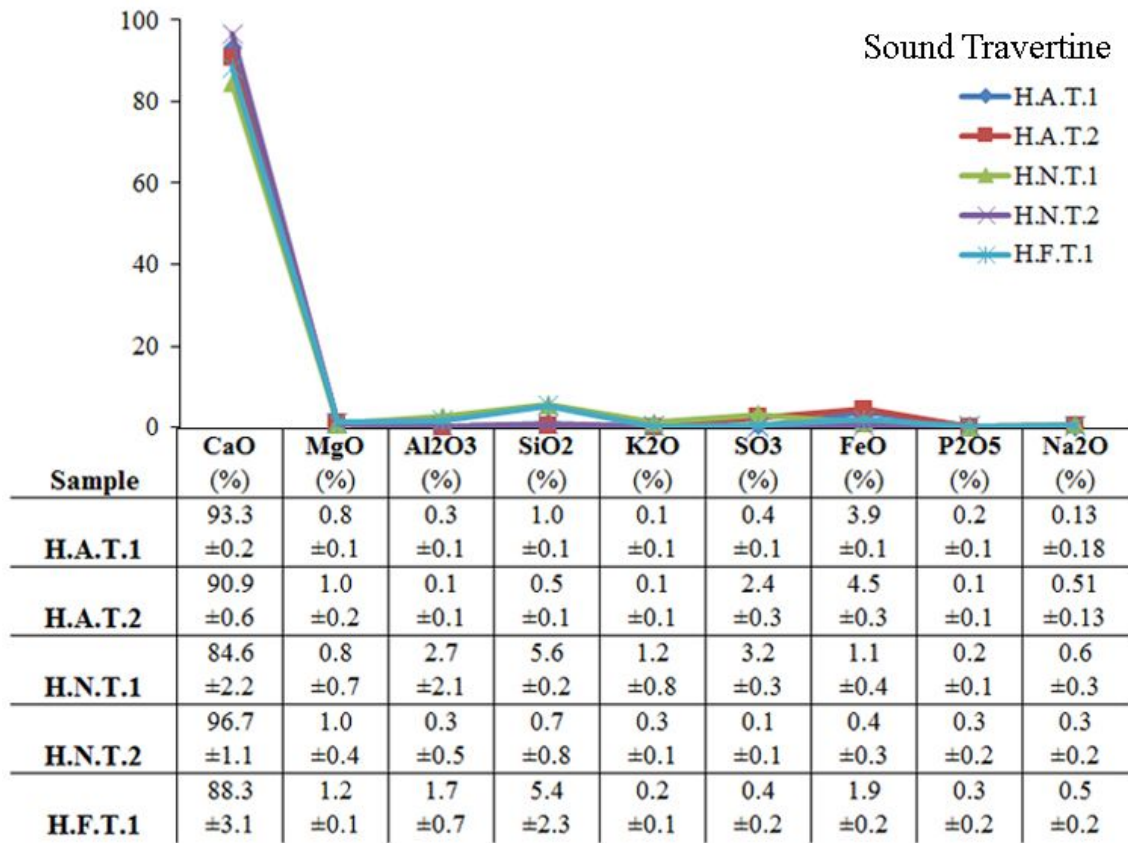


Figure 3.4. The amounts of major and minor elements in sound inner cores of travertine

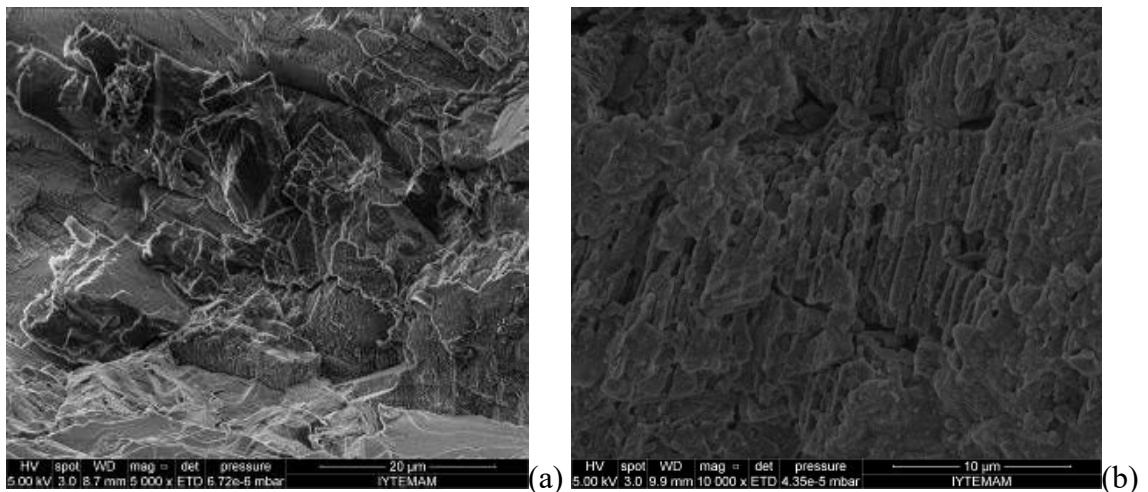


Figure 3.5. Calcite crystals of sound inner cores of marble (Ai.Te.M.1) (a) and travertine (H.N.T.1) (b)

## **3.2. Characteristics of Patina on Marble and Travertine**

The properties of yellow patina samples formed on stone surfaces show some differences with respect to the sound inner cores of marble and travertine. In this part of the study, the mineralogical composition, microstructural and chemical characteristics of patina formation were determined to have a better understanding of properties of yellow patina formation on marble and travertine surfaces for the purpose of their conservation in the archaeological sites.

Mineralogical composition of the samples were determined by XRD and FT-IR analyses of collected patina samples.

Microstructural characteristics were deciphered by magnified SEM images. Chemical composition and in-depth analyses were determined by SEM-EDX, TGA and LIBS analyses.

### **3.2.1. Mineralogical Composition of Yellow Patina**

The XRD patterns indicated that the yellow patina formed on marble surfaces collected from Aizanoi and Aphrodisias are mainly composed of calcium oxalate in the form of weddellite ( $\text{CaC}_2\text{O}_4 \cdot 2\text{H}_2\text{O}$ ) or whewellite ( $\text{CaC}_2\text{O}_4 \cdot \text{H}_2\text{O}$ ), gypsum ( $\text{CaSO}_4 \cdot 2\text{H}_2\text{O}$ ), quartz ( $\text{SiO}_2$ ), and calcite ( $\text{CaCO}_3$ ) minerals in general (Figure 3.6). Brushite ( $\text{CaHPO}_4 \cdot 2\text{H}_2\text{O}$ ) was also determined in one of the yellow patina samples collected from the marble wall of Zeus Temple in Aizanoi (Figure 3.6). Similarly, whewellite, gypsum, quartz and calcite minerals were observed on the XRD patterns of yellow patina on travertine samples collected from Hierapolis archaeological site (Figure 3.7). Calcite and quartz were the only minerals present in the XRD patterns of patina samples on marble collected from temple in Sardis and on travertine collected from fountain in Hierapolis (Figure 3.6, Figure 3.7).

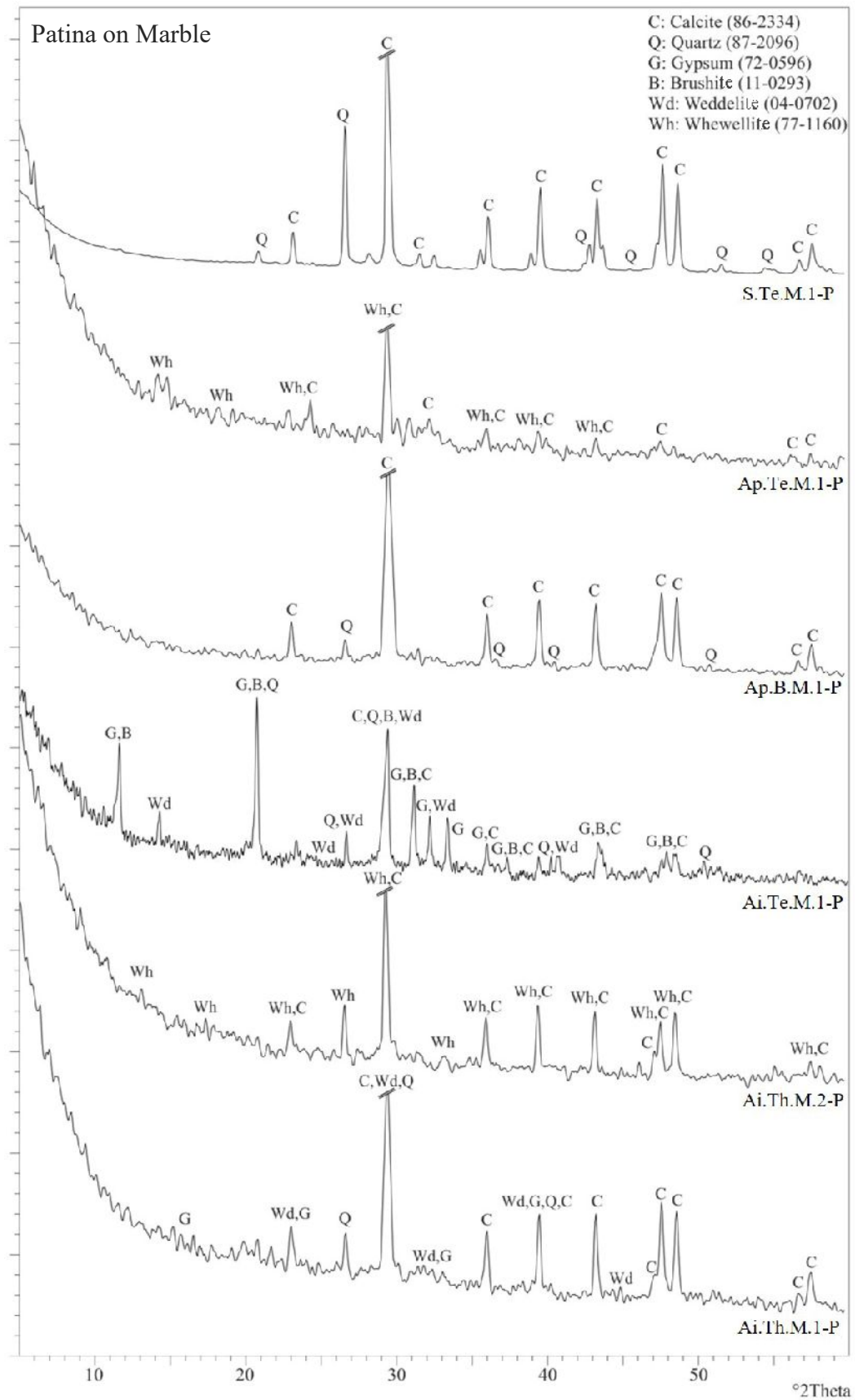


Figure 3.6. XRD patterns of patina samples formed on marble surfaces of various buildings in Aizanoi, Aphrodisias and Sardes archaeological sites

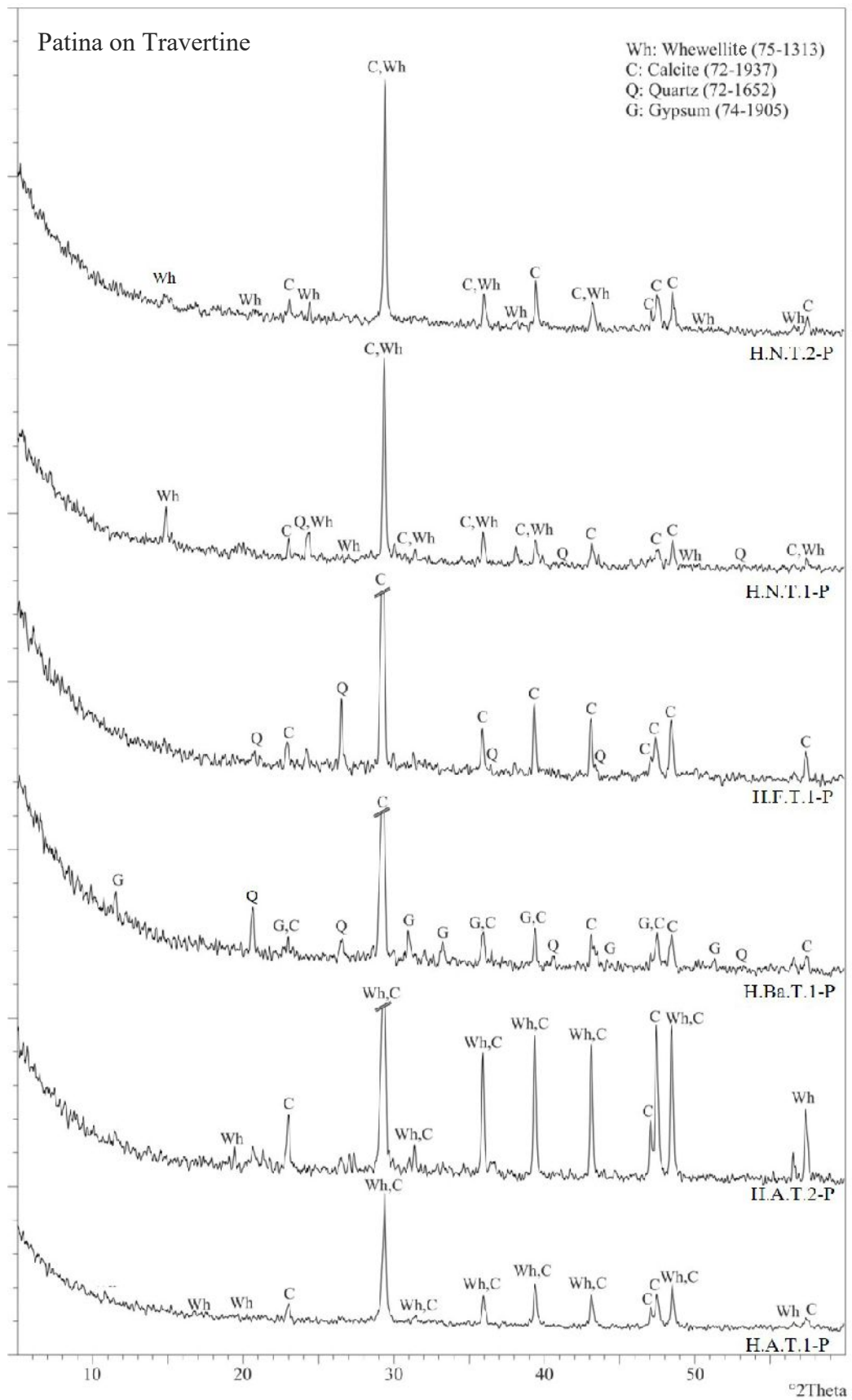


Figure 3.7. XRD patterns of patina samples formed on travertine surfaces of various buildings in Hierapolis archaeological site

The mineralogical composition of yellow patina was also determined by FT-IR (Figure 3.8, Figure 3.9). FT-IR results of the same marble and travertine samples presented one form of hydrated oxalate as whewellite characterized by the bands at around 1635, 1323 and 783  $\text{cm}^{-1}$  (Figure 3.8, Figure 3.9). Two of the prominent bands at 1635 and 1323  $\text{cm}^{-1}$  are related with  $\text{OH}^-$  vibrations and  $\text{C}=\text{O}$  stretching presenting in whewellite (Rodriguez et.al. 2011). The absorbance bands at around 2925, 2927 and 2850  $\text{cm}^{-1}$  are assigned to C-H stretching showing the presence of organic compounds in the patina which may be the sign of biologic tissues in the stones. The stretching and bending vibrations of calcite ( $\text{CaCO}_3$ ) with the bands at  $\sim 2513$ , 1797, 1430, 876, 712  $\text{cm}^{-1}$  and quartz ( $\text{SiO}_2$ ) at  $\sim 1031$   $\text{cm}^{-1}$  were also observed. Hence, these bands are ascribed to carbonates at around 1430  $\text{cm}^{-1}$ , and to silicates at around  $\sim 1030$   $\text{cm}^{-1}$  in the previous studies (Rodriguez et.al. 2011). Gypsum was determined at 3546, 3409, 1146, 1119, 671, 470  $\text{cm}^{-1}$ . In addition, brushite is determined with the bands at 1054, 566  $\text{cm}^{-1}$  in the same yellow patina sample (Ai.Te.M.1) promoting its XRD results (Figure 3.8).

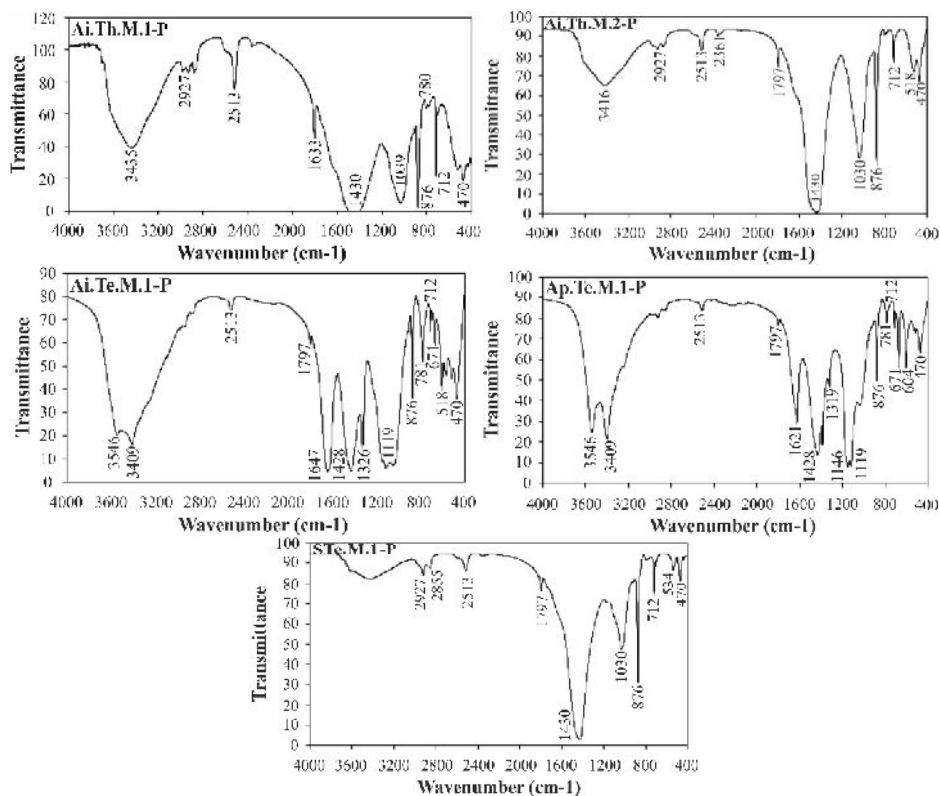


Figure 3.8. FT-IR graphs of patina samples on marble in Aizanoi, Aphrodisias and Sardes archaeological sites

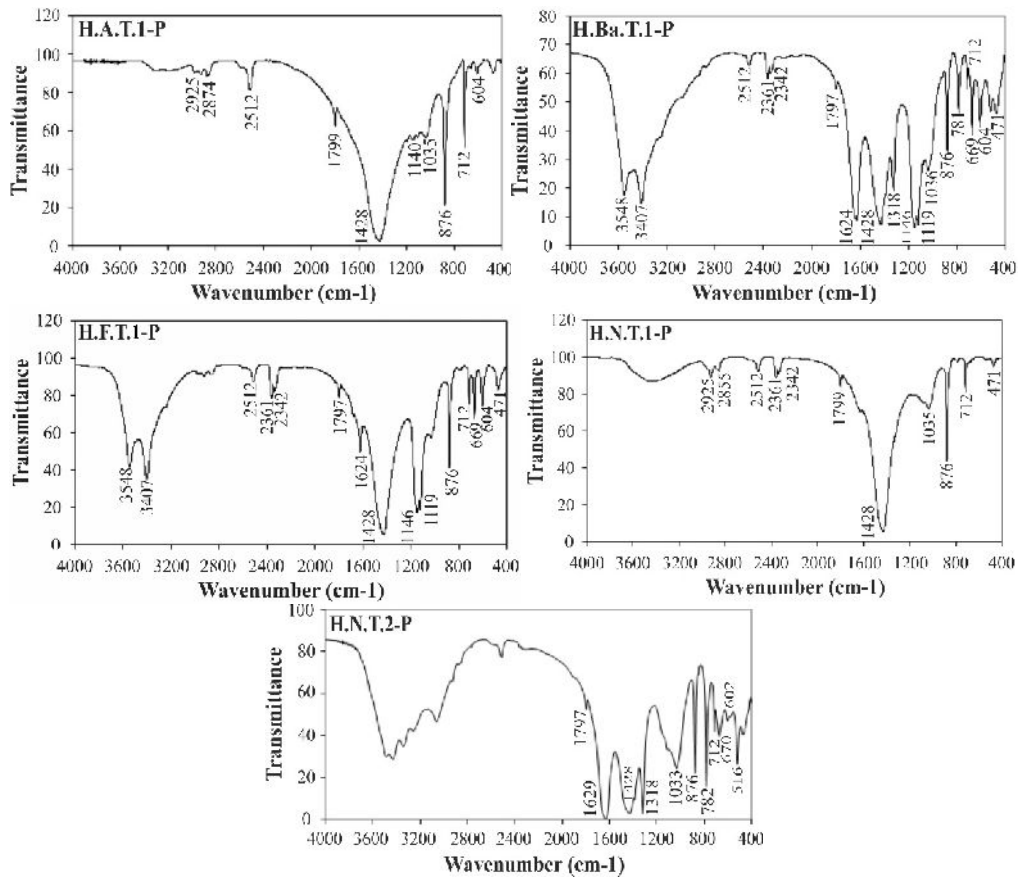


Figure 3.9. FT-IR graphs of patina samples on travertine in Hierapolis archaeological site

The yellow patina was found to be composed of mainly calcium oxalate (whewellite or weddellite), gypsum, quartz and calcite in the previous studies (Table 3.1). But further, brushite, kaolinite, hydroxyapatite, hematite, potassium, feldspar, clays, dolomite, smectite, halite, fluorite were determined in some of them (Table 3.1). Among all, the minerals such as calcium oxalate, gypsum, quartz and calcite are in accordance with the XRD and FT-IR results of marble and travertine surfaces in this study (Table 3.2). Calcium oxalate is the major constituent of yellow patina. It was determined on four of six marble surfaces (Table 3.2). Yellow patina is not perceived on yellow travertine by naked eye because of the original color of the stone. However, it has similar mineralogical composition with yellow colored marble surfaces including calcium oxalate as the major constituent in travertine surfaces.

The yellow colored calcium oxalate was formed as a result of the chemical change of marble and travertine surfaces. The origin of calcium oxalate is explained with two

major causes as biological and anthropogenic factors in the previous studies (Del Monte and Sabbioni 1987, Lazzarini and Salvadori 1989). At first case, the oxalic acid produced by the biological agents reacts with calcium carbonate (Del Monte and Sabbioni 1987). In the second case, the previously applied man-made coatings including calcium caseinate, egg protein, and animal glue etc. weathers chemically (Lazzarini and Salvadori 1989). In both cases, calcium oxalate layer is formed on the calcareous stone surfaces as a result of the weathering.

Gypsum is observed on two monuments located in Aizanoi and one monument in Aphrodisias. Gypsum is a weathering product of chemical reaction observed on calcareous stones located in an air polluted atmosphere (Böke 2003). Thus, it can be considered as a sign of air pollution in Aphrodisias and Aizanoi archaeological sites. The gypsum formation on calcareous stone surfaces necessitates taking environmental precautions for air pollution in the mentioned archaeological sites.

Quartz is probably carried to the stone surface with clays deposited on the surfaces of stones. Clay deposition may be transferred to the surface of the stone by external factors such as wind or water etc (Polikreti and Maniatis 2003). The existence of clays on the exterior and the interior parts of the stone accelerates its weathering by swelling and providing accurate conditions for the growth of algae, lichen, moss, etc. which also cause physical and chemical weathering of original stone materials (Chen et al. 2000, Press and Siever 2002). Clays expand in moist environment and cause the formation of fissures and cracks in stone (Scherer 2006).

Brushite is observed only in one of the yellow patina samples collected from temple in Aizanoi (Table 3.2). It is not observed in the mineralogical analyses of the previously studied monuments and sites (Table 3.1). Brushite is formed at low pH by reaction of phosphate-rich solutions with marble granules as calcite at temperatures between 20-37°C (Tas 2011). It can be concluded that, this material may have formed as a result of chemical reaction of calcite crystals with phosphate in the presence of water.

Table 3.1. The mineralogical analyses results of yellow patina formation in literature

| The reference study          | Case Study Area or Building / (Century it was built)  | Stone Type         | Analyses Method      | Mineralogical composition of yellow patina formations                               |
|------------------------------|---|--------------------|----------------------|---|
| Del Monte and Sabbioni 1987  | 295 monuments, artifacts and natural outcrops in Rome (from various periods)  | Marble, Limestone  | XRD                  | Whewellite, weddelite, quartz, gypsum, calcite                                      |
| Lazzarini and Salvadori 1989 | Cathedral and Church of S.Zeno, Verona (12 <sup>th</sup> century AD)  | Marble             | XRD                  | Weddelite, quartz, gypsum, calcite  |
| Caner and Böke 1989          | Temple of Zeus Temple of Augustus, Turkey (25-20 BC)  | Marble             | XRD, FT-IR           | Whewellite Whewellite, weddelite  |
| Watchman 1991                | Oxalate rich crusts in Australia  | Siliceous rocks    | XRD, FT-IR           | Whewellite  |
| Fassina 1995                 | A Critani Pillars, Ca'd'Oro Façade (15 <sup>th</sup> century AD) Madonna dell'Orto Church (14 <sup>th</sup> century AD) | Marble             | XRD                  | Whewellite, gypsum, calcite, fluorite   |
| Garcia-Valles et al. 1997    | Tarragona Cathedral, Barcelona (12 <sup>th</sup> century AD)  | Limestone, Marble  | XRD, FT-IR, SEM      | Weddelite, quartz, gypsum, calcite, hydroxyapatite, halite                          |
| Garcia-Valles et al. 2000    | Belevi marble quarry, Ephesus, Turkey (14 <sup>th</sup> century BC)   | Marble             | XRD, FT-IR           | Weddelite, quartz, calcite,   |
| Zagari et.al. 2000           | Romanic Tower of Loches in France (11 <sup>th</sup> century AD)   | Limestone          | XRD                  | Quartz, gypsum, calcite, smectite, halite   |
| Bario et al. 2002            | Cathedral of Cleida, Spain (13-15 <sup>th</sup> century AD)   | Dolostone          | XRD                  | Weddelite, quartz, gypsum, calcite, dolomite  |
| Buergo and Gonzalez 2003     | Palacio de Nuevo Baztan (18 <sup>th</sup> century AD)   | Limestone          | XRD, FT-IR           | Calcium oxalate, calcite, quartz, gypsum, potassium, feldspar, clays                |
| Polikreti and Maniatis 2003  | Propylea in Acropolis, Athens (437 BC)  | Marble             | XRD                  | Quartz, calcite, hydroxyapatite   |
| Rampazzi et al. 2004         | Churches of San Pierino, San Fredione, San Michele (11-12 <sup>th</sup> century AD)                                     | Marble             | FT-IR                | Whewellite, gypsum, calcite, silicates,   |
| Kalaitzaki 2005              | Parthenon in Acropolis, Athens (5 <sup>th</sup> century BC)   | Marble             | XRD, FT-IR           | Whewellite, weddelite, quartz, gypsum, calcite, kaolinite, hydroxyapatite, hematite |
| Rodriguez et.al. 2011        | Romanesque Church of Torme (12 <sup>th</sup> century AD)  | Dolomite           | XRD                  | Weddelite, calcite, dolomite  |
| Pinna et al. 2015            | Church of Orsanmichele, Florence (15 <sup>th</sup> century AD)  | Marble             | FT-IR, Raman Spectr. | Weddelite, whewellite, gypsum, calcite  |
| <b>Badur 2017</b>            | Aizanoi & Aphrodisias, Hierapolis, Turkey (from various monuments and periods)  | Marble, Travertine | XRD, FT-IR           | Weddelite, whewellite, quartz, gypsum, calcite, brushite                            |

Table 3.2. The table representing the determined minerals in XRD and FT-IR analyses of patina on marble and travertine samples

| Sample Type       | Sample Name        | Minerals observed in XRD spectrums                   | Minerals determined in FT-IR spectrums      |
|-------------------|--------------------|--|---|
| <b>MARBLE</b>     | <b>Ai.Th.M.1_P</b> | Weddelite<br>Gypsum<br>Quartz<br>Calcite             | Whewellite<br>Calcite                       |
|                   | <b>Ai.Th.M.2_P</b> | Calcite<br>Whewellite                                | Calcite<br>Whewellite                       |
|                   | <b>Ai.Te.M.1_P</b> | Weddelite<br>Gypsum<br>Calcite<br>Quartz<br>Brushite | Whewellite<br>Gypsum<br>Calcite<br>Brushite |
|                   | <b>Ap.B.M.1_P</b>  | Quartz<br>Calcite                                    | -   |
|                   | <b>Ap.Te.M.1_P</b> | Whewellite<br>Calcite                                | Whewellite<br>Gypsum<br>Calcite             |
|                   | <b>S.Te.M.1_P</b>  | Quartz<br>Calcite                                    | Calcite                                     |
| <b>TRAVERTINE</b> | <b>H.A.T.1_P</b>   | Whewellite<br>Calcite                                | Calcite                                     |
|                   | <b>H.A.T.2_P</b>   | Whewellite<br>Calcite                                | Calcite<br>Gypsum                           |
|                   | <b>H.Ba.T.1_P</b>  | Gypsum<br>Quartz<br>Calcite                          | Weddelite<br>Gypsum<br>Quartz<br>Calcite    |
|                   | <b>H.F.T.1_P</b>   | Quartz<br>Calcite                                    | Gypsum<br>Quartz<br>Calcite                 |
|                   | <b>H.N.T.1_P</b>   | Whewellite<br>Quartz<br>Calcite                      | Whewellite<br>Calcite                       |
|                   | <b>H.N.T.2_P</b>   | Whewellite<br>Calcite                                | Weddelite<br>Gypsum<br>Quartz<br>Calcite    |

### 3.2.2. Microstructural Characteristics of Yellow Patina

The magnified SEM images of marble and travertine surfaces were investigated in detail to determine the microstructural characteristics and thickness of yellow patina formed on calcite crystals of marble and travertine.

The coarse grained calcite crystals were observed in the magnified SEM images of sound inner cores of both of the stone types (Figure 3.10 (a)). The well interlocked coarse grained calcite crystals of marble are covered with leaf shaped euhedral calcium oxalate crystals forming a homogeneous nodular surface on the original stone substrata (Figure 3.10 (a, b), Figure 3.11(a)). It is clearly observed as a film layer on magnified SEM images of marble (Figure 3.11(a)).

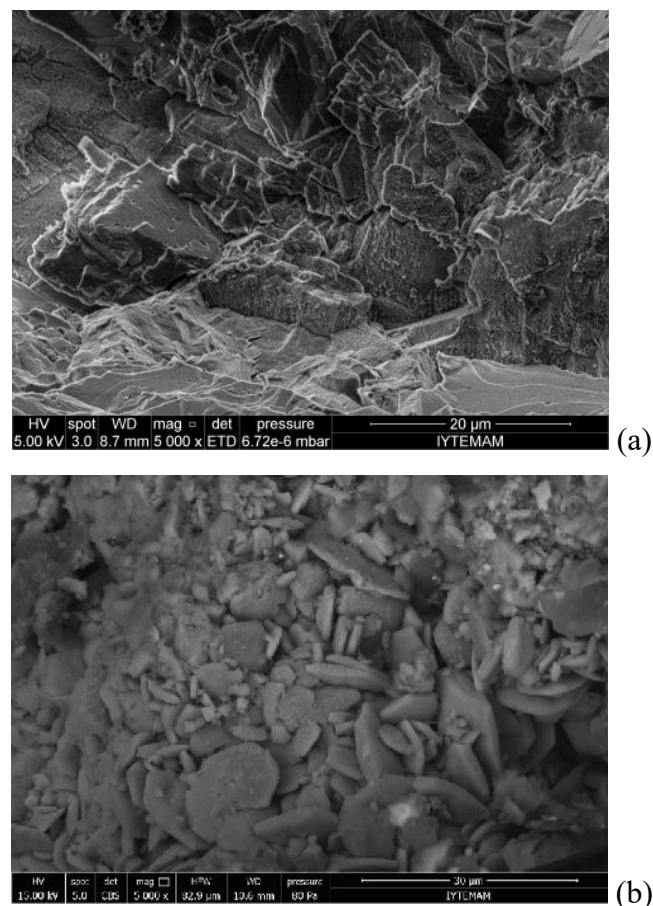


Figure 3.10. SEM images of one representative marble sample (Ai.Te.M.1) showing calcite (a) and calcium oxalate crystals formed on it (b)

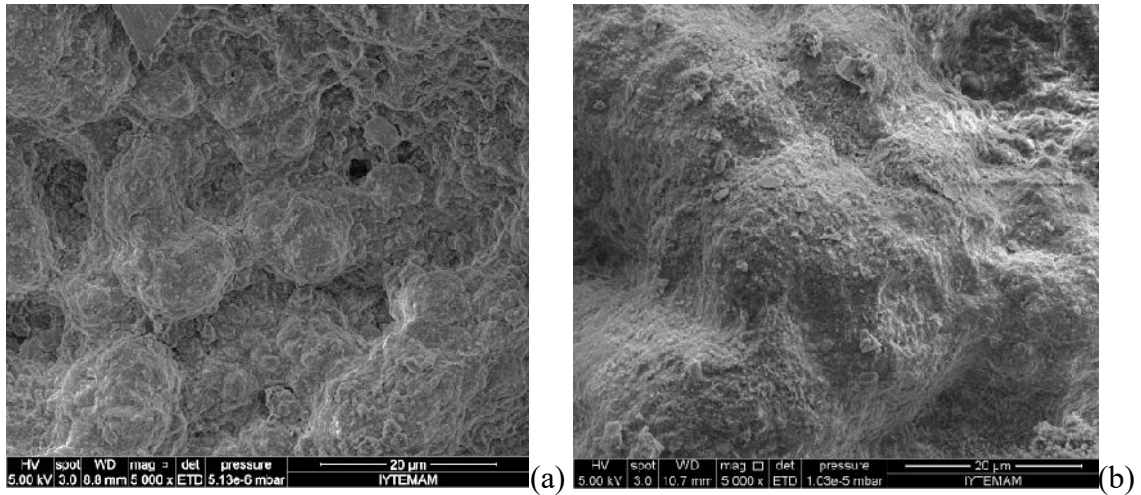


Figure 3.11. Magnified SEM images showing the outer nodular appearance of calcium oxalate layer on marble (Ai.Th.M.1 (a)) and travertine (H.N.T.1 (b))

Calcium oxalate formation could not be distinguished by naked eye on yellow travertine surfaces because of its color. However, the thin patina layer was determined on the magnified SEM-EDX images of yellow travertine surfaces representing same microstructural characteristics with the patina layer formed on marble surfaces (Figure 3.11(b)). According to the SEM images of travertine surfaces, it forms a smooth and nodular surface covering the crystals of porous substratum of travertine (Figure 3.11(b)). The same microstructure is also observed as depositions in the pores, even at the inner cores of some travertine samples because of the porous micro structural characteristic of stone (Figure 3.12(c)). It is not well interlocked with the stone which have cavities and fissures at the intersection zone of patina and inner parts (Figure 3.12(d)).

The microstructural studies of patina formation included the determination of thickness of the patina layer formed both on marble and travertine surfaces. The thickness of the samples were measured from the broken parts of the samples by the help of visual analyses to decide the beginning and end of the patina layer from the magnified SEM sections of each sample. It was able to be measured on four marble samples. It was between 78-123 µm (Figure 3.13 (a)); 95-243 µm (Figure 3.13 (b)); 76-164 µm (Figure 3.13 (c)) and around 54 µm (Figure 3.13 (d)) on marble samples. The thickness of the patina could not be observed on SEM images of marble samples of Bouleuterion in Aphrodisias and temple in Sardes although they are yellow in color.

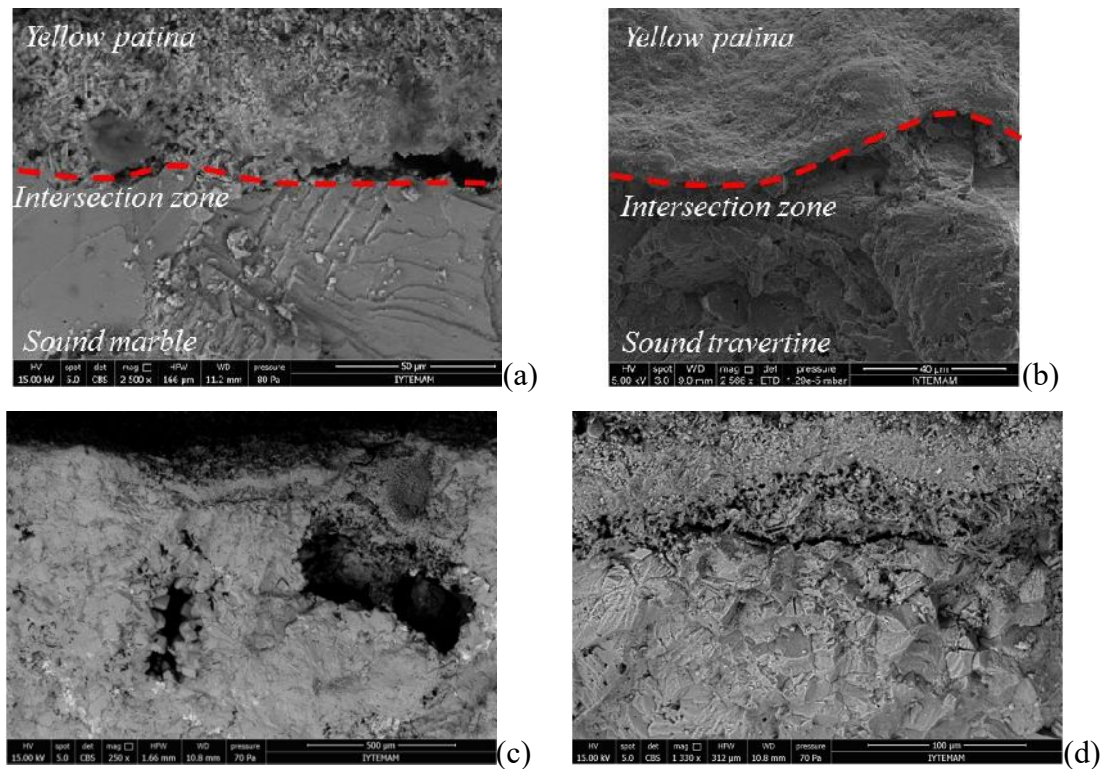


Figure 3.12. SEM images of yellow patina on marble (Ai.Th.M.1 (a)) and travertine surfaces (H.N.T.1 (b)), sections representing the yellow patina, inner core and intersection of both (H.Ba.T.1 (c, d))

The thickness of the yellow patina was able to be determined on only three of the travertine samples on magnified SEM images. It was between 73-154  $\mu\text{m}$  (Figure 3.14 (a)) and around 55  $\mu\text{m}$  (Figure 3.14(b)) on two of the travertine samples. The thinnest layer has 6  $\mu\text{m}$  thickness among all stone samples (Figure 3.14(c)).

The results of magnified SEM images indicate that the thickness of yellow patina layer varies between 6 and 250 $\mu\text{m}$  on marble and travertine surfaces (Table 3.3). The thickness of yellow patina was determined in the previous studies on different cases in the literature. These studies were focused on yellow patina formed on dolostone, limestone and mostly marble. The results of these studies are in agreement with the thicknesses of yellow patina determined on the studied marble and travertine surfaces varying in a wide range with the thickness of 10 to 500  $\mu\text{m}$  according to the optic microscope and SEM-EDX results (Table 3.4). Hence, the thickness of patina formation may vary due to the period of aging, microclimatic and environmental factors, the type of the original stone material etc. which should be investigated in a more comprehensive way in the following studies.

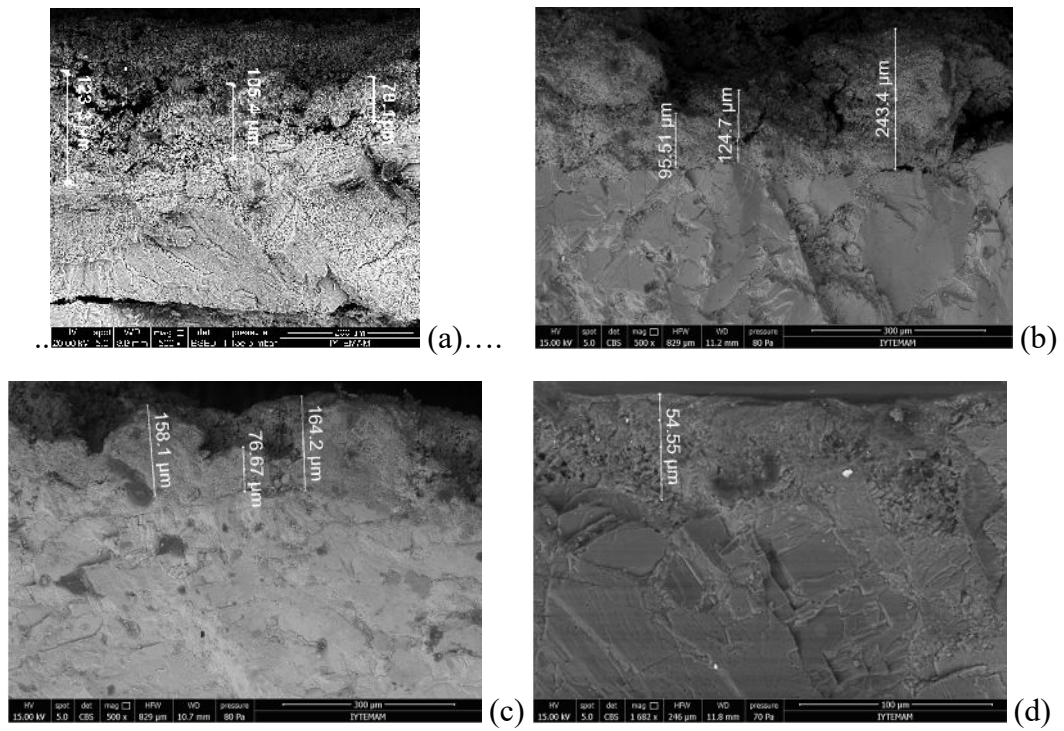


Figure 3.13. SEM images of the intersection of marble and patina with its thickness (Ai.Th.M.1 (a), Ai.Th.M.2 (b), Ai.Te.M.1 (c), Ap.Te.M.1 (d))

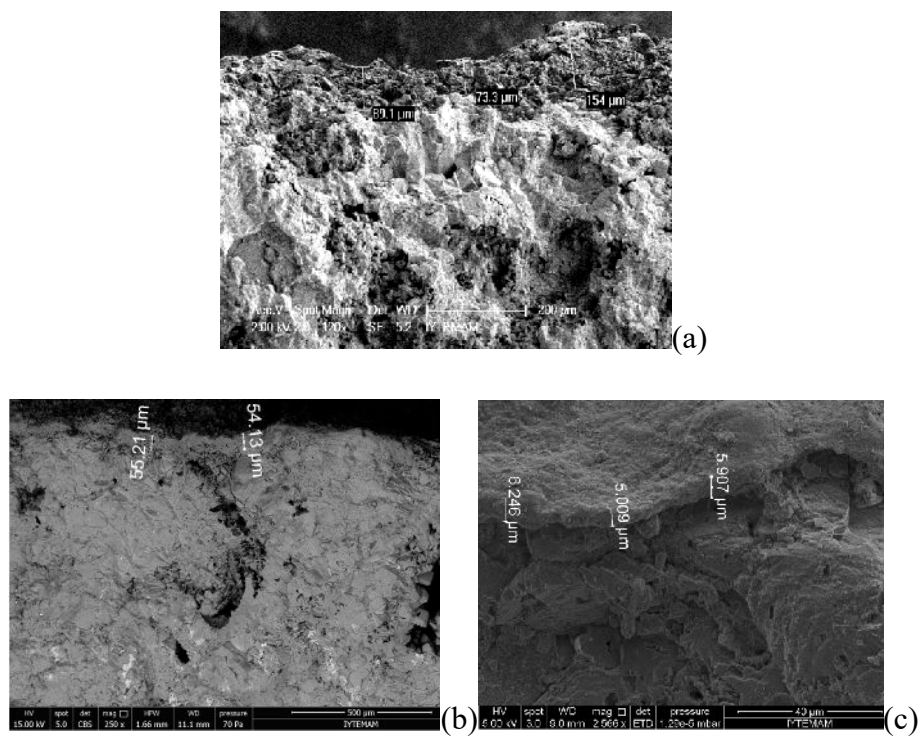


Figure 3.14. SEM images of the intersection of travertine and patina with its thickness (H.A.T.1 (a), H.Ba.T.1 (b), H.N.T.1 (c))

Table 3.3. The thickness of yellow patina determined in SEM-EDX analyses

| Stone type | Sample    | Thickness of the patina samples ( $\mu\text{m}$ ) |
|------------|-----------|---|
| Marble     | Ai.Th.M.1 | ~78-105   |
|            | Ai.Th.M.2 | ~95-243   |
|            | Ai.Te.M.1 | ~76-164   |
|            | Ap.Te.M.1 | ~54   |
|            | Ap.B.M.1  | -   |
| Travertine | H.A.T.1   | ~ 73-154  |
|            | H.A.T.2   | -   |
|            | H.Ba.T.1  | -   |
|            | H.N.T.1   | ~ 55  |
|            | H.F.T.1   | ~ 6   |

Table 3.4. The thickness of yellow patina determined in literature survey

| The reference study         | Case Study Area or Building / (Century it was built)   | Stone type        | Analyses Method       | Thickness of yellow patina formation ( $\mu\text{m}$ ) |
|-----------------------------|--|-------------------|-----------------------|--|
| Fassina 1995                | A Critani Pillars, Ca'd'Oro Façade (15 <sup>th</sup> century AD)<br>Madonna dell'Orto Church (14 <sup>th</sup> century AD) | Marble            | SEM-EDX               | ~110-150   |
| Garcia - Valles et al. 1997 | Tarragona Cathedral, Barcelona (12 <sup>th</sup> century AD)   | Limestone, Marble | SEM, Optic microscope | ~100-200   |
| Garcia - Valles et al. 2000 | Belevi marble quarry, Ephesus, Turkey (14 <sup>th</sup> century BC)  | Marble            | Optic microscope      | ~10-300  |
| Barrio et al. 2002          | Cathedral of Cleida, Spain (13-15 <sup>th</sup> century AD)  | Dolostone         | SEM, Optic microscope | ~100-500   |
| Buergo Gonzales 2003        | Palacio de Nuevo Baztan (18 <sup>th</sup> century AD)  | Limestone         | SEM, Optic microscope | ~ 80-200   |
| Rampazzi et al. 2004        | Churches of San Pierino, San Fredione, San Michele (11-12 <sup>th</sup> century AD)  | Marble            | SEM-EDX               | ~ 60-200   |
| Kalaitzaki 2005             | Parthenon in Acropolis, Athens (5 <sup>th</sup> century BC)  | Marble            | Optic microscope      | ~100-150   |

### 3.2.3. Chemical Composition of Yellow Patina

The chemical composition of the yellow patina samples were determined by SEM-EDX, TGA and LIBS analyses. The results of LIBS analyses were also checked by in-depth profiling in order to determine the elemental distribution of yellow patina from surface to the sound inner cores with respect to its thickness on stones.

The SEM-EDX results of yellow patina on marble revealed that the patina is composed of CaO (11-64%), MgO (~4%), Al<sub>2</sub>O<sub>3</sub> (3-15%), SiO<sub>2</sub> (19-46%) and FeO (1.5-25%). SO<sub>3</sub> is observed only in two of the samples taken from temples in Aizanoi (29%) and Aphrodisias (11%) (Figure 3.15). SEM-EDX results of yellow patina on travertine resembled the results of patina on marble. According to the SEM-EDX results, yellow patina on travertine is composed of CaO (37-87%), MgO (~3%), Al<sub>2</sub>O<sub>3</sub> (0.3-11%), SiO<sub>2</sub> (0.3-36%), FeO (1-11%) and SO<sub>3</sub> (1-3%). Among all, one travertine sample, which was taken from bath, represents high percentage of SO<sub>3</sub> (~43%) (Figure 3.16). The presence of SO<sub>2</sub> (as wet and dry deposition on the surface of marble and travertine) may be related with air pollution in the studied site (Figure 3.15). It comes from the gypsum precipitation observed as black crust due to air pollution. It is formed on calcareous stones as a result of the reaction of SO<sub>2</sub> with calcium carbonate in the presence of water (Böke 2003). These findings are in agreement with previous studies carried out on yellow patina formation concentrating on marble surfaces of ancient monuments around the world (Table 3.5). Their results resemble with the results of this study with the high amounts of Ca and moderate amounts of Al, Si, S and Fe (Table 3.5).

When the results of sound inner cores and yellow patina samples are compared, Al, Si and Fe ratios are higher on the surfaces of stone samples according to sound inner cores (Figure 3.15, Figure 3.16). It is probably related with clay deposition on the surfaces of the stones.

The ratio of P (phosphorus) differs in some studies according to the SEM-EDX results of studied marble and travertine surfaces (Figure 3.15, Figure 3.16). The high (phosphorus) content (16-44%) is related with the weathering of man-made resins as calcium caseinate on stone surfaces for conservation purposes in the previous studies (Polikreti and Maniatis 2003, Fassina 1995, Lazzarini and Salvadori 1989) (Table 3.5). However, in this study, the P content (0-4.66%) is not close to the P content (16-44%) of the previously studied cases. It is most probably carried from the environment.

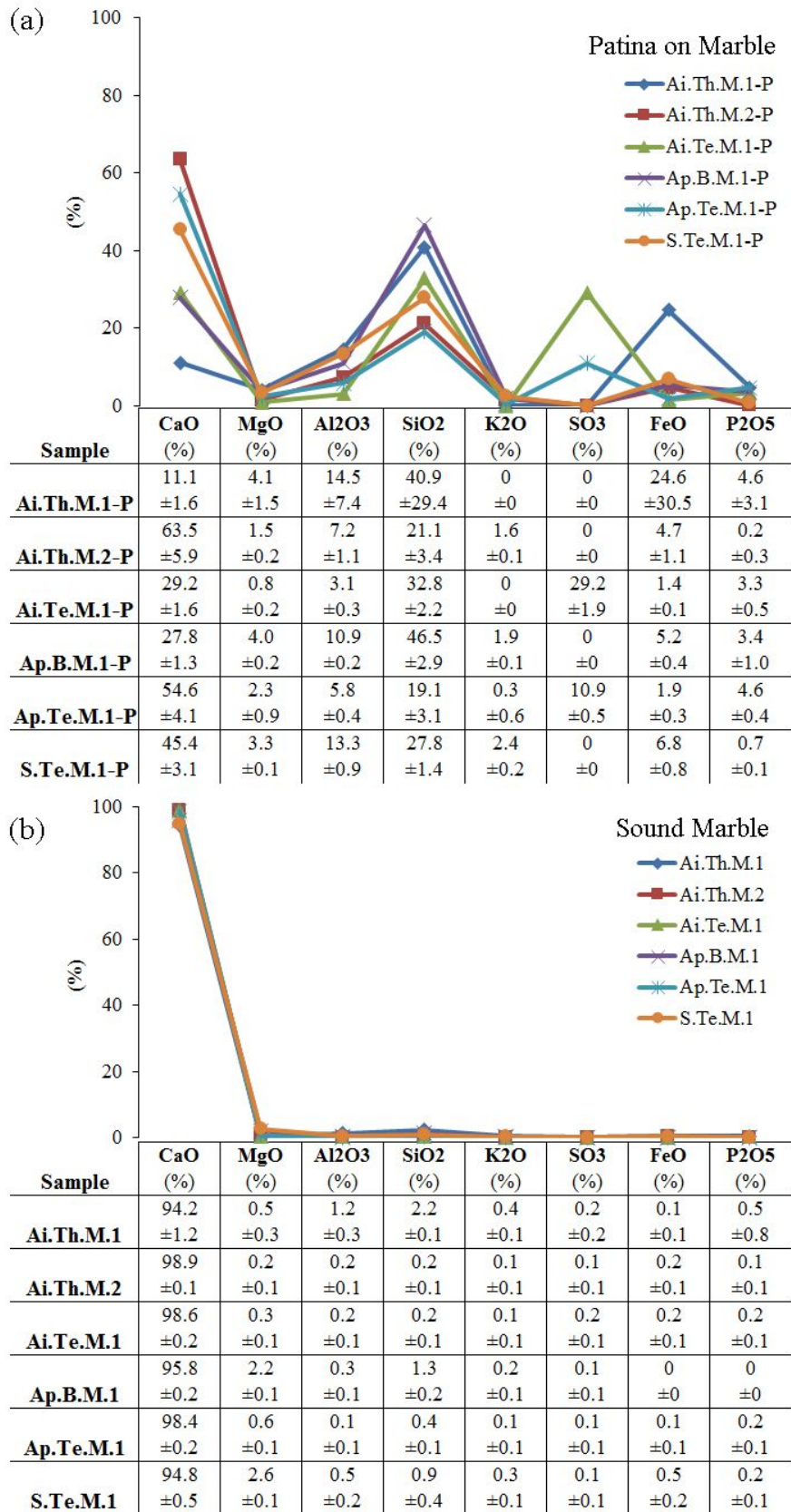


Figure 3.15. The amounts of major and minor elements in yellow patina formation (a) and sound inner cores (b) of marble samples

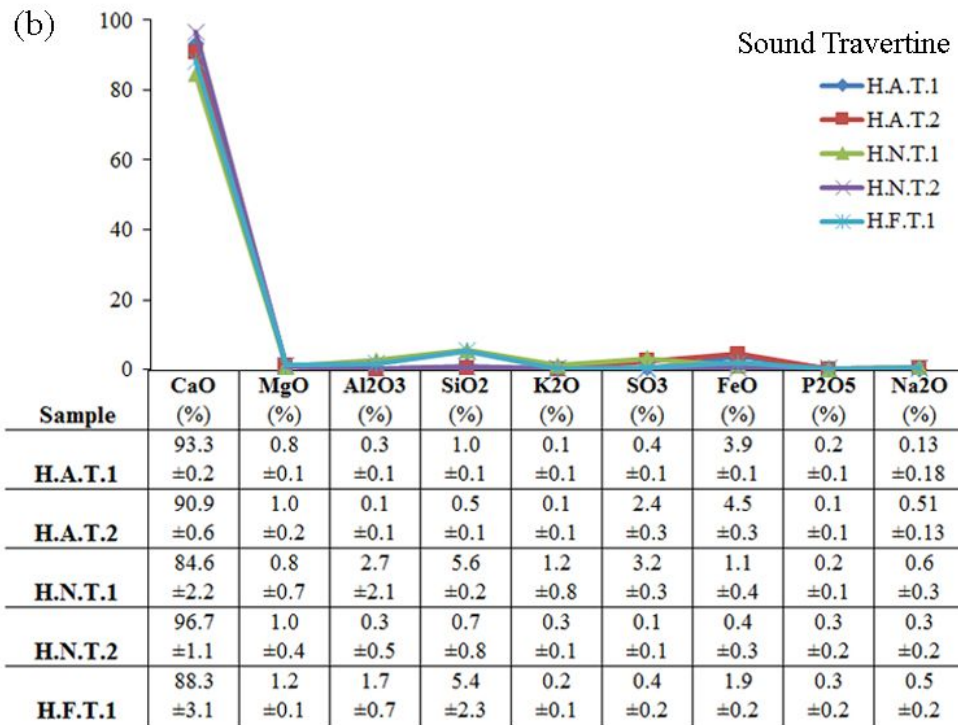
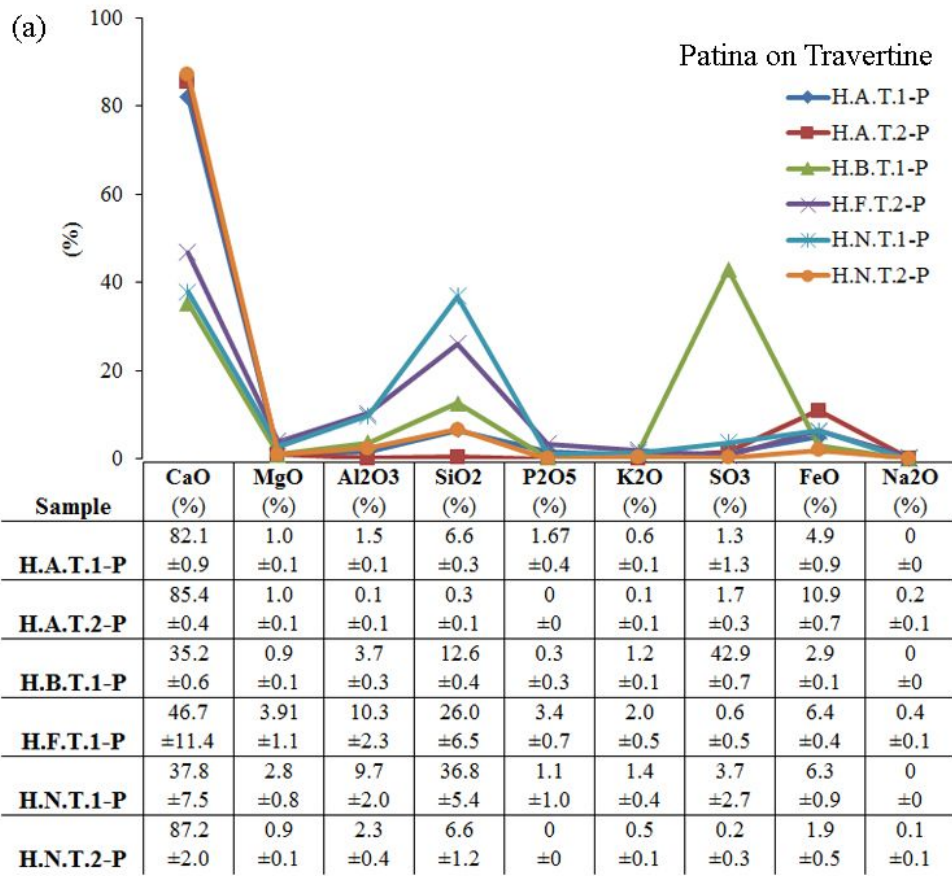


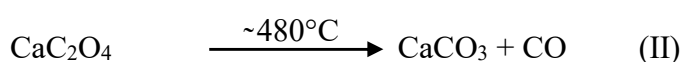
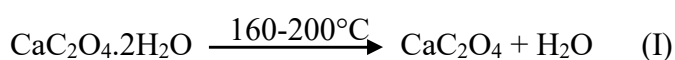
Figure 3.16. The amounts of major and minor elements in yellow patina formation (a) and sound inner cores (b) of travertine samples

Table 3.5. Comparison of chemical composition of yellow patina in some studies in the literature

| <b>The reference study</b>   | <b>Case Study Area / Building</b>  | <b>Stone Type</b> | <b>Analyses Method</b> | <b>CaO (%)</b> | <b>MgO (%)</b> | <b>Al<sub>2</sub>O<sub>3</sub> (%)</b> | <b>SiO<sub>2</sub> (%)</b> | <b>SO<sub>3</sub> (%)</b> | <b>FeO (%)</b> | <b>P<sub>2</sub>O<sub>5</sub> (%)</b> |
|------------------------------|--|-------------------|------------------------|----------------|----------------|--|----------------------------|---------------------------|----------------|---------------------------------------|
| Lazzarini and Salvadori 1989 | Arch of Titus (1 <sup>st</sup> century AD)   | Marble            | Microprobe Analyses    | –              | –              | 7.00                                   | 25.00                      | –                         | 5.00           | 20.00                                 |
| Fassina 1995;                | A Critani Pillars, Ca'd'Oro Façade (15 <sup>th</sup> century AD)<br>Madonna dell'Orto Church (14 <sup>th</sup> century AD) | Marble            | SEM-EDX                | 66.00          | –              | 29.00                                  | 22.00                      | 3.00                      | 4.42           | 16.2                                  |
| Garcia-Valles et al. 1997    | Tarragona Cathedral, Barcelona (12 <sup>th</sup> century AD)   | Limestone, Marble | SEM-EDX                | 55.86          | 0.40           | 5.23                                   | 20.58                      | 0.90                      | 4.42           | 8.64                                  |
| Polikreti and Maniatis 2003  | Propylea in Acropolis, Athens (437 BC)   | Marble            | SEM-EDX                | 50.40          | –              | 0.17                                   | 2.76                       | 2.19                      | –              | 44.3                                  |
| Kalaitzaki 2005              | Parthenon in Acropolis, Athens (5 <sup>th</sup> century BC)  | Marble            | SEM-EDX                | 56.54          | 0.60           | 29.00                                  | 22.50                      | 1.15                      | 4.69           | 6.86                                  |
| <b><i>Badur 2017</i></b>     | Aizanoi & Aphrodisias, Turkey (from various monuments and periods)   | Marble            | SEM-EDX                | <b>38.64</b>   | <b>2.68</b>    | <b>9.18</b>                            | <b>27.84</b>               | <b>6.70</b>               | <b>7.49</b>    | <b>2.84</b>                           |
| <b><i>Badur 2017</i></b>     | Hierapolis, Turkey<br>Aizanoi & Aphrodisias, Hierapolis, Turkey (from various monuments and periods)                       | Travertine        | SEM-EDX                | <b>62.47</b>   | <b>1.79</b>    | <b>4.64</b>                            | <b>14.86</b>               | <b>8.44</b>               | <b>5.59</b>    | <b>1.09</b>                           |

The chemical characteristics of the samples were investigated by TGA that were carried out for the determination of thermal behavior of same powder sample prepared by scratching the yellow patina sample from the marble and travertine surfaces.

The TGA results were in agreement with the mineralogical tests and SEM-EDX results of two marble (Ai.Te.M.1 and Ap.Te.M.1) and one travertine sample (H.Ba.T.1) representing the thermal behavior of calcium oxalate decomposition in TGA graphs (Figure 3.17, Figure 3.18). It is observed in three steps as follows (Rodriguez et.al. 2011):



The first weight loss was observed in the first step due to the initial loss of hygroscopic water in the material around 160-200°C. In the second step, CO and organic material is lost as a result of calcium oxalate combustion transformed into calcium carbonate around 480°C. Finally, CO<sub>2</sub> is lost as a result of thermal decomposition of calcium carbonate around 650°C as the last step of thermal decomposition process of calcium oxalate (Rodriguez et.al. 2011). Considering this, the weight losses of 5%, 7% and 15% were attributed to evolved water molecule, carbon monoxide and carbon dioxide respectively in calcium oxalate patina which was shown in Table 3.6 with the mentioned intervals in detail (Ai.Te.M.1, Ap.Te.M.1 and H.Ba.T.1) (Table 3.6).

The TGA graph of one travertine sample (H.F.T.1) differed from the other TGA graphs showing endothermic peaks at around 65°C and 240°C. It was related with the dehydration procedure of gypsum (Yu and Brouwers 2011). The weight loss of gypsum observed on the surface of H.F.T.1 occurred in two steps with 0.47 % and 2.55 % respectively due to the loss of hygroscopic water content and decomposition of CaSO<sub>4</sub>·0.5H<sub>2</sub>O to CaSO<sub>4</sub> respectively as it was explained with the reactions below. The presence of gypsum in the TGA graph of H.F.T.1-P is in accordance with the mineralogical and chemical analyses results of the same sample (Table 3.6, Figure 3.18). The weight loss with 27.25% content observed around 650°C have been caused by the decomposition of CaCO<sub>3</sub> presented in the same powder specimen scratched from the surface of travertine sample (Table 3.6, Figure 3.18).



The rest of the samples have similar TGA graphs representing the thermal behavior of calcite minerals (Ai.Th.M.1, Ap.B.M.1, S.Te.M.1, H.A.T.1, H.A.T.2 and H.N.T.1) (Figure 3.17, Figure 3.18). The weight losses were observed between 0.19% and 9.80 % at around 200°C and between 16% and 39% at around 650°C. These losses occur due to the loss of hygroscopic water content and combustion of calcium carbonate resulting with the removal of CO respectively in the TGA graphs of the mentioned samples in accordance with the mineralogical and chemical analyses results (Figure 3.17, Figure 3.18, Table 3.6)

Table 3.6. Weight losses of the samples during TGA analyses

| <b>Calcium oxalate</b>   | <b>~200°C</b> | <b>~480°C</b>    | <b>~650°C</b> |
|--------------------------|---------------|------------------|---------------|
| Ai.Te.M.1_P              | 5.61          | 6.32             | 10.32         |
| Ap.Te.M.1_P              | 3.98          | 8.12             | 16.08         |
| H.Ba.T.1_P               | 6.36          | 7.16             | 15.24         |
| <b>Gypsum</b>            | <b>~65°C</b>  | <b>105-240°C</b> | <b>~650°C</b> |
| H.F.T.1_P                | 0.47          | 2.55             | 27.25         |
| <b>Calcium carbonate</b> | <b>~200°C</b> |                  | <b>~650°C</b> |
| Ai.Th.M.1_P              | 9.80          |                  | 27.87         |
| Ai.Th.M.2_P              | 6.89          |                  | 16.24         |
| Ap.B.M.1                 | 5.38          |                  | 25.78         |
| S.Te.M.1                 | 4.79          |                  | 25.25         |
| H.A.T.1_P                | 0.19          |                  | 33.75         |
| H.A.T.2_P                | 0.66          |                  | 35.82         |
| H.N.T.1_P                | 2.35          |                  | 39.10         |

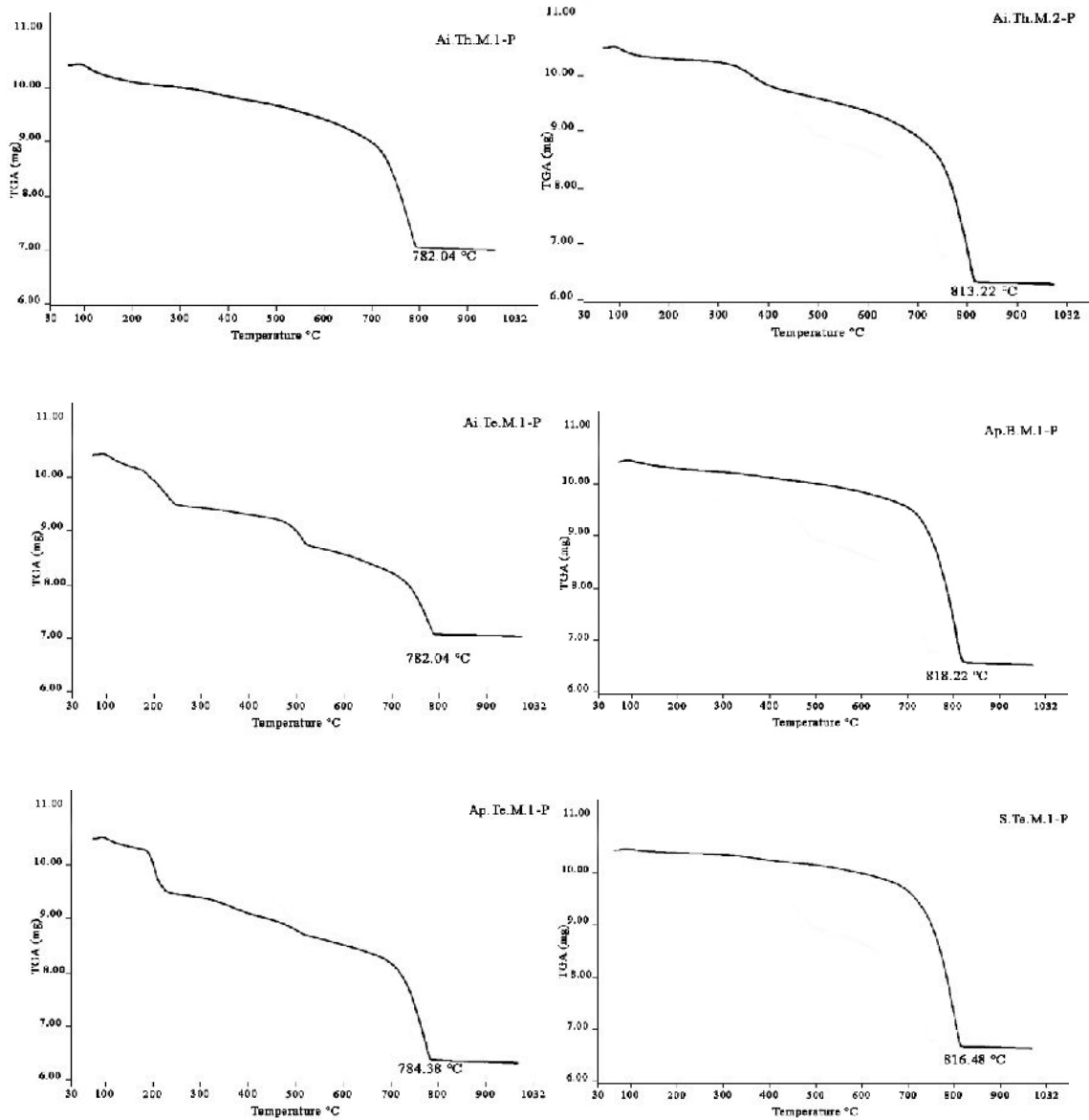


Figure 3.17. TGA graphs of patina samples taken from marble surfaces

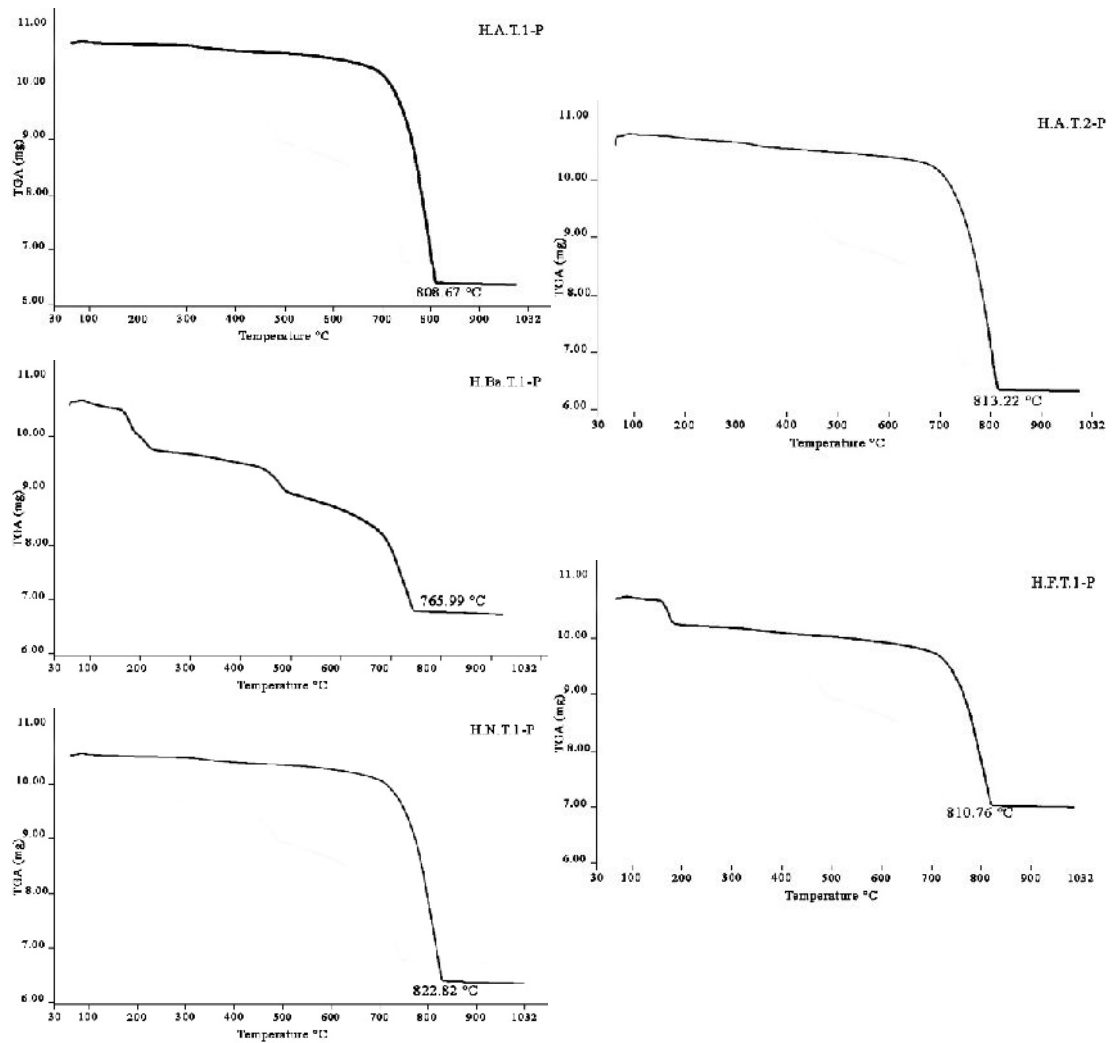


Figure 3.18. TGA graphs of patina samples taken from travertine surfaces

In addition to SEM-EDX and TGA analyses, the lateral and in-depth LIBS analyses were also performed on the yellow patina covered marble and travertine surfaces to determine their chemical composition.

The SEM-EDX results indicated that the yellow patina is composed of high amounts of CaO and SiO<sub>2</sub> and low amounts of MgO, Al<sub>2</sub>O<sub>3</sub>, K<sub>2</sub>O, FeO and P<sub>2</sub>O<sub>5</sub> (Figure 3.15, Figure 3.16). In addition to SEM-EDX results, lateral LIBS analyses corresponded the presence of C(I), Ca(I), Si(I), Al(I), Mg(I) and Fe(I) in the yellow patina and sound inner parts separately showing good agreement with XRD, FT-IR and SEM-EDX results (Figure 3.19). The concentrations of these elements change in the yellow patina covered surfaces according to sound parts of marble and travertine which is obvious from the SEM-EDX and LIBS results. The SEM-EDX indicated that CaO is lower, and MgO,

$\text{Al}_2\text{O}_3$ ,  $\text{SiO}_2$ ,  $\text{K}_2\text{O}$ ,  $\text{FeO}$  and  $\text{P}_2\text{O}_5$  are higher in the yellow patina layer according to the sound inner cores. It was obvious from the LIBS spectrums of the same samples showing the comparison of atomic emission lines of C, Si, Al and Fe of sound inner core with the spectrum containing lower signal intensities (spectrum below) and yellow patina with the spectrum containing higher signal intensities (spectrum above) (Figure 3.19).

The semi-quantitative data obtained from the lateral LIBS spectrums of Ai.Th.M.1 which is the most representative sample among all the samples were used to draw the graph of the ratios of elements in the patina and sound inner core (Figure 3.20). The results indicated that C content is 7 times, Al is 3.3 times, Si is 114 times and Fe is 3.7 times higher on the surfaces of marble where calcium oxalate patina formed (Figure 3.19, Figure 3.20, Table 3.7).

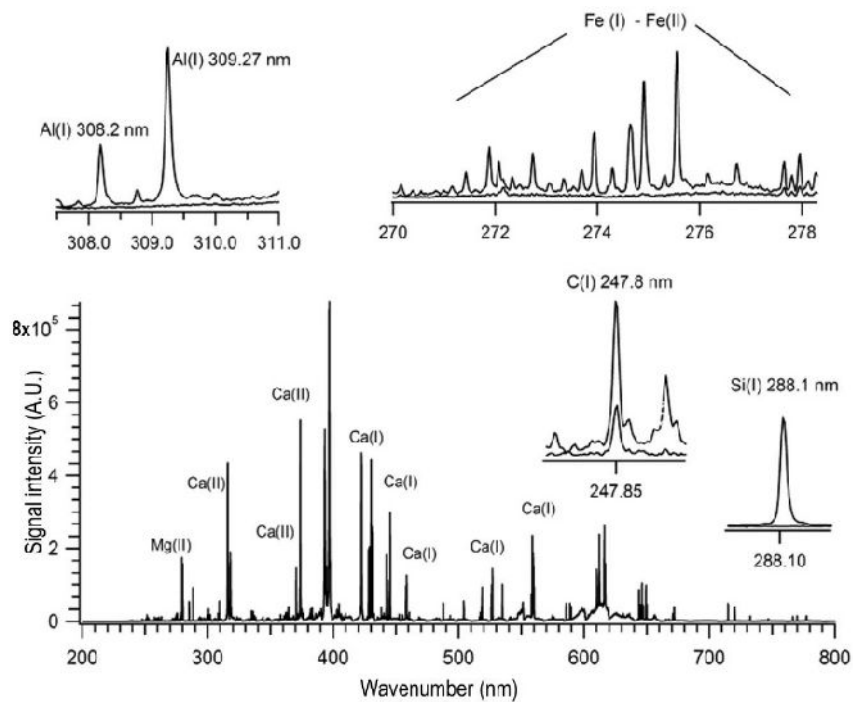


Figure 3.19. Atomic emission lines of C, Si, Al and Fe of sound inner core (spectrum below) and yellow patina (spectrum above) by LIBS spectrum of marble (Ai.Th.M.1)

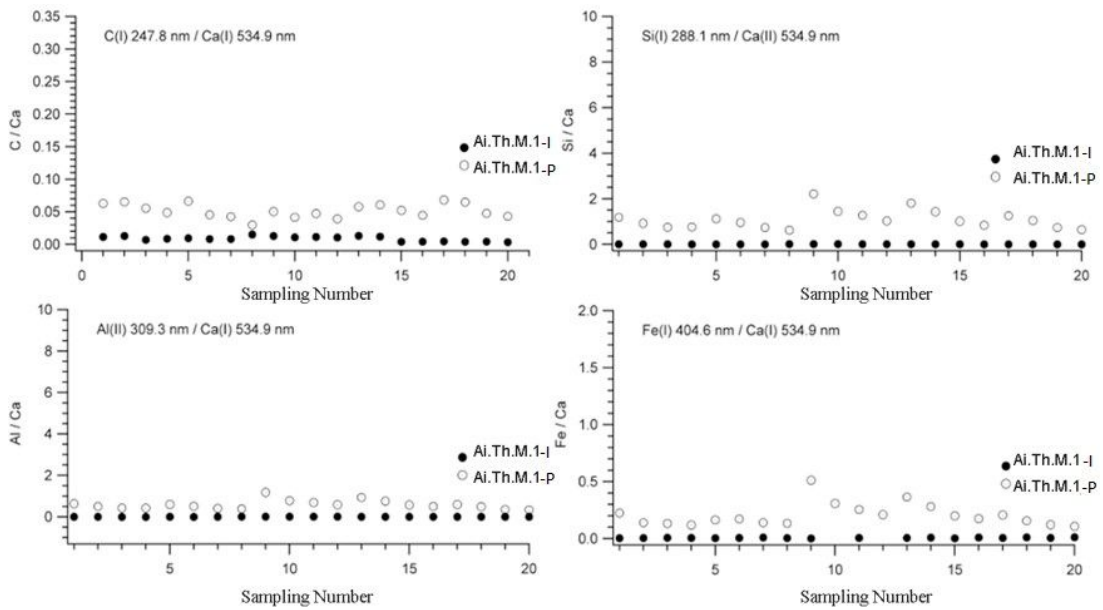


Figure 3.20. The graphs showing the ratios of C, Si, Al and Fe signals to Ca signal in the yellow patina (Ai.Th.M.1-P) and sound inner cores of marble sample (Ai.Th.M.1-I)

Table 3.7. C/Ca, Al/Ca, Fe/Ca and Si/Ca ratios in the patina according to the inner core of yellow patina covered marble

| Ratio | Patina | Inner Core |
|-------|--------|------------|
| C/Ca  | 7x     | x          |
| Al/Ca | 3.3x   | x          |
| Fe/Ca | 3.7x   | x          |
| Si/Ca | 114x   | x          |

The same lateral LIBS analyses was performed on one representative travertine sample showed similarities with the yellow patina spectrum of marble sample. It represented higher signal intensities of Ca and lower signal densities of C, Si, Al, Mg and Fe according to sound inner core (Figure 3.21). It is related with the difference of material characteristics of yellow patina and sound inner cores of marble and travertine. As it was determined from XRD and FT-IR analyses, the yellow patina is mainly composed of calcium oxalate with minor amounts of gypsum, quartz and calcite. However, the sound inner cores are mainly composed of calcite with the minor amounts of quartz. When the

chemical composition of these two layers are considered, it is expected to observe differences in the chemical composition of these two materials as natural which are explained in detail as follows:

The chemical formula of yellow patina as calcium oxalate ( $\text{CaC}_2\text{O}_4$ ) and sound inner core as calcium carbonate ( $\text{CaCO}_3$ ) are the main factors of the elemental variation about C and Ca. They include same elements as Ca, C and O. However, when the LIBS spectrums of both layers are compared, the atomic emission line of Ca is lower in the weathered surfaces and higher in the sound inner parts. SEM-EDX results resemble with LIBS spectrum showing the higher concentrations of Ca in the sound inner cores of marble and travertine (Figure 3.15, Figure 3.16). It can be explained with the chemical formula of sound inner parts calcite and calcium oxalate of collected marble and travertine samples. For this purpose, the molecular weight of  $\text{CaC}_2\text{O}_4$  and  $\text{CaCO}_3$  was calculated according to the molar mass of element contents of both minerals considering the atomic mass and number of atoms (Table 3.8). The mass percent of each element was calculated considering the molecular weight of these two minerals considering the values presented in Table 3.8.

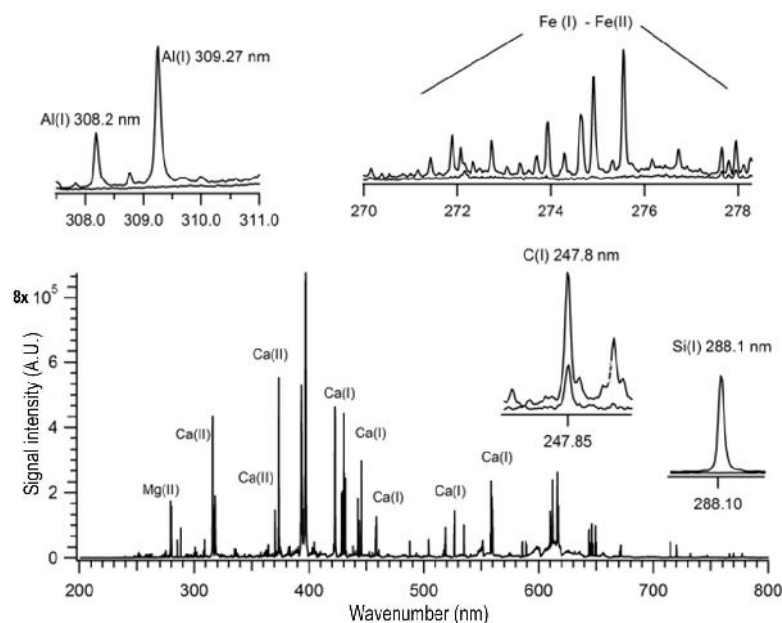
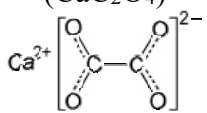
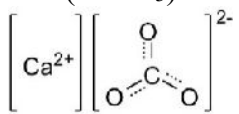


Figure 3.21. Atomic emission lines of C, Si, Al and Fe of sound inner core (spectrum below) and yellow patina (spectrum above) by LIBS spectrum of travertine (H.N.T.1)

Table 3.8. The molecular weight and mass percent of each element in calcium oxalate and calcium carbonate (Source: <http://www.convertunits.com/>)

| Mineral   | Element | Atomic Mass | # of Atoms | Mass Percent (%) | Total molecular weight (g/mol) |
|---|---------|-------------|------------|------------------|--------------------------------|
| <u>Calcium oxalate</u><br>(CaC <sub>2</sub> O <sub>4</sub> )<br> | Ca      | 40.078      | 1          | 31.287           | 128.097                        |
|   | C       | 12.0107     | 2          | 18.753           |                                |
|   | O       | 15.9994     | 4          | 49.960           |                                |
| <u>Calcium carbonate</u><br>(CaCO <sub>3</sub> )<br>             | Ca      | 40.078      | 1          | 40.043           | 100.0869                       |
|   | C       | 12.0107     | 1          | 12.000           |                                |
|   | O       | 15.9994     | 3          | 47.957           |                                |

The results of the molecular weight calculations indicated that Ca ratio is lower considering its mass percent in the yellow patina samples (31.287% in calcium oxalate) with respect to the sound inner cores of stones (40.043% in calcium carbonate) (Table 3.8). The results of SEM-EDX and LIBS analyses are in accordance with these calculations showing the high ratios of Ca in the sound inner cores (Figure 3.15, Figure 3.16, Figure 3.6).

When the same calculations were made for C concentration in both parts, it is obvious that C ratio is higher in the yellow patina samples (18.75% in calcium oxalate) with respect to the sound inner cores of stones (12% in calcium carbonate) (Table 3.8). The results of LIBS analyses are in accordance with these calculations showing the high ratios of C in the yellow patina layers according to the sound inner cores of the stones (Figure 3.19, Figure 3.20, Figure 3.21).

The chemical mineralogical and compositions of clay minerals were not investigated in detail in this study. However, the higher values of Al, Si and Fe are most probably related with the clay deposition incorporated in in the yellow patina during its formation which shows good agreement with the previously studied cases (Table 3.2) (Del Monte and Sabbioni 1987). Mg and Fe may be transformed from the environment as windborne particles just as together with clay minerals (Del Monte and Sabbioni 1987). The existence of clays on the exterior and the interior parts of the stone accelerates its weathering by promoting physical and biological weathering of stone (Chen et al. 2000,

Press and Siever 2002). Clays expand in moist environment and cause the formation of fissures and micro cracks in stone by swelling (Scherer 2006). They also provide optimum conditions for the growth of biological formations as algae, lichen, moss, etc. which also cause physical and chemical weathering of stone (Chen et al. 2000, Press and Siever 2002). Within this respect, the generation of biological forms were determined by FT-IR analysis of the yellow patina formation on marble and travertine surfaces considering the absorption bands around  $2800\text{ cm}^{-1}$  as organic materials and biologic tissues. It was a sign of the weathering of stone by the effects of clays and biological growth in the studied marble and travertine surfaces (Figure 3.8, Figure 3.9) (Chen et al. 2000, Press and Siever 2002).

The in-depth LIBS analyses were also used to provide semi-quantitative data about the purity and thickness of yellow patina on marble and travertine surfaces which will be mentioned in detail in the following part.

### **3.2.3.1. The Elemental Distribution of Stone Samples from Surface to the Inner Cores**

The chemical composition of stones was also investigated considering the elemental distribution of patina from surface to the sound inner cores which also helped to decipher its thickness by using in-depth LIBS profiling.

The LIBS analysis was performed to determine the elemental variation of marble and travertine samples by applying repetitive laser shots on one point (Figure 2.9(b)). It resulted with the formation of nearly  $1\mu\text{m}$  depth crater after each shot on the surface. The elemental composition of each crater shaped area showed the presence of C(I), Ca(I), Si(I), Al(I), Mg(I) and Fe(I) as it was determined by LIBS, SEM-EDX, XRD and FT-IR analyses of yellow patina (Figure 3.22, Figure 3.23). The in-depth LIBS graphs corresponded to the results of mineralogical and chemical analyses of yellow patina indicating the increase of Ca and decrease of C, Si, Al, Mg and Fe ratios due to calcium oxalate formation and clay deposition on stone surfaces (Figure 3.14, Figure 3.25, Figure 3.26, Figure 3.27, Figure 3.28, Figure 3.29, Figure 3.30, Figure 3.31, Figure 3.33 and Figure 3.32).

This information was also evaluated considering the semi quantitative data which was gathered from the signal intensities of each elements included. The signal intensities of C(I), Ca(I), Si(I), Al(I), Mg(I) and Fe(I) were investigated by calculating their peak

areas in LIBS spectrums to show them on the graphs according to depth. It helped to figure out the trend lines of each element from yellow patina formed surface to the sound inner core of marble and travertine samples. The curve in the trend line of an element ends when the laser reaches the sound inner core and the layer transition occurs. Within this respect, patina was lost between almost the first 5<sup>th</sup> to 25<sup>th</sup> laser shots with respect to the end of curved and beginning of straight trend line of the elements in yellow patina samples on marble (Figure 3.24, Figure 3.25, Figure 3.26, Figure 3.28). The results are similar for patina samples determined on travertine surfaces (Figure 3.29, Figure 3.30, Figure 3.31, Figure 3.32, Figure 3.33). Considering approximately 1  $\mu\text{m}$  depth craters which formed after each laser shot, the thickness of each patina samples was estimated to vary around a few tens of microns on marble and travertine surfaces in general.

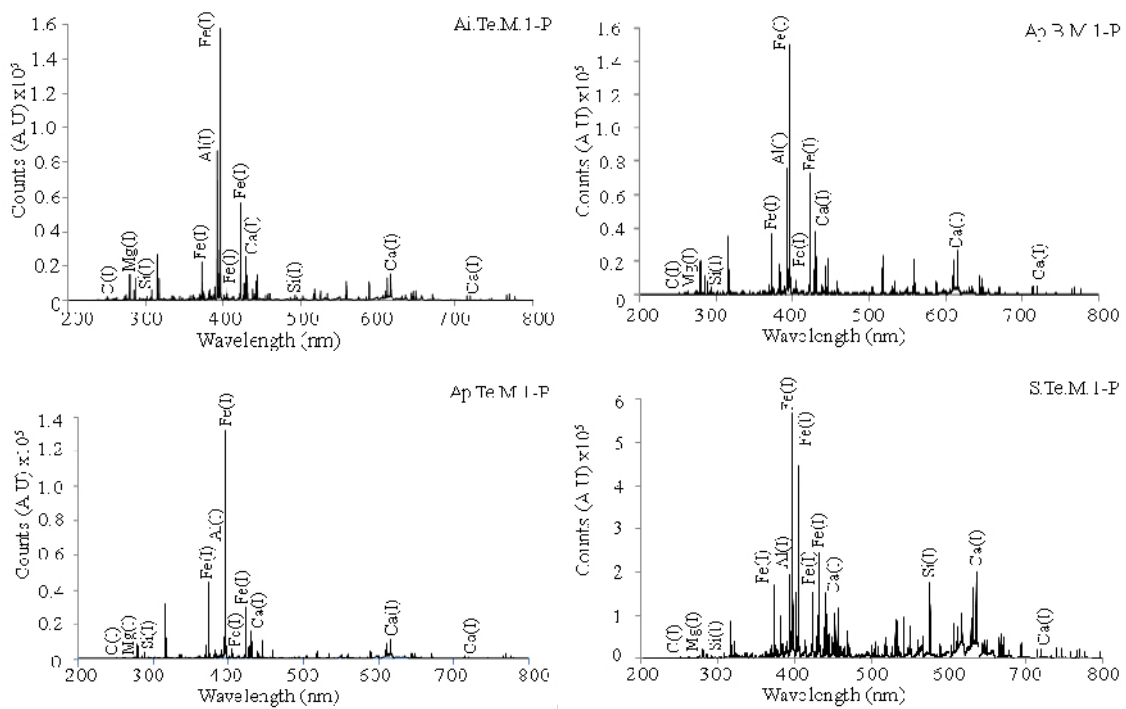


Figure 3.22. Atomic emission lines of C, Ca, Mg, Si, Al and Fe of yellow patina on marble samples by LIBS spectrum

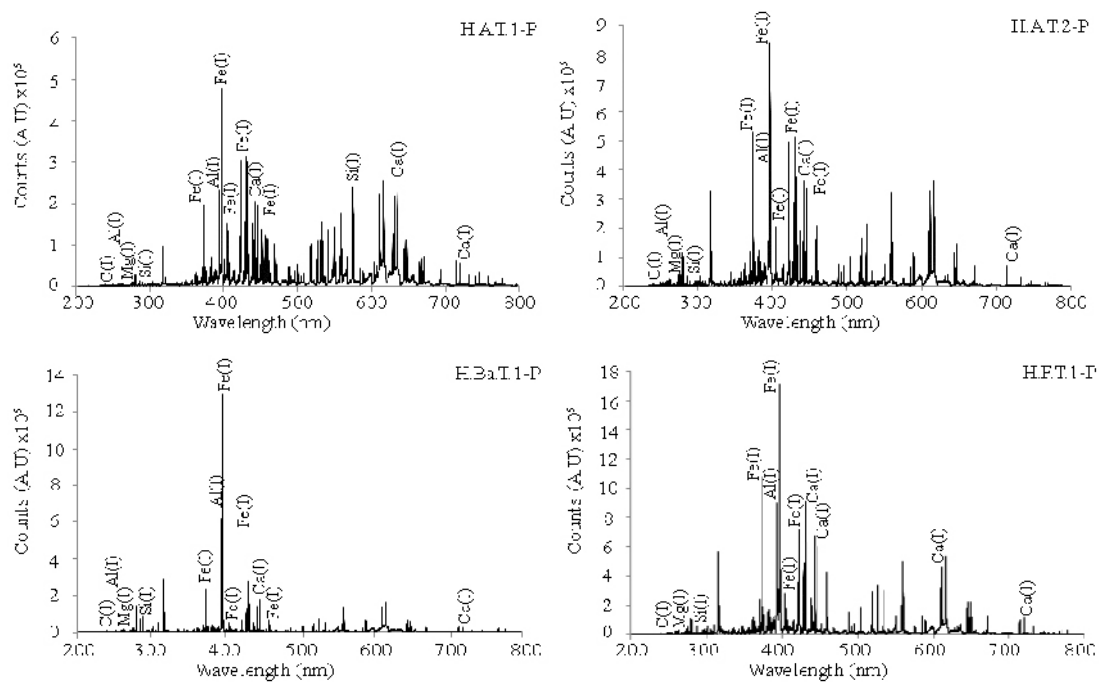


Figure 3.23. Atomic emission lines of C, Ca, Mg, Si, Al and Fe of yellow patina on yellow travertine samples by LIBS spectrum

The LIBS graph of one of the marble sample taken from theatre in Aizanoi (Ai.Th.M.2) indicated that the patina layer was lost at around 15<sup>th</sup> laser shot and continued by a straight line in the following shots indicating the thickness of patina around 15  $\mu\text{m}$  depth from the surface (95-243  $\mu\text{m}$  in SEM) (Figure 3.24 (a), Table 3.9). The C/Ca intensity decreased until the 15<sup>th</sup> shot. The Si/Ca, Al/Ca, Fe/Ca and Mg/Ca have been also in the same trend. On the contrary, Ca intensity differentiated from other elements showing an increase from surface to the inner core. Also, the straight line of Ca began after 50<sup>th</sup> shot. SEM-EDX mapping images were in accordance with LIBS results showing the decrease of Si, Al and Fe and increase of Ca from surface to the inner parts. With this point of view, the increase of Fe together with Si and Al indicated the presence of clay minerals on the surface of the stone. The decrease of Mg and C elements from surface to the inner core is not clear in mapping analyses where it is obvious in their LIBS graphs (Figure 3.24 (b)).

The LIBS graph of one marble sample taken from temple in Aizanoi indicated that C/Ca, Si/Ca, Al/Ca and Fe/Ca ratios decreased and signal intensity of Ca increased and stabilized around 50<sup>th</sup> laser shot from surface to the inner parts of showing the

thickness of patina as 50  $\mu\text{m}$  approximately (76-164  $\mu\text{m}$  in SEM) (Ai.Te.M.1) (Figure 3.25 (a), Table 3.9). Mapping images were similar for Si, Al, and Ca showing an increase from surface to the inner parts (Figure 3.25 (b)). In addition to this, the presence of S element was also determined in mapping analyses of the same sample. It was also corresponded by the mineralogical analysis of patina with high amounts of S content due to gypsum formation (Table 3.2, Figure 3.15).

Another LIBS graphs of marble sample taken from bouleuterion in Aphrodisias (Ap.B.M.1) showed the thickness of the yellow patina probably about 15  $\mu\text{m}$  according to the decrease and the formation of straight trend line for C/Ca, Mg/Ca, Si/Ca, Al/Ca and Fe/Ca (Figure 3.26 (a)). The decrease was also observed in the mapping analyses of Mg, Si and Al (Figure 3.26 (b)). The variation was observed as an increase for Ca not only in LIBS graphs but also in SEM-EDX mapping analyses due to the original stone material underlying patina formation (Figure 3.26 (b)).

The yellow patina samples on marble was also taken from the temple in Aphrodisias (Ap.Te.M.1). The LIBS graphs of this sample were in accordance with its SEM-EDX results (Figure 3.15, Figure 3.27 (a)). The variation of C/Ca, Si/Ca, Mg/Ca and Fe/Ca showed a decrease and provided a straight line when the original stone substrata was probably reached after the 10<sup>th</sup> shot showing that the thickness of patina was around 10  $\mu\text{m}$  ( $\sim$ 54  $\mu\text{m}$  in SEM) (Figure 3.27 (a), Table 3.9). In this sample, aluminum could not be evaluated because of an experimental error which caused Al/Ca values to scatter in the LIBS graphs. However, the mapping analyses of Al together with Si deposition clearly showed the presence of clay minerals on the surface of the stone sample. S was another element that was determined in the SEM-EDX and mapping analyses as it was proved by the results of mineralogical analyses showing the presence of gypsum resulting from air pollution on the surface of the stone (Figure 3.27 (b), Table 3.2). Ca showed the trend as an increase from surface to the inner core due to high Ca content of the original stone substrata with respect to calcium oxalate patina on the stone surface (Figure 3.27 (b)).

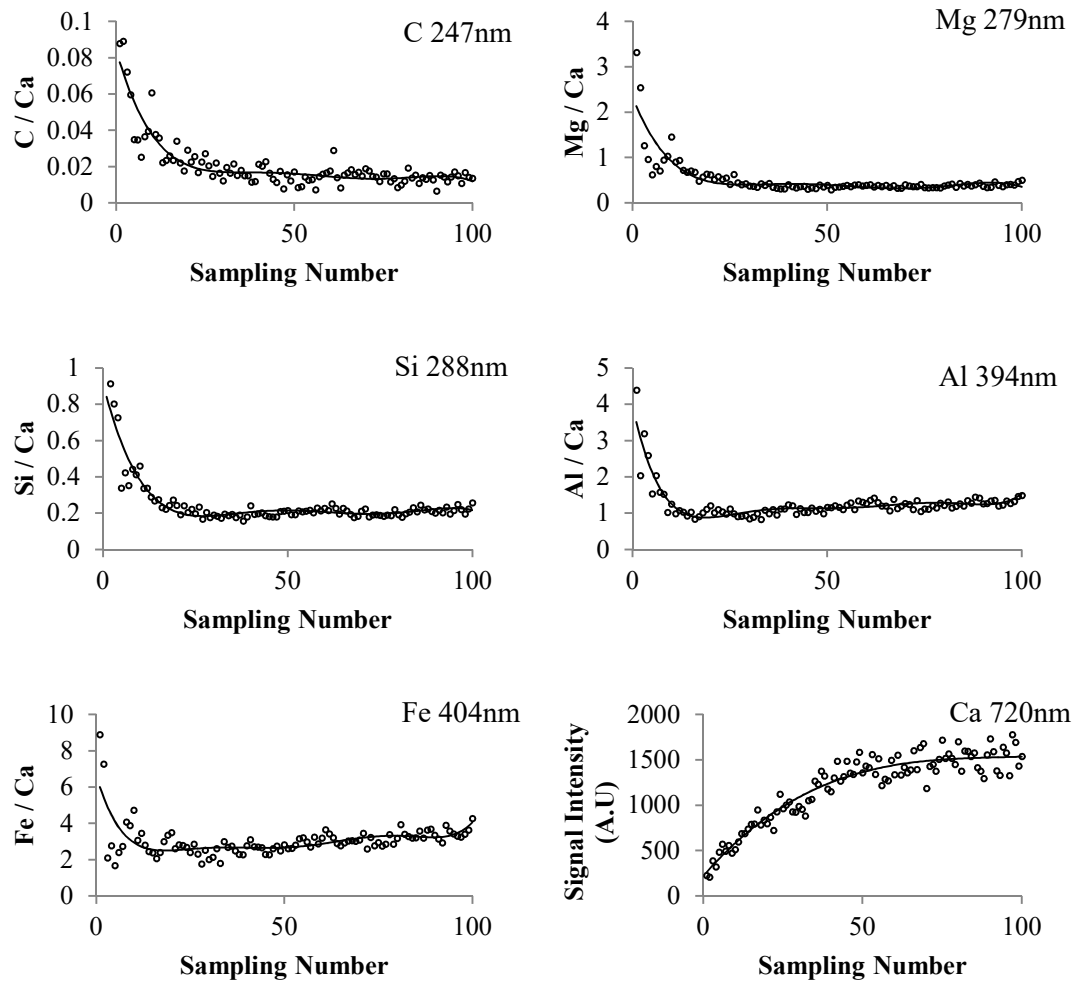
In Sardis, the surface of the marble sample taken from the temple was yellow in color which caused the assumption that a calcium oxalate patina may have formed on the stone surface as it was determined on other samples (S.Te.M.1). However, the mineralogical and chemical composition of the sample was not assigning the presence of a calcium oxalate but quartz and calcite on the marble surface (Table 3.2). The results of LIBS graphs indicated a decrease in C/Ca, Si/Ca, Mg/Ca and Fe/Ca ratio and increase in

Ca signal intensity until the 10<sup>th</sup> shot which was probably related with clay deposition on stone surface (Figure 3.28). As proof, quartz and calcite crystals were determined in mineralogical analyses (Table 3.2). The mapping analyses was not satisfactory to compare the results of both analyses because patina layer could not be detected in SEM-EDX analysis.

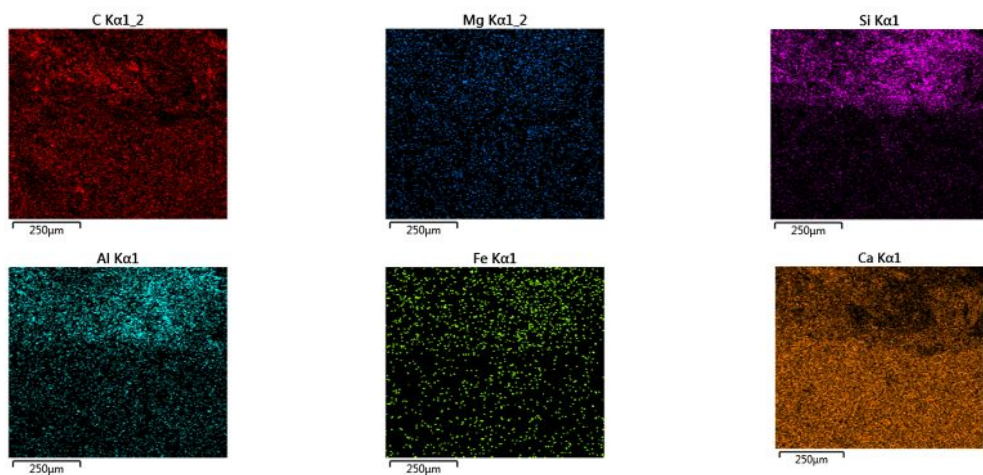
The in-depth analyses were also applied on travertine samples collected from Hierapolis. The results were similar with the results of marble considering the changes of trend line for C, Si, Al, Fe, Mg and Ca due to the transition from yellow patina to the sound inner cores of the stone. It was used to estimate the thickness of patina as well as in marble samples. The LIBS graphs of travertine sample taken from necropolis (H.N.T.1) indicated that C, Si, Al, Fe and Mg decrease from surface to the inner core. However, the decrease began after a small period of increase around the 10<sup>th</sup> shot (Figure 3.29). It may be related with the porous and heterogeneous characteristic of travertine. The trend line of the elements were normalized after 10<sup>th</sup> shot and curved until 25<sup>th</sup> shot estimating the thickness of patina as 25  $\mu\text{m}$  (55  $\mu\text{m}$  in SEM) (Figure 3.29, Table 3.9).

The LIBS graph of the sample taken from travertine in Hierapolis Agora (H.A.T.1) indicated that there was a fluctuation in the graphs of Fe/Ca and Mg/Ca variations around 30<sup>th</sup> shot (Figure 3.30 (a)). However, the trend lines of other elements were in agreement with the patina formation on the surface of a stone specimen. The patina layer was probably lost at around 20<sup>th</sup> shot indicating the thickness as 20  $\mu\text{m}$  (73-154  $\mu\text{m}$  in SEM) (Table 3.9). SEM-EDX mapping results were in accordance with LIBS graphs showing the decrease of Al and Si and increase of Ca from surface to the inner core of travertine (Figure 3.30 (b)).

The LIBS graphs of another travertine sample from Agora in Hierapolis showed similarities with the other travertine results (H.A.T.2). The curve of the trend line ended with the repetitive laser shots, patina layer was probably lost and the original stone surface was probably reached at around 25<sup>th</sup> shot (Figure 3.31). The decrease of C, Si, Mg, Al and Fe, and increase of Ca with respect to depth of the stone was obvious on the LIBS graphs of the sample showing agreement with mineralogical test results with the determination of calcium oxalate and calcite as a patina layer with different characteristics on travertine surfaces (Figure 3.31). The mapping analyses was not satisfactory to compare the results of both analyses because patina layer could not be detected in SEM-EDX analysis.



(a)



(b)

Figure 3.24. Variation of C, Mg, Si, Al and Fe signal intensities normalized to Ca signal with respect to depth in LIBS (a) and SEM-EDX mapping of Ai.Th.M.2 (b)

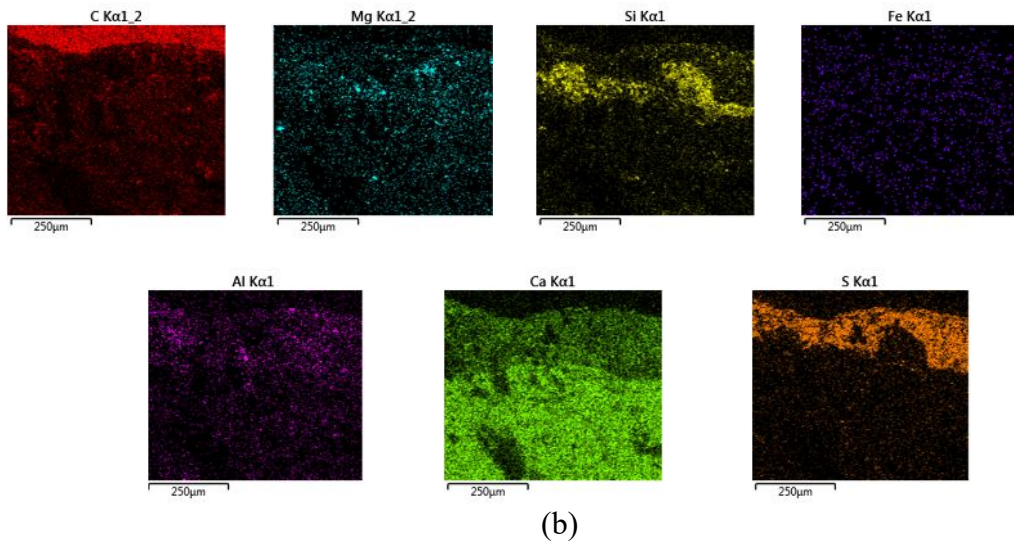
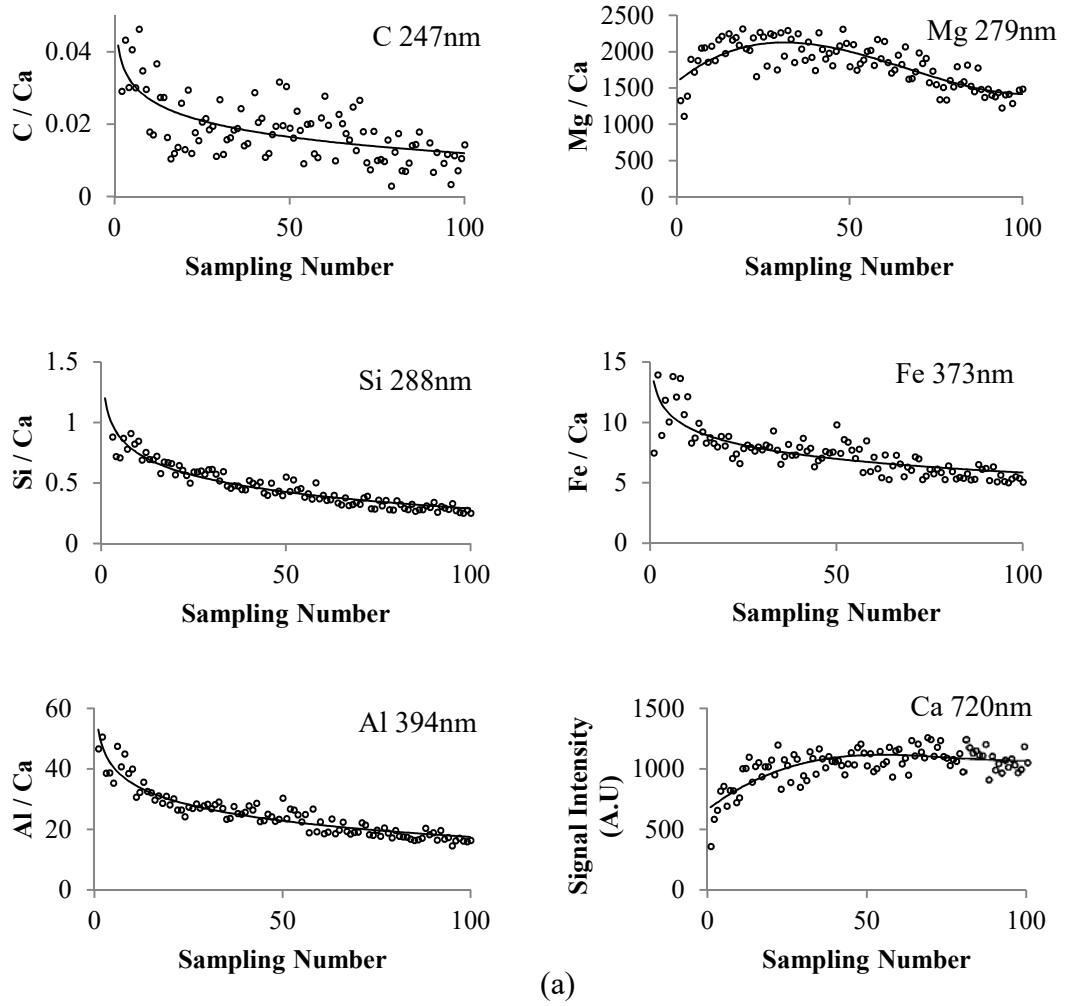
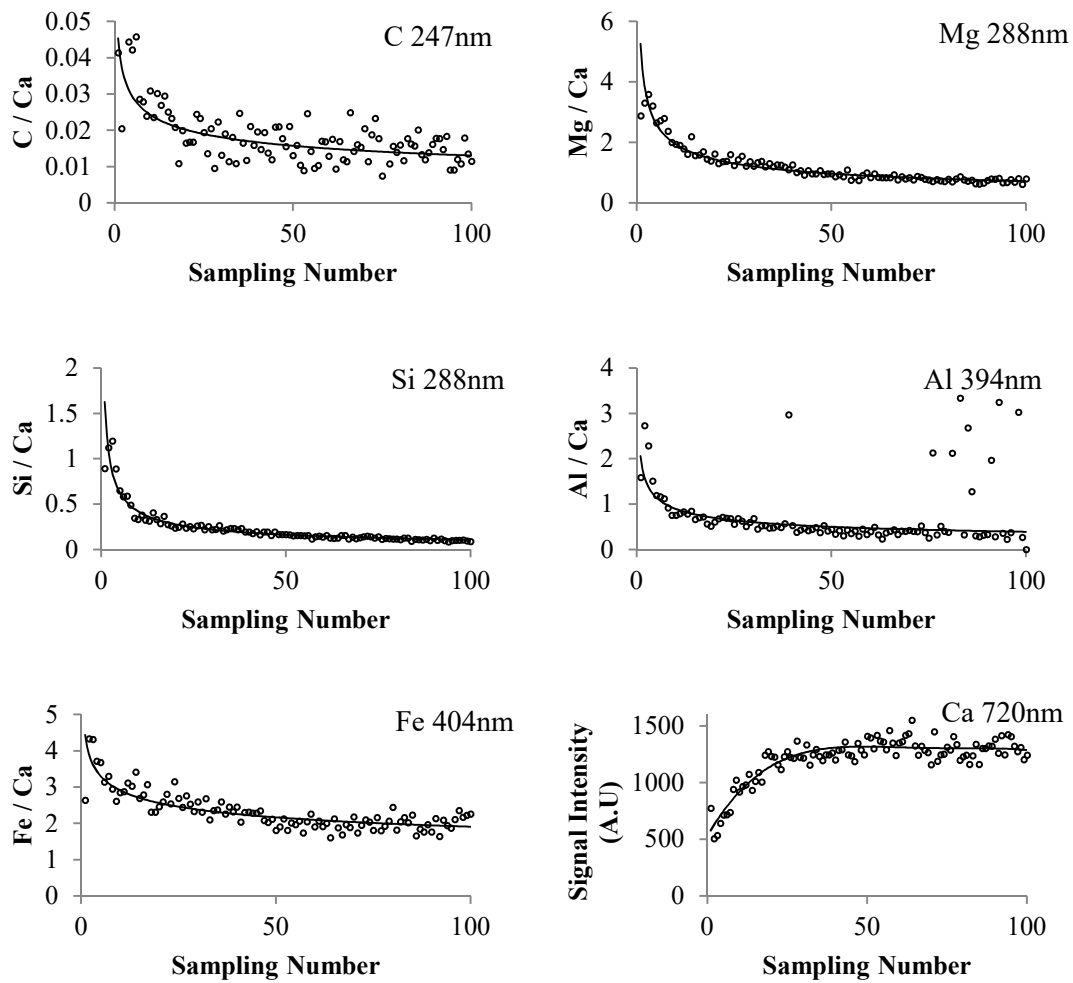
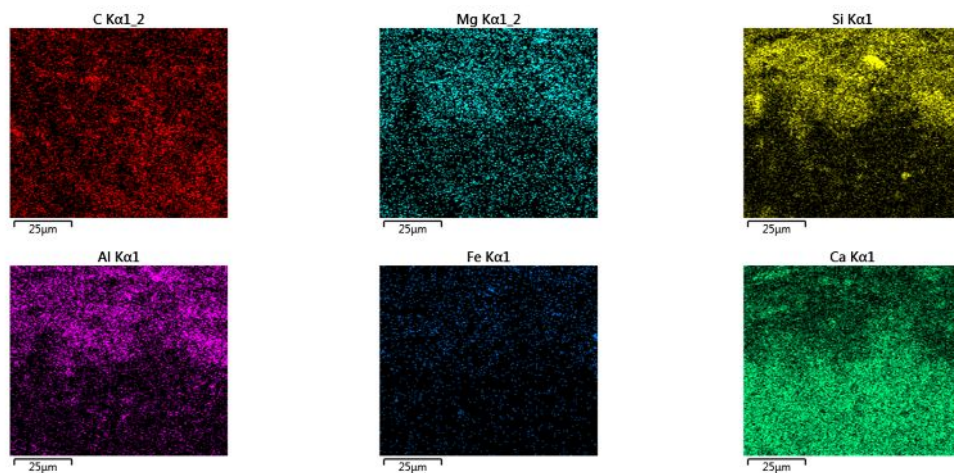


Figure 3.25. Variation of C, Mg, Si, Al and Fe signal intensities normalized to Ca signal with respect to depth in LIBS (a) and SEM-EDX mapping of Ai.Te.M.1 (b)

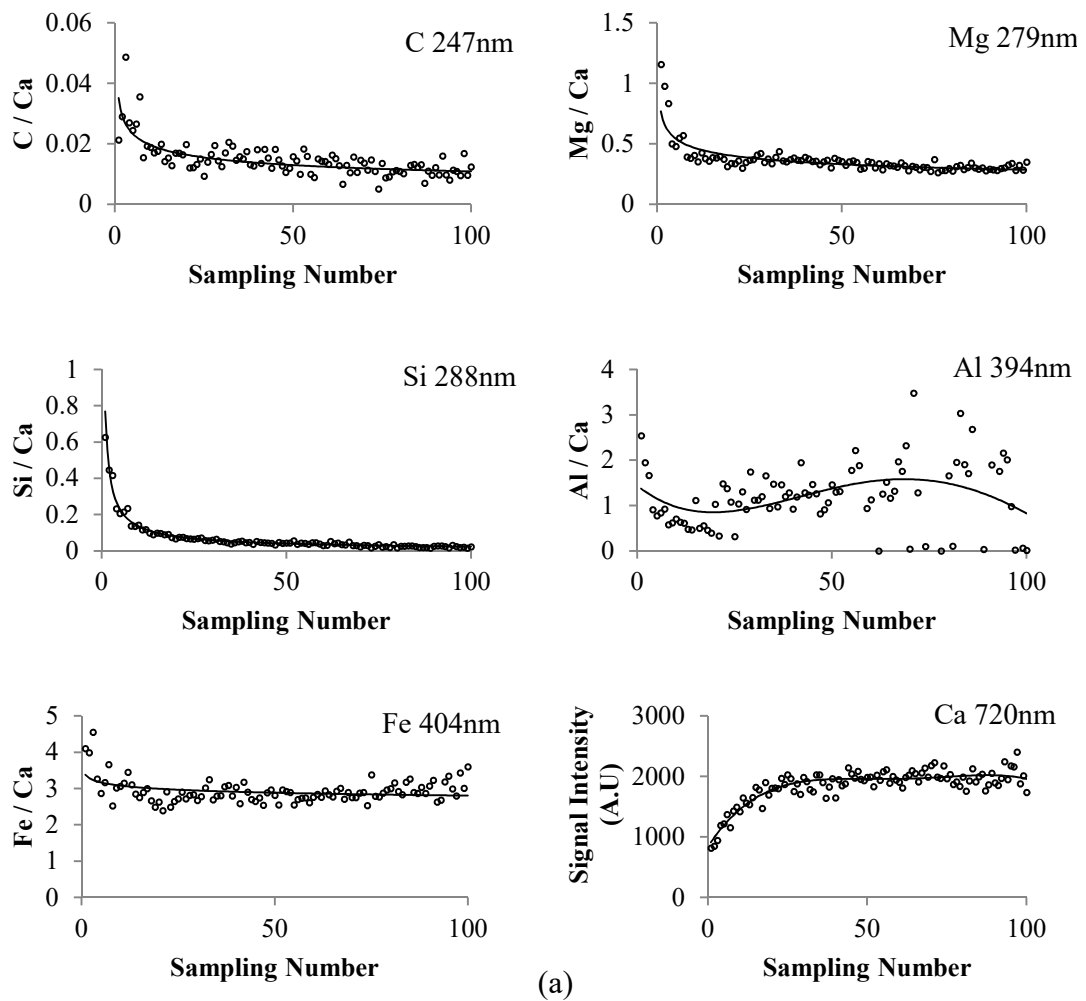


(a)

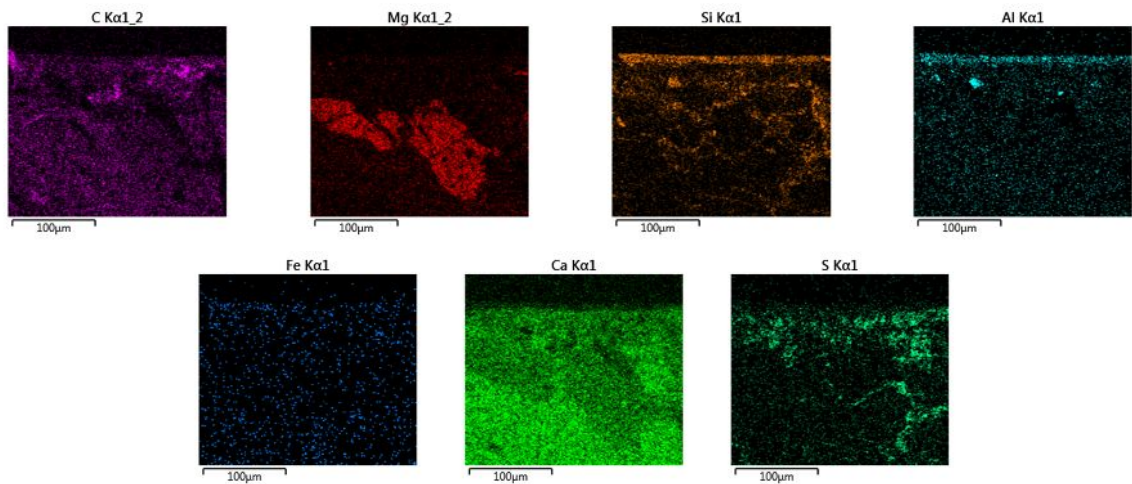


(b)

Figure 3.26. Variation of C, Mg, Si, Al and Fe signal intensities normalized to Ca signal with respect to depth in LIBS (a) and SEM-EDX mapping of Ap.B.M.1 (b)



(a)



(b)

Figure 3.27. Variation of C, Mg, Si, Al and Fe signal intensities normalized to Ca signal with respect to depth in LIBS (a) and SEM-EDX mapping of Ap.Te.M.1 (b)

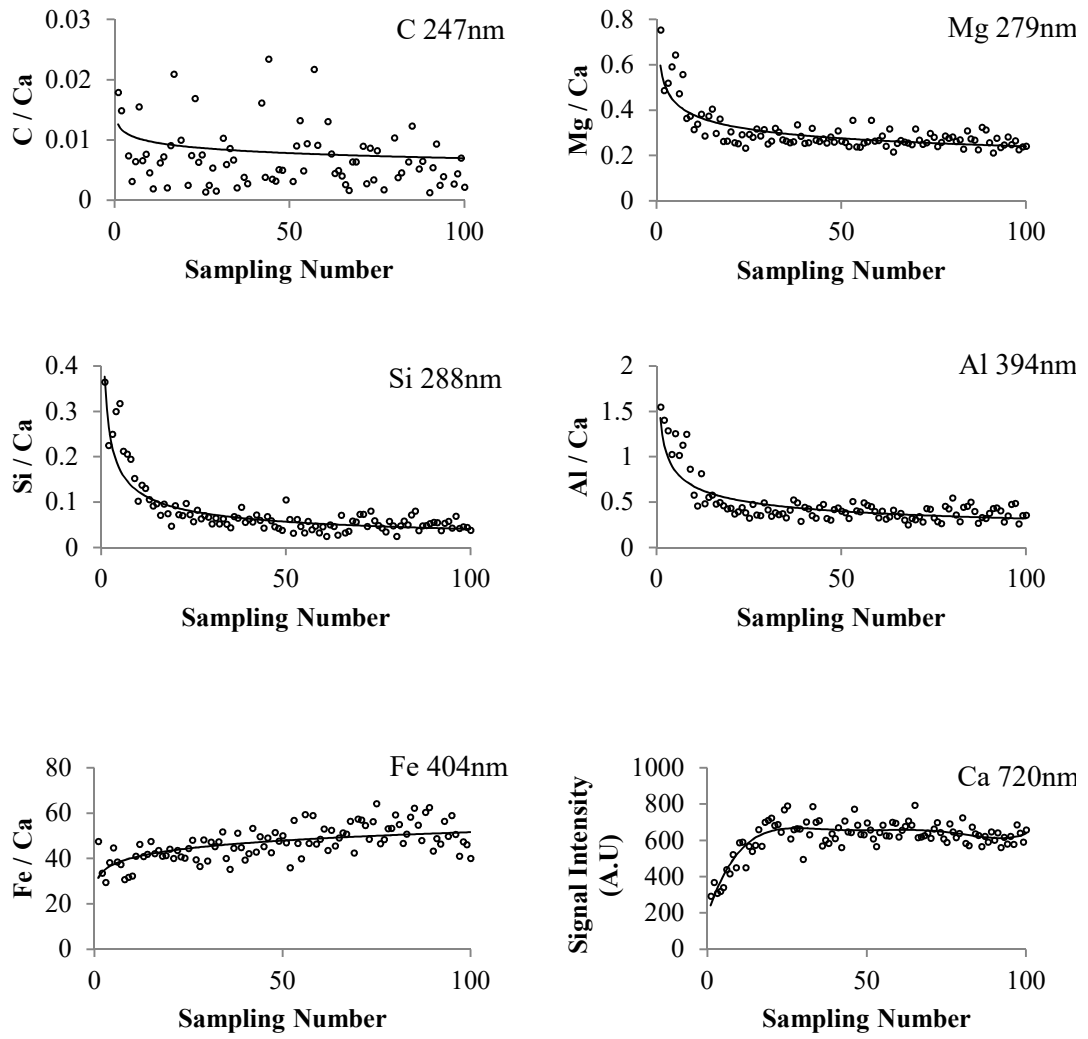


Figure 3.28. Variation of C, Mg, Si, Al and Fe signal intensities normalized to Ca signal with respect to depth for S.Te.M.1 in LIBS

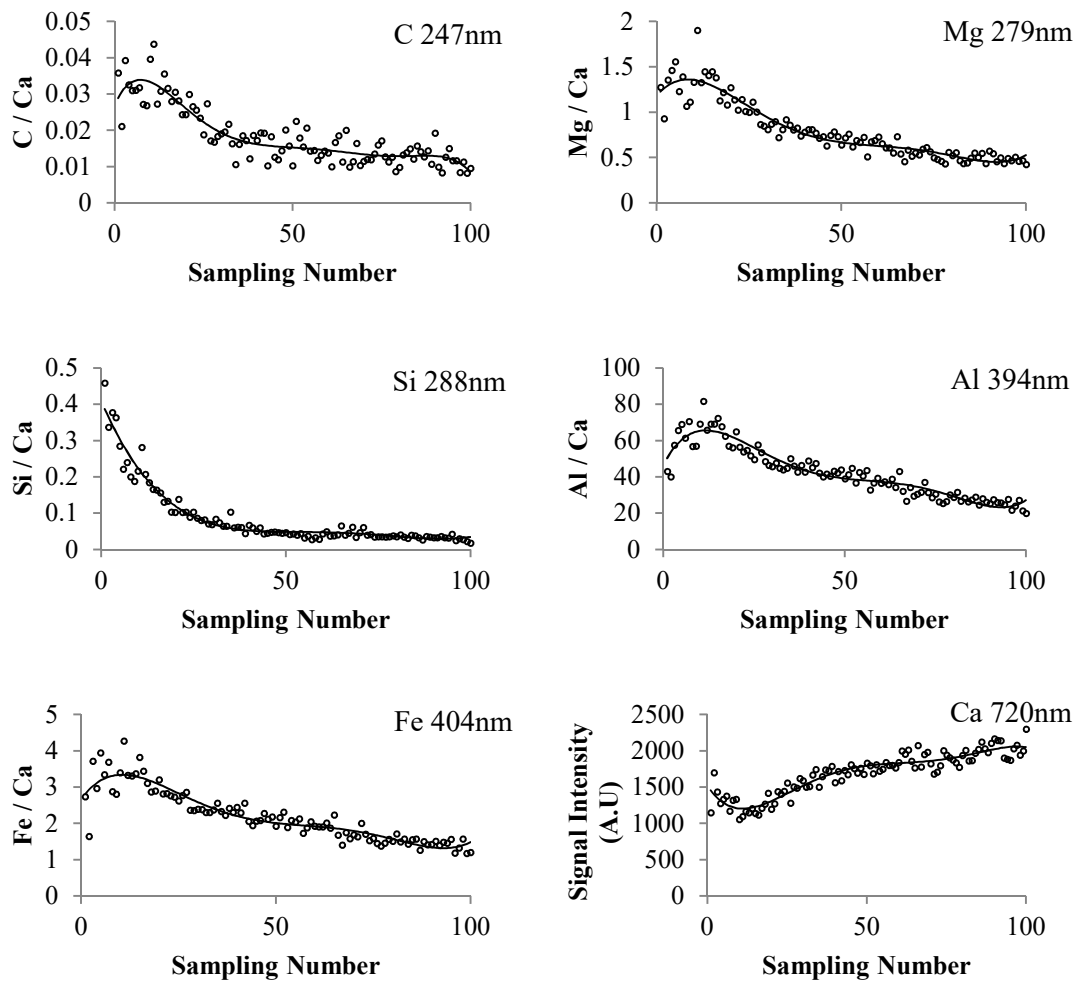


Figure 3.29. Variation of C, Mg, Si, Al and Fe signal intensities normalized to Ca signal with respect to depth for H.N.T.1 in LIBS

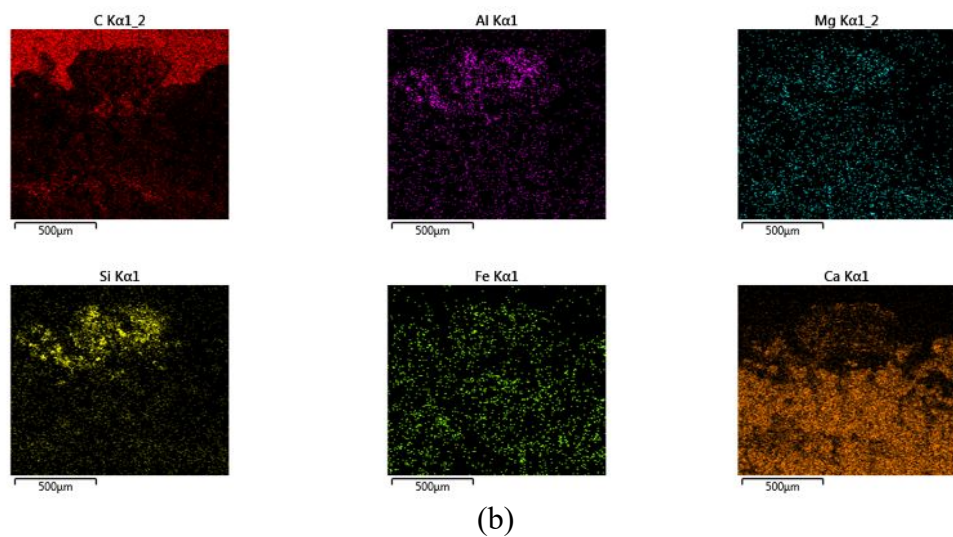
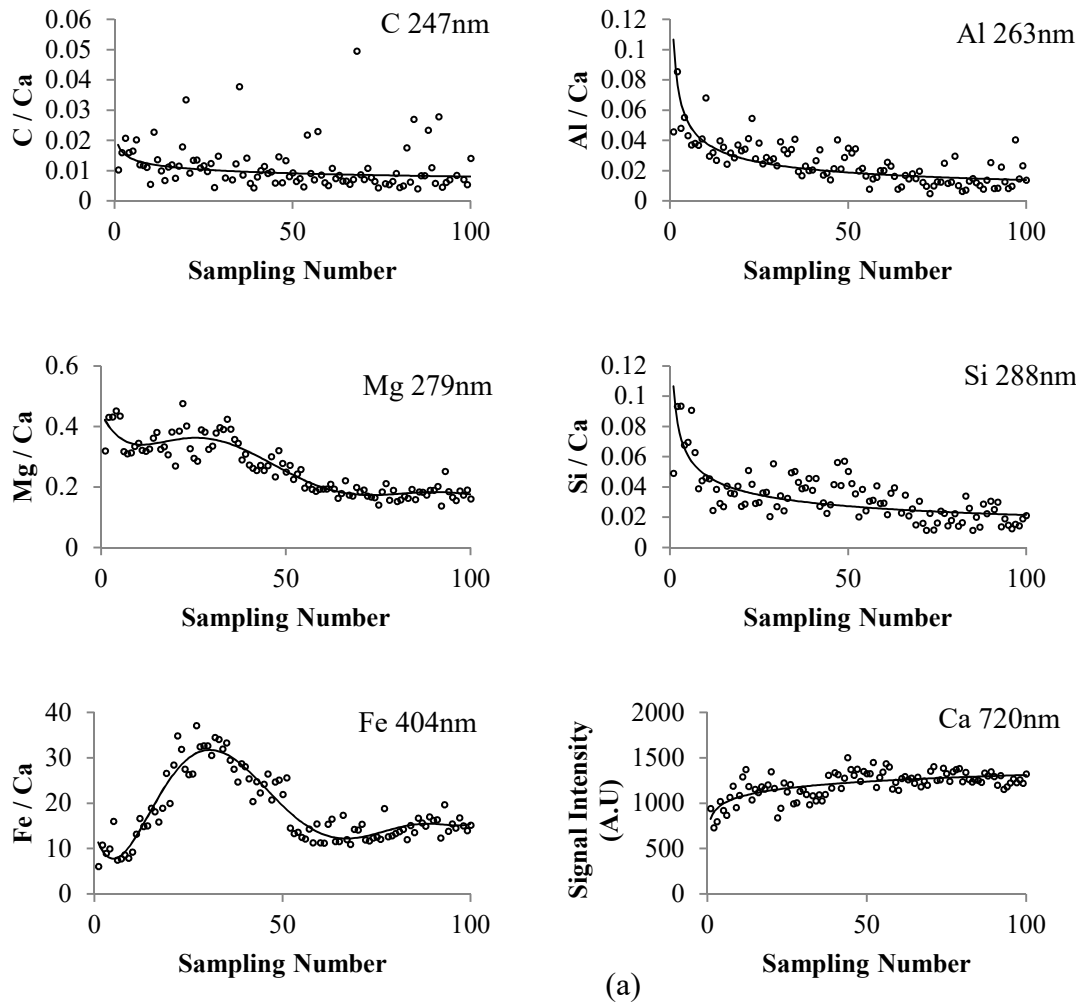


Figure 3.30. Variation of C, Mg, Si, Al and Fe signal intensities normalized to Ca signal with respect to depth in LIBS (a) and SEM-EDX mapping of H.A.T.1 (b)

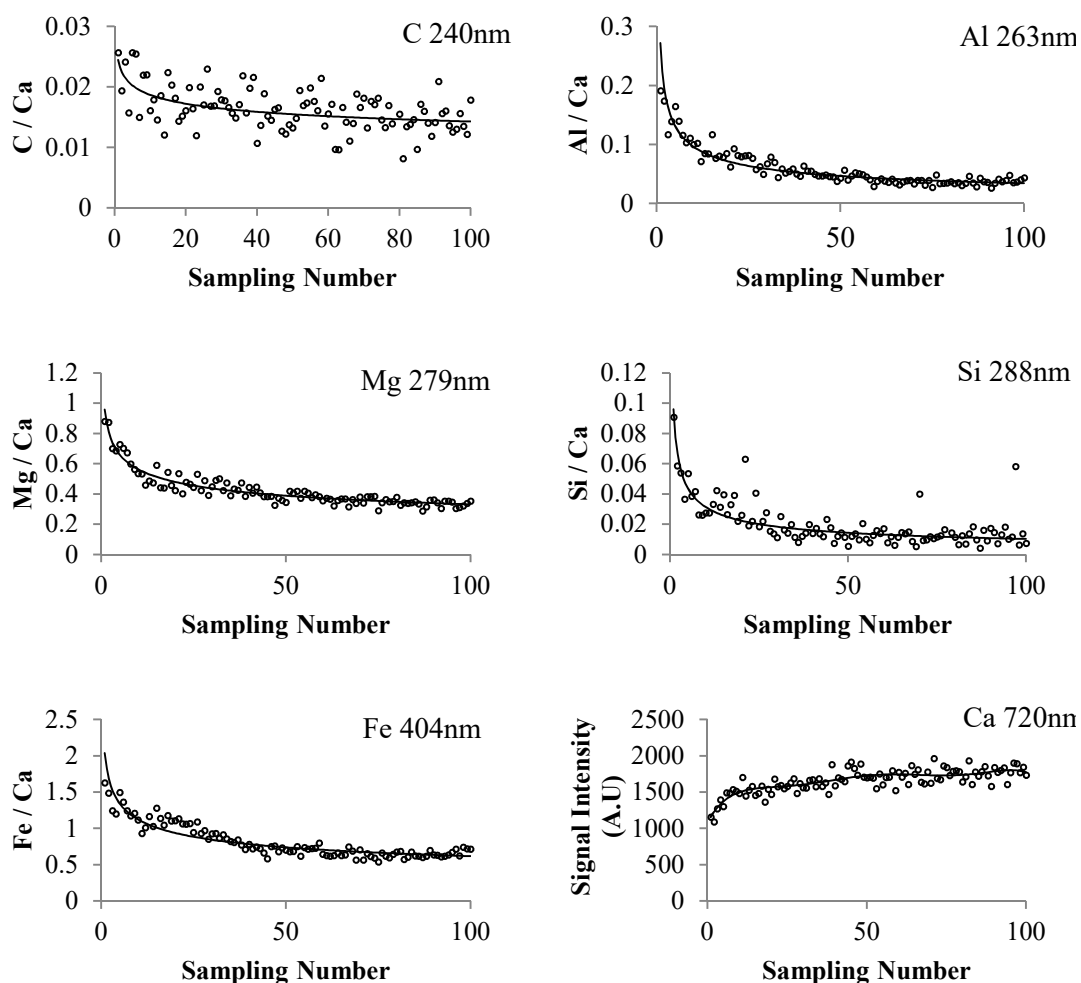


Figure 3.31. Variation of C, Mg, Si, Al and Fe signal intensities normalized to Ca signal with respect to depth for H.A.T.2 in LIBS

The LIBS graphs of the sample taken from the fountain in Hierapolis (H.F.T.1) indicated that C, Mg, Si, Al and Fe decreased, and Ca increased from surface to the inner parts of the stone and the patina layer was probably lost at about 15<sup>th</sup> shot estimating its thickness as 15  $\mu\text{m}$  (6  $\mu\text{m}$  in SEM) (Figure 3.32, Table 3.9). The mapping analysis was not satisfactory to compare the results of both analyses.

The LIBS graphs of travertine sample taken from bath in Hierapolis (H.Ba.T.1) showed the decrease of C, Si, Mg, Al and Fe and increase of Ca with respect to depth until the 10<sup>th</sup> shot when the patina was probably lost and original surface was reached (Figure 3.33 (a)). SEM-EDX mapping of Si, Al and Ca were coherent with LIBS (Figure 3.33 (b)).

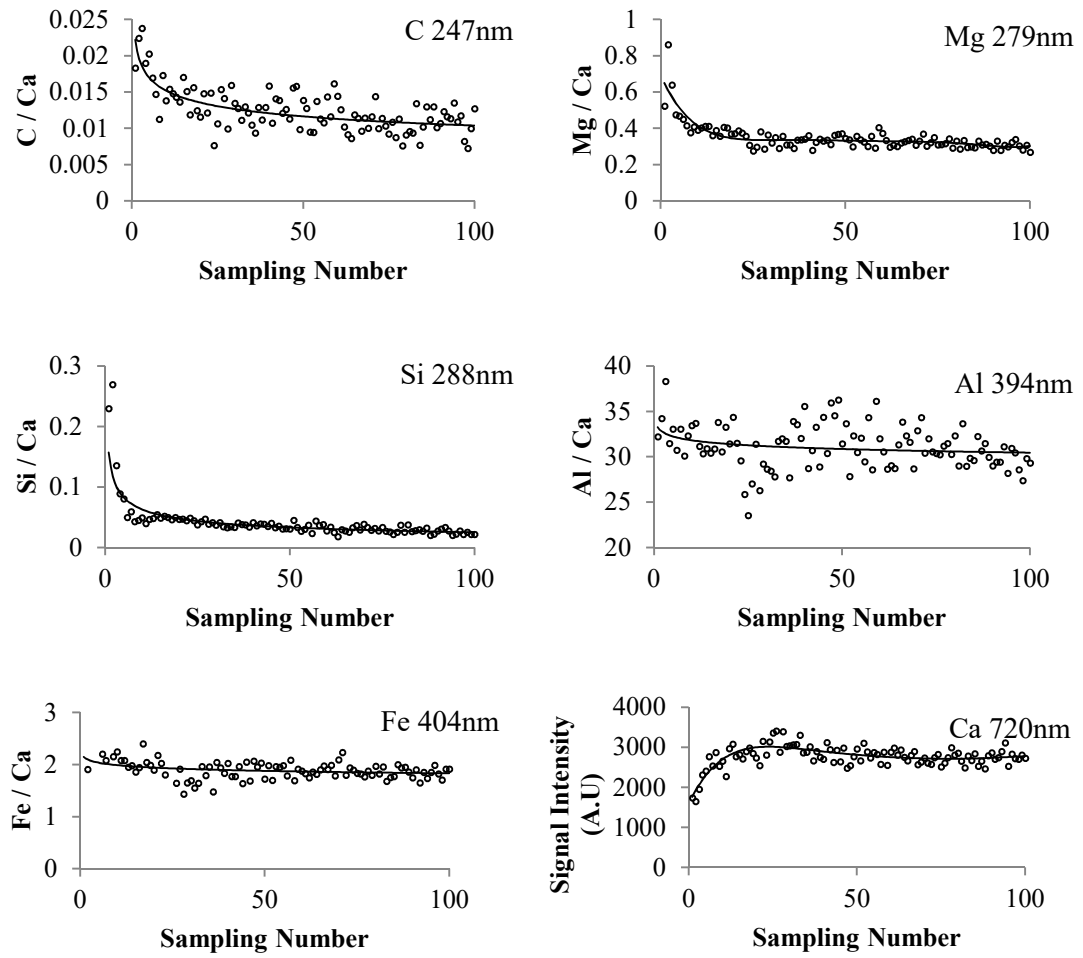
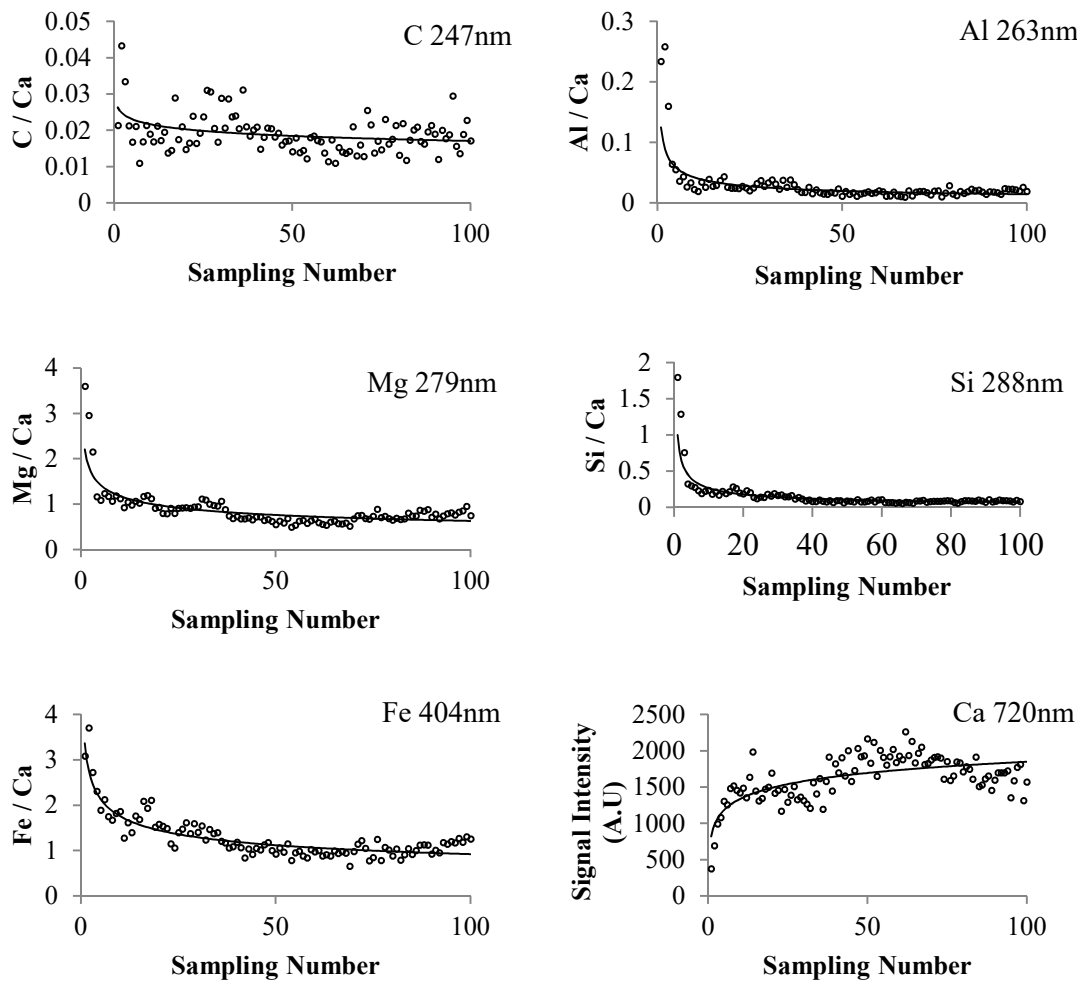
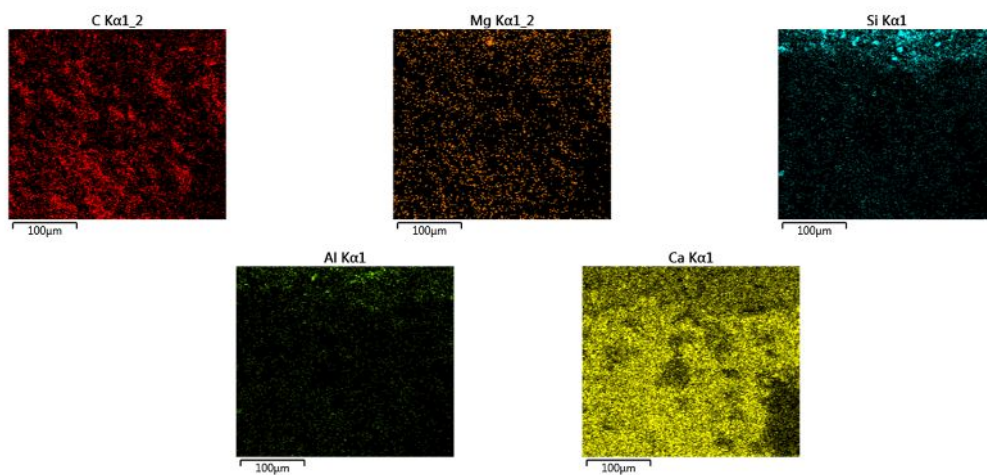


Figure 3.32. Variation of C, Mg, Si, Al and Fe signal intensities normalized to Ca signal with respect to depth for H.F.T.1 in LIBS



(a)



(b)

Figure 3.33. Variation of C, Mg, Si, Al and Fe signal intensities normalized to Ca signal with respect to depth in LIBS (a) and SEM-EDX mapping of H.Ba.T.1 (b)

LIBS analyses were also used for multiple purposes as determination of chemical composition and thickness of patina on marble and travertine surfaces as in SEM-EDX analyses. In LIBS analyses, the change of the trend lines of each element was used to estimate the thickness of the patina layer formed on marble and travertine surfaces. The trend lines became a straight line when the patina layer was over during the repetitive laser shots. Thus, the changes in the trend line of the elements showed that the thickness of the patina formation on marble and travertine surfaces were around a few tens of microns for each of the samples according to LIBS results (Table 3.9).

The thickness of patina samples determined by SEM-EDX analyses show differences from the LIBS analyses (Table 3.9). In SEM-EDX analyses, the position of the sample may be angled and may mislead the user with subjective interpretations. In addition to this, the thickness determined by SEM-EDX are in a wide range with respect to LIBS. It can be concluded that the in-depth LIBS analyses, which directly measure the layer changes on the specimens, are probably more precise and sensitive with respect to visual SEM-EDX analyses to conclude the thickness of the patina regardless of subjective interpretations of the user. Thus, the use of in-depth LIBS profiling is critical in the determination of thickness of patina on marble and yellow travertine surfaces.

Table 3.9. The thickness of patina formations determined by SEM-EDX and LIBS analyses

| Stone Type | Sample    | Thickness of yellow patina formation (µm) |                       |
|------------|-----------|---|-----------------------|
|            |           | SEM-EDX results                           | In-depth LIBS results |
| Marble     | Ai.Th.M.1 | ~78-105                                   | -                     |
|            | Ai.Th.M.2 | ~95-243                                   | ~15                   |
|            | Ai.Te.M.1 | ~76-164                                   | ~50                   |
|            | Ap.Te.M.1 | ~54                                       | ~10                   |
|            | Ap.B.M.1  | -   | ~15                   |
| Travertine | H.A.T.1   | ~ 73-154                                  | ~30                   |
|            | H.A.T.2   | -   | ~25                   |
|            | H.Ba.T.1  | -   | ~10                   |
|            | H.N.T.1   | ~ 55                                      | ~25                   |
|            | H.F.T.1   | ~ 6                                       | ~15                   |

The result of these calculations show consistency with respect to the chemical compositions of patina on the surface for each sample. SEM-EDX analyses corresponded to these results considering the weathering of calcium carbonate surfaces. It can be evaluated that the calcium oxalate patina forms a compact layer on the surface of marble and travertine in general. However, the thickness of the samples change free from the ratios and elemental composition formed on the original calcium carbonate material according to the results of in-depth LIBS analyses. The calcium oxalate, gypsum or clay minerals could form a homogeneous film layer on stone surfaces, but it can also be deposited on some points in the pores of the stones which cause a higher thickness of the patina. The LIBS and SEM-EDX analyses give a general information about the thickness of the patina giving the minimum and maximum limits of it formed on calcareous stone surfaces.

LIBS graphs also showed that the first five shots give detailed information about the chemical composition of yellow patina layer superficially where it displays the highest signal intensities of patina. Within this respect, the high signal intensities and the average values of peak areas of first five shots of each sample were calculated to gather information about the elemental composition of the first 5  $\mu\text{m}$  depth patina on the calcareous stone surfaces for each element for marble and travertine separately (Table 3.10, Table 3.11). These calculations were illustrated in Figure 3.34 and Figure 3.35 to evaluate the differences of element ratios for marble and travertine samples graphically (Figure 3.34, Figure 3.35). Their results indicated that C, Si, Al, Mg and Fe contents are higher in the patina layers according to the sound inner cores of marble (Table 3.10, Figure 3.34). Then same trend was also observed in the travertine graphs for each element, which show good agreement with the previously mentioned chemical and mineralogical analyses results of patina formation observed on both of the stone types (Table 3.11, Figure 3.35).

When all the results of chemical tests are evaluated, it is observed that the C ratio of the samples decrease from surface to the sound inner cores of marble and travertine samples because of the differences in chemical composition of calcium oxalate and calcium carbonate. C content is higher in calcium oxalate ( $\text{CaC}_2\text{O}_4$ -yellow patina surface) with respect to calcium carbonate ( $\text{CaCO}_3$ -the major mineral of marble and travertine) considering their mass percent in the total molecular weight as it was mentioned before. The presence of organic materials is another factor of the increase in the C content of stone surfaces. Ca ratio gets higher from surface to the inner cores of the stones which is

also related with Ca content of calcium carbonate and calcium oxalate observed as yellow patina on stone surfaces.

Mg, Al and Si are present with minor ratios in the sound inner parts of stones according to the SEM-EDX results of marble and travertine samples as mentioned. They increase in the yellow patina zone as it is also understood from the LIBS results of the surfaces of same samples. This increase is almost impossible to be distinguished from the SEM-EDX mapping results for Mg. However, the higher ratios of Al and Si elements are clearly observed on the SEM-EDX mapping images of the sample sections. The increase of these elements are related with the clay deposition incorporated in the patina layer on the stone surfaces. The clays may be carried from the environment as windborne particles on the climate exposed marble and travertine surfaces.

The increase of Fe is visible during in-depth profiling of LIBS in marble and travertine in accordance with the SEM-EDX results. However, it is not so clear in the SEM-EDX mapping images of the prepared marble and travertine sections. Fe is observed on the yellow colored stone surfaces denser according to the inner cores of the carbonate stones as a weathering product. It may be related with clay deposition considering the high amounts of Fe together with Al and Si on all of the stone surfaces.

Another possible cause of iron precipitation is related with the oxidation, mobilization and precipitation process of metal compounds carried from the inner cores or neighboring materials of the stones in the presence of water. According to this mechanism, the water penetrates from exterior surface to the inner parts of the stone when the exterior surface of the stones gets wet. In the interior, the minerals that contain iron compounds are dissolved and  $\text{Fe}^{2+}$  is moved to the dry surfaces by water and oxidized to form  $\text{Fe}^{3+}$  (Oguchi 2001, Press and Siever 2002). When considering the minor amounts of Fe together with Al and Si in the sound inner cores of marble and travertine, they may also be carried from the environment, either.

Table 3.10. The signal intensity ratios of elements considering the average values of ~5  $\mu\text{m}$  thick area in in-depth LIBS analyses of yellow patina and sound inner core of marble

| Samples          | C/Ca   |            | Mg/Ca  |            | Si/Ca  |            | Al/Ca  |            | Fe/Ca  |            |
|------------------|--------|------------|--------|------------|--------|------------|--------|------------|--------|------------|
|                  | Patina | Inner Core | Patina | Inner Core | Patina | Inner Core | Patina | Inner Core | Patina | Inner Core |
| <b>Ai.Th.M.2</b> | 0.07   | 0.01       | 1.74   | 0.36       | 0.64   | 0.20       | 2.76   | 1.10       | 4.54   | 2.59       |
| <b>Ai.Te.M.1</b> | 0.05   | 0.02       | 2.33   | 1.85       | 0.79   | 0.46       | 42.04  | 25.18      | 13.09  | 7.92       |
| <b>Ap.B.M.1</b>  | 0.10   | 0.04       | 3.69   | 1.23       | 1.70   | 0.37       | 1.32   | 0.89       | 1.69   | 0.73       |
| <b>Ap.Te.M.1</b> | 0.03   | 0.01       | 0.79   | 0.35       | 0.39   | 0.04       | 1.57   | 1.17       | 3.82   | 2.79       |
| <b>S.Te.M.1</b>  | 0.01   | 0.01       | 0.60   | 0.27       | 0.29   | 0.06       | 1.31   | 0.38       | 38.80  | 48.29      |

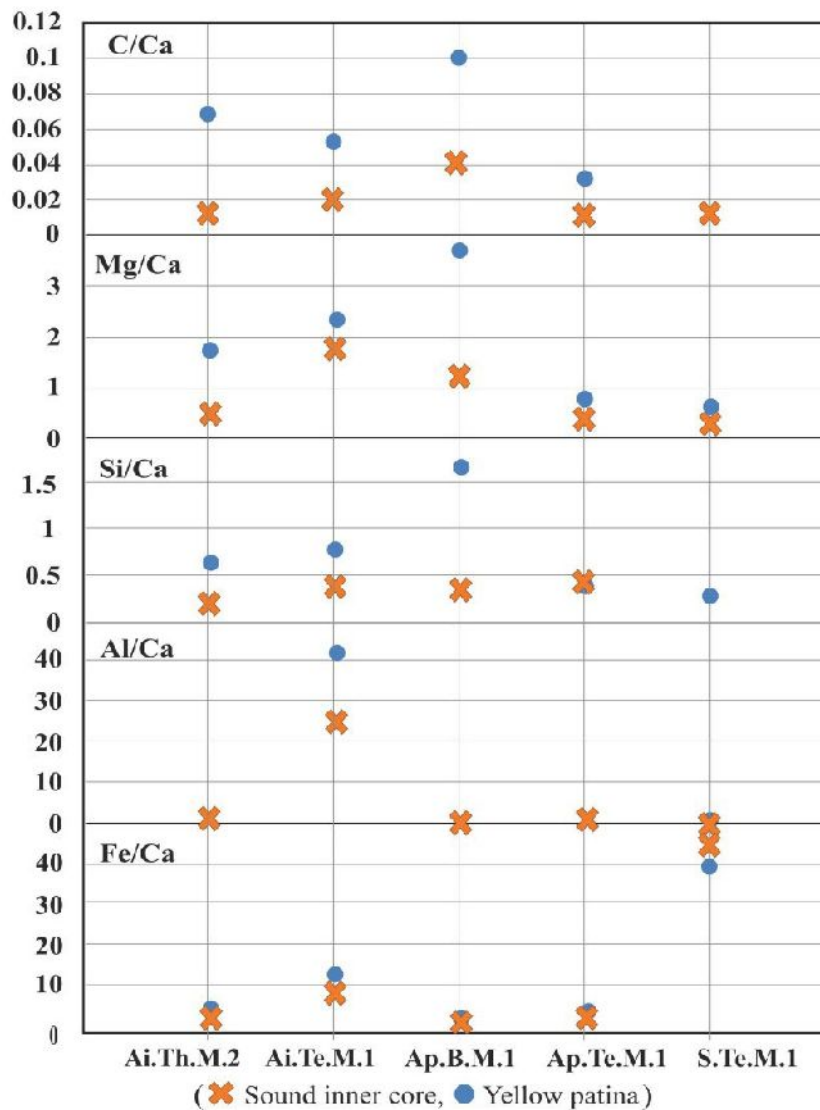


Figure 3.34. Graph showing the average content of C, Mg, Si, Al and Fe in the superficial layer of patina (~first 5  $\mu\text{m}$  depth) and inner core of marble using LIBS

Table 3.11. The signal intensity ratios of elements considering the average values of ~5  $\mu\text{m}$  thick area in in-depth LIBS analyses of yellow patina and sound inner core of travertine

| Samples  | C/Ca   |            | Mg/Ca  |            | Si/Ca  |            | Al/Ca  |            | Fe/Ca  |            |
|----------|--------|------------|--------|------------|--------|------------|--------|------------|--------|------------|
|          | Patina | Inner Core | Patina | Inner Core | Patina | Inner Core | Patina | Inner Core | Patina | Inner Core |
| H.A.T.1  | 0.02   | 0.01       | 0.41   | 0.28       | 0.08   | 0.05       | 0.05   | 0.03       | 8.58   | 13.24      |
| H.A.T.2  | 0.02   | 0.01       | 0.78   | 0.36       | 0.06   | 0.01       | 0.16   | 0.04       | 1.41   | 0.72       |
| H.Ba.T.1 | 0.03   | 0.02       | 2.23   | 0.64       | 0.90   | 0.08       | 0.15   | 0.02       | 2.74   | 1.05       |
| H.F.T.1  | 0.02   | 0.01       | 0.58   | 0.35       | 0.13   | 0.03       | 33.59  | 33.74      | 1.63   | 1.89       |
| H.N.T.1  | 0.03   | 0.01       | 1.38   | 0.70       | 0.34   | 0.05       | 64.92  | 41.90      | 3.51   | 2.12       |

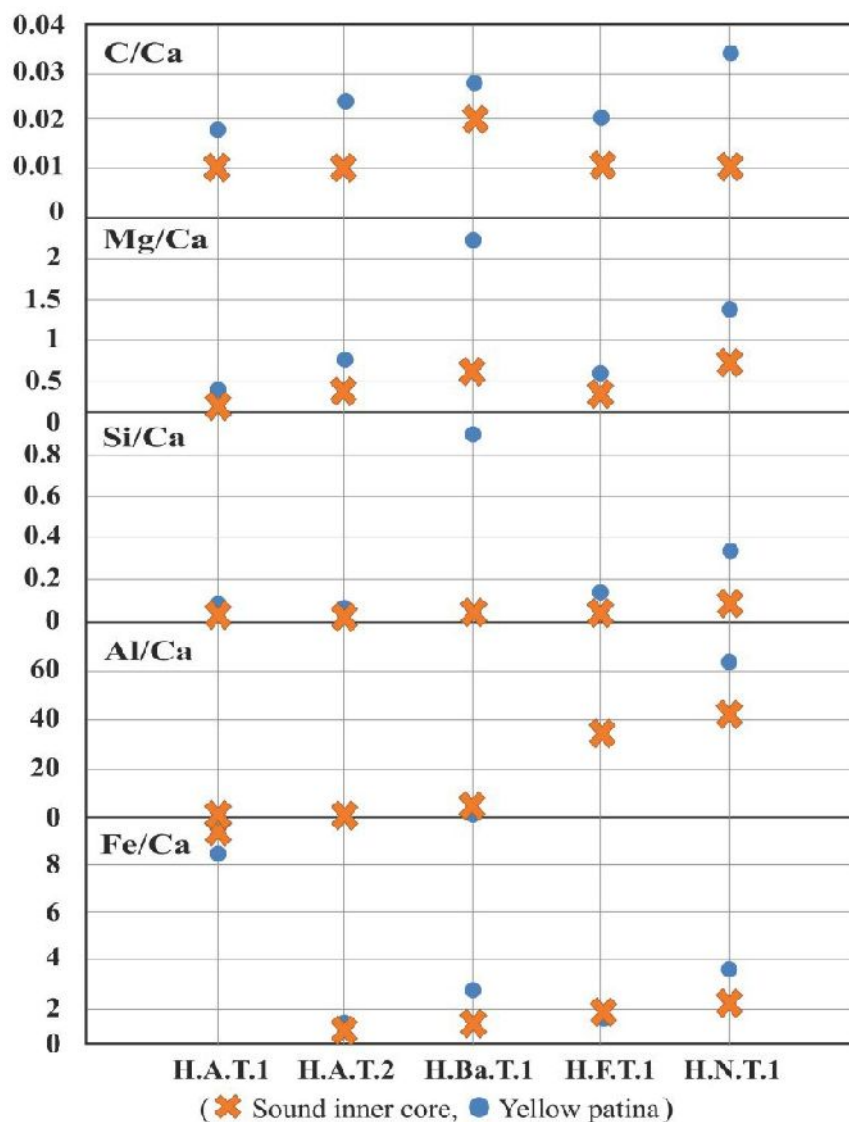


Figure 3.35. Graph showing the average content of C, Mg, Si, Al and Fe in the superficial layer of patina (~first 5  $\mu\text{m}$  depth) and inner core of travertine using LIBS

### **3.3. The Source of $\text{CaC}_2\text{O}_4$ and Yellow Color of Calcium Oxalate Patina on Marble and Travertine**

The source of yellow patina formation was investigated by mineralogical and chemical analyses in the limits of this study. The results showed that calcium oxalate is the main source of yellow patina formation on calcareous stone surfaces as it is observed from the XRD and FT-IR patterns of nine of twelve marble and travertine samples in accordance with the previous studies (Table 3.1, Table 3.2). However, the yellow color was also observed on the stone surfaces that calcium oxalate was not determined. Hence in the rest of other yellow patina samples, calcite is observed as the major component of the samples collected from the surfaces of S.Te.M.1, Ap.B.M.1 and H.F.T.1 (Table 3.2).

In this study, calcium oxalate formation was most probably formed due to the biological actions detected on the facades of studied marble and travertine monuments in the scope of this study (Figure 3.36). The determination of organic compounds in FT-IR analyses were the signs of biogenic activities on marble and travertine surfaces (Figure 3.8, Figure 3.9). In addition to this, the traces of lichen thalli and living organism itself determined on SEM images were also determined as biological agents settled on the surfaces and even in the pores of calcite rich stones (Figure 3.37). The biological origin of oxalate formation is assumed when there is no trace of brush strokes which is a sign of previously applied man-made treatment on stone surfaces (Del Monte and Sabbioni 1987). The lack of any brushstrokes on marble and travertine strengthen the biological origin theory for the case study samples in accordance with the Del Monte and Sabbioni's biological origin theory (Del Monte and Sabbioni 1987). Hence, anthropogenic origin is almost impossible considering the sizes of the archaeological monuments for such a conservation intervention which is easy to be applied for small objects.

Biological formations produce oxalic acid on the surfaces of stones. The oxalic acid reacts with calcium carbonate which is the major mineral of calcareous stones. As a result of this chemical reaction, calcium oxalate forms on the surfaces of stones. Calcium oxalate is colorless to bright yellow in original form (Garcia-Valles et al. 1997). However, this layer is observed in different hues of yellow to brown in color on marble and travertine surfaces (Figure 3.38, Figure 3.39).



Figure 3.36. Biological formations on the marble walls of Zeus Temple in Aizanoi

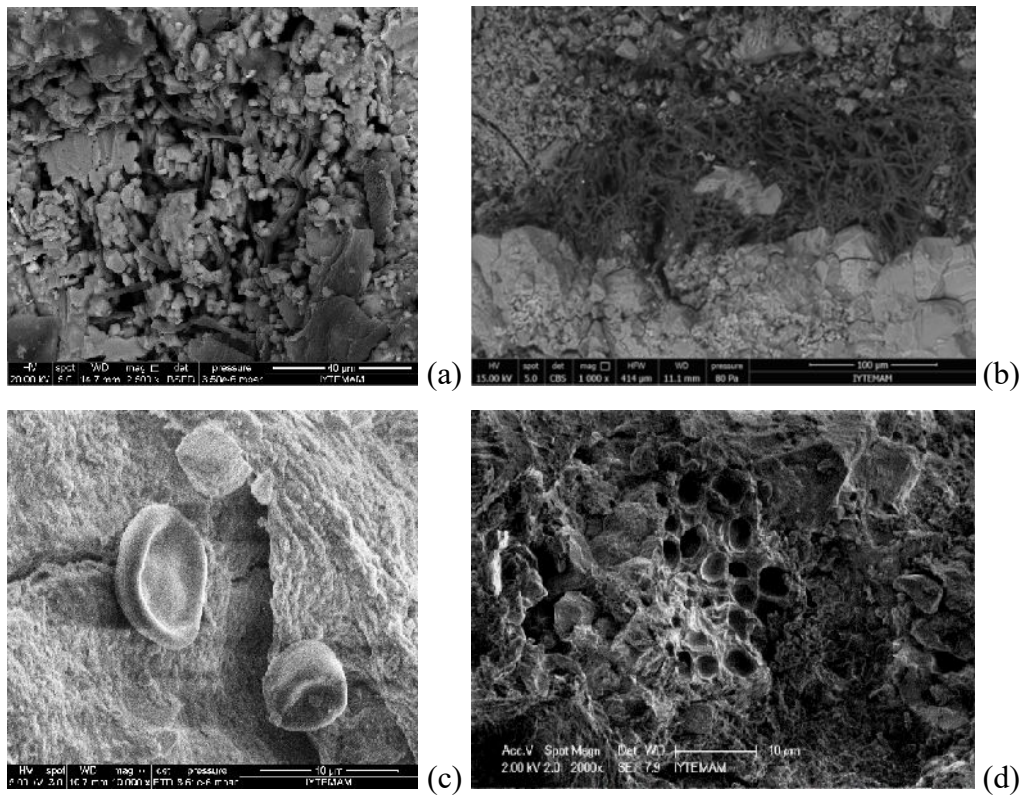


Figure 3.37. SEM images of lichen formations (H.A.T.1 (a, b), H.N.T.1 (c)) and traces of living organisms (H.N.T.1 (d)) in the yellow patina formations of travertine surfaces

Besides the yellow color of calcium oxalate covered stone surfaces, three of the stone samples, which calcium oxalate could not be determined, were also observed as yellow in color. When evaluated in this manner, yellowing may form with the presence of clay minerals and Fe precipitation on calcareous stone surfaces regardless from calcium oxalate formation. Clay minerals could be transformed by wind or water, or may be a weathering product formed on marble and travertine surfaces (Polikreti and Maniatis 2003). In this study, the increase of Si/Ca and Al/Ca together with Fe/Ca ratios on the stone surfaces indicates the presence of clays and dirt on stone surfaces, which may be the main cause of yellow color on climate exposed marble and travertine stones.

Another possible cause of yellow appearance of the weathered stone surface of calcium oxalate formation on the stone surface is directly related with the precipitation of leachable iron elements on stone surfaces carried from the inner cores or neighboring materials of the stones. As a result of this process, iron containing colored minerals precipitate on the surfaces of stones and calcium oxalate layers were observed in different hues of yellow on stone surfaces (Oguchi 2001, Press and Siever 2002). Fe may be carried from the environment, also (Kalaitzaki 2005). In this study, there was an increase of Fe precipitation on marble and travertine surfaces strengthening the possibility of source of yellowing for calcium oxalate formation on calcareous stone surfaces probably carried from the environment. It increased from 0.00-0.49 % to 1.48-24.68 % for marble samples, and 0.38-4.50 % to 1.97 and 10.98% for travertine samples. Kalaitzaki discuss Fe precipitation by refusing the possibility of Fe elements leaching from the inner parts of marble and travertine (Kalaitzaki 2005). Because he points out that calcareous stones do not include much Fe element to leach from the interior of the stone. Thus he explains it with the wind-born Fe elements coming from the surroundings. He also suggests that it may be related with the weathering of organic products applied for the conservative purposes on the surface of the stones (Kalaitzaki 2005). However, the possibility of the leachable iron elements should be investigated in detail for marble and travertine stone separately in order to have accurate information about it.

Yellowing is also formed as a result of colored mineral coatings (Garcia-Valles et al.1997). It was observed in a case study in Catalonia focusing on the colorless characteristic of weddelite formed on marble surfaces. According to the results of this research, the yellow color of the calcium oxalate layer was related with iron precipitation. Iron is related with the weathering of chlorophylls on the stone surfaces (Garcia-Valles et al.1997).

Different hues of the same elements are related with the precipitation in the pores and on the surfaces of the stones. Patina formation is darker on the areas that are precipitated in the craters of stone surfaces. In addition to this, the patina formations are darker on the surfaces that are protected from rain and water (Kalaitzaki 2005). It is proved in a research study focusing on the characterization of protective patinas applied on historical building surfaces (Buergo and Gonzales 2003). In this research, the scientists evaluate the yellow color on 4 facades of the building. The hue of the patina gets more intense in lower areas of the building and in areas protected from rain wash and solar radiation (Buergo and Gonzales 2003). Considering this, the different hues of the same color should be handled as the same patina type on the same monument surfaces.

Considering all the results of the study, the increase of Fe, Al and Si on the surfaces of marble and travertine show that the yellowing of colorless stone surfaces and calcium oxalate layer may be because of the precipitation of leachable iron elements and clay deposition on the surfaces of stones.



Figure 3.38. Different hues of yellow patina on marble ruins of Zeus Temple in Aizanoi



Figure 3.39. Different hues of yellow patina on travertine ruins of Necropolis in Hierapolis

## CHAPTER 4

### CONCLUSION

The conservation interventions of patina formed on the surfaces of stone monuments should be evaluated within a comprehensive approach in the archaeological excavations considering the material characteristics of patina and stone under it. In this study, the mineralogical composition and microstructural and chemical characteristics of patina formed on marble and yellow travertine surfaces were investigated in order to constitute a conservation approach for patina formation on calcareous stone surfaces in the archaeological sites.

The mineralogical composition, micro-structural and chemical characteristics of stones and patina were determined by using XRD, FT-IR, SEM-EDX, TGA and LIBS on marble used in Aizanoi, Aphrodisias and Sardes archaeological sites; and on yellow travertine used in Hierapolis archaeological site.

Marble and yellow travertine is composed of mainly calcite ( $\text{CaCO}_3$ ) together with the minor amounts of quartz ( $\text{SiO}_2$ ) minerals in general. CaO was determined with major amounts, and MgO,  $\text{Al}_2\text{O}_3$ ,  $\text{SiO}_2$ ,  $\text{SO}_3$  and FeO were determined with minor amounts in the chemical composition of marble and yellow travertine samples.

The patina layer was mainly composed of calcium oxalate in the form of weddellite ( $\text{CaC}_2\text{O}_4 \cdot 2\text{H}_2\text{O}$ ) or whewellite ( $\text{CaC}_2\text{O}_4 \cdot \text{H}_2\text{O}$ ). Gypsum ( $\text{CaSO}_4 \cdot 2\text{H}_2\text{O}$ ), quartz ( $\text{SiO}_2$ ) and calcite ( $\text{CaCO}_3$ ) minerals were also observed. Calcium oxalate was the main source of yellow patina formation providing a homogeneous protective layer on the calcareous stone surfaces against the weathering effect of water because it is less soluble in water than calcite. It is most probably formed because of the reaction between calcite crystals and oxalic acid that biological formations produce on the stone surfaces. Calcium oxalate is colorless in origin. However, it is observed in different hues of yellow on marble and yellow travertine surfaces because of leachable Fe elements or clay and dirt deposited in the same layer.

C, Mg, Al, Si, S and Fe decrease; and Ca increase from the surface to the inner parts of marble and travertine. The higher amount of C is related with its molar mass in calcium oxalate patina with respect to calcite rich marble and travertine material. The

higher amounts of Al and Si together with Fe elements are signs of clay deposition carried from the environment by the effect of wind or water. S is related with gypsum formed on stone due to air pollution. The increase of Ca in the sound inner cores of stone is related with the molar mass of Ca in calcite, which is the main mineral of marble and travertine with respect to calcium oxalate.

The patina formation was determined on both marble and yellow travertine surfaces representing a homogeneous and nodular film layer with euhedral crystals on the coarse grained calcite crystals of marble and travertine surfaces. It is deposited in the pores of travertine in some cases, also.

The thickness of the yellow patina layer is also another critical issue that should be regarded before intervention. In this study, the thickness of patina was determined as a few tens of microns according to the results of LIBS and SEM-EDX analyses. The LIBS results are more precise according to SEM-EDX results indicating the importance of in-depth LIBS profiling for the determination of patina layer on marble and yellow travertine surfaces for this type of studies. These analyses also show that it is almost impossible to clean the patina layer without intervention to the original stone material.

Gypsum and clay minerals were also present in the same layer with minor amounts. Gypsum is easily dissolved in the presence of water resulting with the loss of original stone material. In addition to this, swelling and shrinkage of clay minerals are also affective in the physical weathering of stones. Thus, it can be concluded that gypsum and clay minerals in the calcium oxalate layer may cause to speed the weathering of marble and travertine. However, it is almost impossible to clean them from the stone surfaces without detriment to the original building material or calcium oxalate patina and should be conserved in the conservations studies of the selected cases.

Based on the results of visual analyses and experimental methods, this study sheds light to constitute a conservation approach for the interventions of yellow patina formation observed on marble and travertine monuments. It recommends avoiding irreversible interventions as cleaning of patina for the conservation of the historical building materials in the archaeological sites. The calcium oxalate patina should be protected with respect to the principles of international charters on the protection of patina layer on stone surfaces. Patina represents the authentic and historical value of buildings and monuments in the archaeological sites. It may include information about the former environmental conditions and past civilizations, also. Thus, it should be regarded as a part of the building or monument with all its characteristic and conserved as the witnesses of

the bygone time. In addition to this, calcium oxalate is a less soluble material in water according to calcite representing a protective patina against weathering of marble and travertine surfaces with the effect of water. If this layer is cleaned from the calcareous stone surface, it causes the original stone material to be subjected to the environmental conditions. It results with the rapid weathering of climate exposed original stone material by water or humid environment which was protected under the patina layer for many years.

The cleaning of patina may be indispensable in some cases for the long term maintenance of the original stone materials in the archaeological sites. The material characteristics of patina formation may be destructive for the underlying stone substrata. It may include harmful agents as clays and gypsum that was determined in this study. Clays expand in moist environment and cause the formation of fissures and cracks by swelling in the pores and on the exterior surfaces of stones. They also promote the growth of algae, lichen, moss, etc. which also cause physical and chemical weathering of original stone materials. Gypsum is soluble in water. Thus it results with the loss of original stone material. In such a case, it should be removed from the stone surface without detriment to the original building material. The harmless patina layer and original stone surface should be protected as a part of the historical monument.

However, the decision of cleaning intervention is directly related with the formation and material characteristics of patina layer or layers overlapped. In this case, it is almost impossible to clean the harmful agents from the surface of marble and travertine without detriment to the calcium oxalate patina or original stone material. Thus, patina layer should be protected without any intervention. In addition to this, consolidation, stabilization of decay, long term planned maintenance and repair is also essential considering the reversible intervention, no adverse effects and compatibility for the restoration works on original fabric and patina layer. The cleaning of patina should be taken into account if only it causes advanced decay on original materials.

The future works may be planned in various fields considering the results of this thesis. The term “patina” should be precisely mentioned in the international charters by giving a detailed guideline for the conservation interventions for various types of patina formation on the surfaces of stones used in the construction of historical buildings and monuments in cultural heritage studies. In research studies, yellow patina formation may be handled considering the formation mechanism of it in various environments which promotes or reduces its precipitation with the effect of microclimatic conditions,

microorganism types, and mineralogical, chemical and microstructural characteristics of original stone material, formation of patina on different sides of the buildings which may affect its thickness on the monument surfaces.

This study lead conservators about the intervention decisions of yellow patina formed on the surfaces of calcareous stone monuments for the purpose of conservation in the archaeological sites. It indicates that the patina formation should not be disregarded on historical buildings and monument surfaces in the archaeological sites. In conflict, it must be protected with all its authentic characteristics if it is protective against water, air pollution, humidity, climatic shifts etc. according to the original stone material underlying it. Within this respect, the proper diagnosis on the presence and mineralogical composition, and microstructural and chemical characteristics of patina should be made. The causes and aesthetical and functional effects of patina on marble and especially yellow travertine surfaces should be very well investigated and evaluated before deciding conservation interventions and cleaning techniques for stone monuments in the archaeological sites.

## REFERENCES

- Adamo, P., Violante, P. 2000. Weathering of rocks and neogenesis of minerals associated with lichen activity (Review). *Applied Clay Science* 16: 229-256.
- Anglos, D., Miller, J.C. 2009. Cultural Heritage Applications of LIBS, in R. Noll, V. Sturm, M. Stepputat, A. Whitehouse, J. Young, P. Evans. (Eds.) *Industrial applications of LIBS, Fundamentals and Applications*. Cambridge Uni. Press, UK.
- Atalay, R. 2014. Afrodisias Heykel Okulu. *Ulakbilge*. 2 (3):140-149.
- Bario, S.V., Garcia-Valle's, M., Pradel, T., Vendrell-Saz, M. 2002. The red-orange patina developed on a monumental dolostone. *Engineering Geology* 63:31-38.
- Böke, H., Gauri, K.L. 2003. Reducing Marble SO<sub>2</sub> Reaction Rate by the Application of Certain Surfactants. *Water Air and Soil Pollution* 142: 59-70.
- Brandi, C. 1949. The cleaning of pictures in relation to patina, varnish and glazes. *The Burlington Magazine* 556:183-89.
- Buergo, M.A., Gonzalez, R.F. 2003. Protective patinas applied on stony façades of historical buildings in the past. *Construction and Building Materials* 17: 83-89.
- Caner, E.N., Böke, H. 1989. Occurrence of calcium oxalates on marble monuments in Anatolia. *The Proceedings of The oxalate films: origin and significance in the conservation of works of art*. Milano: 299-307.
- Chen, J., Blume, H.P., Beyer, L. 2000. Weathering of rocks induced by lichen colonization—a review. *Catena* 39 (2): 121-146.
- Conforto, L., Felici, M., Monna, D., Serva, L., Taddeucci, A. 1975. A preliminary evaluation of chemical data (trace element) from classical marble quarries in the Mediterranean. *Archeometry* 17(2): 201-213.
- Crispim, C.A., Gaylarde, C.C. 2004. Cyanobacteria and Bioeterioration of Cultural Heritage: A Review. *Microbial Ecology* 48 (1): 1-9.
- Cutler, N.A., Viles, H.A., Ahmad, S., McCabe, S., J.Smith, B. 2013. Algal 'greening' and the conservation of stone heritage structures. *Science of the Total Environment* 442: 152-164.
- Çakır, G.Ö., 2010. Aizanoi Zeus Tapınağının yeniden tarihlendirilmesinin bezeme örgeleri ışığında irdelenmesi. In: *"Arkeolojik Yapı Araştırması. Yöntemler ve Kuramlar I"* Yüksek Lisans Semineri. Mimar Sinan Güzel Sanatlar Üniversitesi, Arkeoloji Bölümü.

- Del Monte, M., Sabbioni, C. 1987. A study of the patina called 'Scialbatura' on Imperial Roman marbles. *Studies in Conservation* 32: 114-121.
- Dakal, T.C., Cameotra, S.S. 2012. Microbially induced deterioration of architectural heritages: routes and mechanisms involved (Review). *Environmental Sciences Europe*, 24: 36.
- Diakumaku, E., Gorbushina, A.A., Krumbein, W.E., Panina, L., Soukharjevski, S. 1995. Black fungi in marble and limestones – an aesthetical, chemical and physical problem for the conservation of monuments. *The Science of the Total Environment* 167: 295-304.
- Di Bonaventura, M. P., Gallo, M. D., Cacchio, P., Ercole, C., and Lepidi, A. 1999. Microbial formation of oxalate films on monument surfaces: *Bioprotection or Biodeterioration?* *Geomicrobiology Journal* (16): 55–64.
- Doherty, B., Pamplona, M., Selvaggii R., Miliani, C., Matteini, M., Sgamellotti, A., Brunetti, B. 2007. Efficiency and resistance of the artificial oxalate protection treatment on marble against chemical weathering. *Applied Surface Science* 253: 4477–4484.
- Fassina, V. 1995. New findings on past treatments carried out on stone and marble monuments' surfaces. *The Science of the Total Environment* 167: 185-203.
- Gadd, G.M. 2007. Geomycology: biogeochemical transformations of rocks, minerals, metals and radionuclides by fungi, bioweathering and bioremediation. *Mycological Research III* 3-49.
- Garcia-Valle's, M., Vendrell-Saz., M., Krumbein, W.E., Urzi, C. 1997. Coloured mineral coatings on monument surfaces as a result of biomineralization: the case of the Terragona cathedral (Catalonia). *Applied Geochemistry* 12: 255-266.
- Garcia-Valle's, M. Urzi, C., De Leo, F., Salamone, P., Vendrell-Saz, M. 2000. Biological weathering and mineral deposits of the Belevi marble quarry (Ephesus, Turkey). *International Biodeterioration and Biodegradation* 46: 221-227.
- Garcia-Valle's, M., Topal, T., Vendrell-Saz, M. 2003. Lichenic growth as a factor in the physical deterioration or protection of Cappadocian monuments. *Environmental Geology* (43): 776–781.
- Garrels, R.M. 1951. *A Textbook of Geology*. USA: Harper & Brothers Publishers.
- Gauri, K. L. and Bandyopadhyay, J. K. 1999. *Carbonate Stone Chemical Behaviour, Durability, and Conservation*. Canada: A Wiley-Interscience Publication John Wiley & Sons Inc.
- Gazzano, C., Favero-Longo, S.E., Iacomussi, P., Piervittori, R. 2013. Biocidal effect of lichen secondary metabolites against rock-dwelling microcolonial fungi, cyanobacteria and green algae. *International Biodeterioration and Biodegradation* 84: 300-306.

- Gauri, K.L., Bandyopadhyay, J.K. 1999. *Carbonate stone: Chemical behavior, durability, and conservation*. USA: A Wiley-Interscience Publication.
- Giakoumaki, A., Melessanaki, K., Anglos, D. 2007. Laser-induced breakdown spectroscopy (LIBS) in archaeological science - applications and prospects. *Analytical and Bioanalytical Chemistry* 387-3 (12): 749-760.
- Grimmer, A.E. 1988. *Keeping it clean: Removing Exterior Dirt, Paint, Stains and Graffiti from Historic Masonry Buildings*. Darby: Diane Publishing Co.
- Hanfmann, G., Ramage, N.H. 1978. Sculpture from Sardis: The Finds through 1975. In: Hanfmann G., Jacobs, S. (Eds.): *Archaeological Explorations of Sardis*. Cambridge, Massachusetts and London, England: Harvard University Press.
- Howe, J. E. 2001. *The Geology of Building Stones*. USA: Donhead Publishing Ltd.
- ICOMOS. "The Venice Charter (1964)". Accessed May 23 2017.  
[http://www.icomos.org/charters/venice\\_e.pdf](http://www.icomos.org/charters/venice_e.pdf)
- ICOMOS. "The Nara Document on Authenticity (1994)". Accessed May 23 2017.  
<http://www.icomos.org/charters/nara-e.pdf>
- ICOMOS. "Principles for the Analysis, Conservation and Structural Restoration of Architectural Heritage in Zimbabwe (2003)". Accessed May 23 2017.  
[https://www.icomos.org/charters/structures\\_e.pdf](https://www.icomos.org/charters/structures_e.pdf)
- ICOMOS. "New Zealand Charter for the Conservation of Places of Cultural Heritage Value (2010)". Accessed May 23 2017.  
[http://www.icomos.org/charters/ICOMOS\\_NZ\\_Charter\\_2010\\_FINAL\\_11\\_Oct\\_2010.pdf](http://www.icomos.org/charters/ICOMOS_NZ_Charter_2010_FINAL_11_Oct_2010.pdf)
- Jokilehto, J. 2002. *A History of Architectural Conservation*. London: Butterworth-Heinemann.
- Kalaitzaki, P.M., Anglos, D., Kilikoglou, V., Zafiropulos, V. 2001. Compositional characterization of encrustation on marble with laser induced breakdown spectroscopy, *Spectrochimica Acta - Part B*: 887-903.
- Kalaitzaki, P.M. 2005. Black crust and patinas on Pentelic marble from the Parthenon and Erectheum (Acropolis, Athens): characterization and origin. *Analytica Chimica Acta* 532: 187-198.
- Krumbein, W., Bogomolova, E., Gorbushina, A., Panina, L., Rybalchenko, O., Ryshov, S., Sagulenko, E., Vlasov, D. 1995. Biodeterioration and conservation status of marble monuments on Crimea. *Transactions on the Built Environment* 15: 195-204.

- Lazic, V., Fantoni, R., Colao, F., Santagata, A., Morone, A., Spizzichino, V. 2004. Quantitative laser induced breakdown spectroscopy analysis of ancient marbles and corrections for the variability of plasma parameters and of ablation rate, *Journal of Analytical Atomic Spectrometry* 19: 429-436.
- Lazic, V., Colao, F., Fantoni, R., Fiorani, L., Palucci, A., Striber, J., Santagata, A., Morone, A., Spizzichino, V. 2005. Spectroscopic monitoring of the laser cleaning applied to ancient marbles from Mediterranean areas. *Lasers in the Conservation of Artworks Springer Proceedings in Physics* 100: 451-456.
- Lazzarini, L., Salvadori, O. 1989. A reassessment of the formation of the patina called 'Scialbatura'. *Studies in Conservation* 34: 20-26.
- Lian, B., Chen, Y., Zhu, L., Yang, R. 2008. Effects of microbial weathering on carbonate rocks. *Earth Science Frontiers* 15 (6): 90-99.
- Long, L. E. 2012. *The regional marble quarries*. In: Ratté, C., De Staebler, P. (Eds.): *The Aphrodisias Regional Survey, Project Aphrodisias* 5 165-201. Mainz.
- Macchia, A., Sammartino, M.P., Laurenzi Tabasso, M.A. 2011. A new method to remove copper corrosion stains from stone surfaces. *Journal of Archaeological Science* 38(6): 1300-1307.
- Macedo, M.F., Miller, A.Z., Dionisoi A., Saiz-Jimenez, C. 2009. Biodiversity of cyanobacteria and green algae on monuments in the Mediterranean Basin: an overview. *Microbiology* 155: 3476-3490.
- Marvasi, M., Donnarumma, F., Frandi, A., Mastromei, G., Sterflinger, K., Tiano, P., Perito, B. 2012. Black microcolonial fungi as deteriogens of two famous marble statues in Florence, Italy. *International Biodeterioration and Biodegradation* 68: 36-44.
- Monroe, J.S., Wicander, R. 2007. *Fiziksel Jeoloji, Yeryuvarı'nın Araştırılması*. Translated by Dirik, K., Şener, M. İstanbul: Berkay Ofset Ltd. Şti.
- Montanari, V. 1996. Patina: surface deposit, alteration or outward appearance? Preliminary considerations for the conservation of stone surfaces in architecture. *Proceedings of the 8<sup>th</sup> International Congress on Deterioration and Conservation of Stone* 929-933. Berlin, Germany.
- Monte, M. 2003. Oxalate film formation on marble specimens caused by fungus. *Journal of Cultural Heritage* 4: 255-258.
- Moropoulou, A., Bisbikou, K., Torfs, K., Van Grieken, R., Zezza, F., Macri, F. 1998. Origin and growth of weathering crust on ancient marbles in industrial atmosphere. *Atmospheric Environment* 32(6): 967-982.
- Niewöhner, P. 2013. Phrygian marble and stonemasonry as markers of regional distinctiveness in late antiquity. In: P. Thonemann (Ed.), *Roman Phrygia: Culture and Society*. Cambridge University Press, England.

- Oguchi, T.C. 2001. Formation of weathering rinds on andesite. *Earth Surface Processes and Landforms* 26: 847-858.
- Pavia, S., Caro, S. 2006. Origin of films on monumental stone. *Studies in Conservation* 51: 177-188.
- Philippot, P. 1966. The idea of patina and cleaning of paintings, in D. Bomford, M. Leonard (Eds.) (2004) *Readings in Conservation of Paintings*. Getty Conservation Institute, Los Angeles.
- Pineda, C.A., Martin, R.T., Hallbauer, D.K., Jacobson, L., Prozesky, V.M., Przybylowicz, W.J. 1997. Geochemical microanalyses of patina layers on rock artefacts from the Central Karoo and Southern Free State, South Africa. *Nuclear Instruments and Methods in Physics Research B* 130: 628-635.
- Pinna, D., Galeotti, M., Rizzo, A. 2015. Brownish alterations on the marble statue in the church of Orsanmichele in Florence: what is their origin? *Heritage Science* 3 (7)
- Plummer, C.C., Carlson D.H., Hammersley, L. 2010. *Physical Geology*, USA: McGraw-Hill.
- Polikreti, K., Maniatis, Y. 2003. Micromorphology, composition and origin of the orange patina on the marble surfaces of Propylaea (Acropolis, Athens). *The Science of the Total Environment* 308: 111-119.
- Press, F., Siever, R. 2002. *Understanding Earth, Third Edition*. New York: W.H. Freeman and Company.
- Prieto, B., Aira, N., Silva, B. 2007. Comparative study of dark patinas on granitic outcrops and buildings. *Science of the Total Environment* 381: 280-289.
- Rampazzi, L., Andreotti, A., Bonaduce, I., Colombini, M.P., Colomco, C., Toniolo, L. 2004. Analytical investigation of calcium oxalate films on marble monuments. *Talanta* 63: 967-977.
- Rodrigues, J.D. 2006. Stone Patina. A controversial concept of relevant importance in conservation. *Conference Paper: International Seminar Theory and Practice in Conservation I*. Lisbon, Portugal.
- Rodriguez, J.L.P., Duran, A., Centeno, M.A., Mzrtinez-Blanes, J.M., Robador, M.D. 2011. Thermal analysis of monument patina containing hydrated calcium oxalates. *Thermochimica Acta* 512: 5-12.
- Ruskin, J. 1849. *The Seven Lamps of Architecture*. Reprinted Noonday Press, New York 1961, Smith E. Jo L. New York: John Willey.
- Schaffer, R.J. 1932. *The Weathering of Natural Building Stones, Special Report No.18*. Garston, Watford: Building Research Establishment.

- Scheerer, S., Ortega-Morales, O., Gaylarde, C. 2009. Microbial Deterioration of stone monuments – an updated overview. *Advances in Applied Microbiology* 66:97-139.
- Scherer, G.W. 2006. Internal Stress and Cracking in Stone and Masonry. In: M.S. Konstadoutos (Ed.), *Measuring, Monitoring and Modeling Concrete Properties*, , 633-641. Netherlands: Springer.
- Siegesmund, S., Weiss, T., Vollbrecht, A. 2002. *Natural Stone, Weathering Phenomena, Conservation Strategies and Case Studies*. London: The Geological Society Press.
- SPAB. “Manifesto of the SPAB by William Morris, (1877)”. Accessed May 23 2017. <http://www.spab.org.uk/what-is-spab/the-manifesto/>
- Spile, S., Suzuki, T., Bendix, J., Simonsen, K.P. 2016. Effective cleaning of rust stained marble. *Heritage Science* (4):12
- Stilgoe, J.R. 2010. On not perceiving urban color. In: G. Poherty (Ed.), *New Geographies 3, Urbanism of Color*. USA: Harvard University Press.
- Stuart, B.H. 2007. *Analytical Techniques in Materials Conservation*. England: John Wiley & Sons, Ltd.
- Tas, A.C. 2011. Granules of brushite and octacalcium phosphate from marble. *Journal of the American Ceramic Society* 94 (11): 3722–3726.
- Toksöz, C. 1996. *Pamukkale - Hierapolis*. Denizli, Turkey: Barış Matbaası.
- Tykot R., Ramage, M. 2002. On the importation of monumental marble to Sardis. In: Herrmann, J., Herz, Jr.N., Newman, R. (Eds.): *Asmosia 5: Interdisciplinary Studies in Ancient Stone* Archetype Publications, London.
- UNESCO. “Aizanoi Antique City (2017)”. Accessed May 23 2017. <http://whc.unesco.org/en/tentativelists/5724/>
- UNESCO. “Hierapolis-Pamukkale (2017)”. Accessed May 23 2017. <http://whc.unesco.org/en/tentativelists/5724/>
- Urzi, C., De Leo, F. 2001. Biodeterioration of Cultural Heritage in Italy: State of Art. *ARIADNE 8 – Advanced Research Workshops: Bio-degradation of Cultural Heritage*. Advanced Research Centre For Cultural Heritage Interdisciplinary Projects.
- Vazquez-Calvo, C. Buergo, M. A., Fort, R. 2007 (a). Overview of recent knowledge of patinas on stone monuments: the Spanish experience. In: Prikryl, R., Smith, B.J. (Eds.): *Building Stone Decay: From Diagnosis to Conservation* 271: 295-307. London: Geological Society, Special Publications.

- Vazquez-Calvo, C., Buergo, M. A., Fort, R., Varas, M.J. 2007 (b). Characterization of patinas by means of microscopic techniques. *Materials Characterization* 58: 1119-1132.
- Vendrell-Saz, M., Krumbein, W.E., Urzi, C., Garcia-Valles, M. 1996. Are patinas of Mediterranean monuments really related to the rock substrate? *Proceedings of the 8<sup>th</sup> International Congress on Deterioration and Conservation of Stone* 609-624. Berlin, Germany.
- Warscheid, Th., Braams, J. 2000. Biodeterioration of stone: a review. *International Biodeterioration & Biodegradation* 46: 343-368.
- Watchman, A.L. 1991. Age and composition of oxalate-rich crusts in the northern territory, Australia. *Studies in Conservation* 36: 24-32.
- Weil, P.D. 1977. A review of history and practice of patination. In: Brown, B.F., Burnett, H.C., Chase, W.T., Goodway, M., Kruger, J., Pourbaix, M. (Eds.): *Proceedings of a Seminar, Corrosion and Metal Artifacts – A Dialogue between Conservators and Archaeologists and Corrosion Scientists*. Maryland: National Bureau of Standards Special Publication.
- Yu, Q.L., Brouwers, H.J.H. 2011. Thermal properties and microstructure of gypsum board and its dehydration products: A theoretical and experimental investigation. *Fire and Materials* 36:575–589,
- Zagari, M., Antonelli, F., Urzi, C. 2000. Biological patinas on the limestones of The Loches Romanic Tower (Touraine, France). In: V. Faccina (Ed.), *Proceedings of the 9th International congress on deterioration and conservation of stone*. 445-451. Elsevier, Amsterdam.
- Zimi, E. 2006. Aphrodisias, City in Asia Minor. In: N. Wilson (Ed.), *Encyclopedia of Ancient Greece*. New York London: Routledge Taylor and Francis Group.

# VITA

## Fulya BADUR

Date of Birth:

14.03.1984

Place of Birth:

Merzifon/ Amasya, TURKEY

Education:

Ph.D., İzmir Institute of Technology, Department of Architecture (2017)

M.Sc., İzmir Institute of Technology, Department of Architectural Restoration (2009)

B.Arch., İzmir Institute of Technology, Department of Architecture (2006)

Working Experience:

Assistant General Manager, Kent Private School, İzmir, Turkey (since 2012)

Research Assistant, Department of Architectural Restoration, İzmir Institute of Technology (2006-2012)

Architect - Arkmim Architecture and Restoration Company (2006)